University of Alberta
Department of Civil &
Environmental Engineering

Structural Engineering Report No. 261

ANALYSIS OF STEEL PLATE SHEAR WALLS USING THE MODIFIED STRIP MODEL

by

Jonah J. Shishkin

Robert G. Driver

and

Gilbert Y. Grondin

November 2005

Analysis of Steel Plate Shear Walls Using the Modified Strip Model

by

Jonah J. Shishkin
Robert G. Driver
and
Gilbert Y. Grondin

Structural Engineering Report 261

Department of Civil and Environmental Engineering
University of Alberta
Edmonton, Alberta, Canada

November 2005

ABSTRACT

Unstiffened steel plate shear walls are an effective and economical method of resisting lateral forces on structures due to wind and earthquakes. Engineers in the workplace require the ability to assess the inelastic structural response of steel plate shear walls using conventional analysis software that is commonly available and is relatively simple and expeditious to use. The strip model, a widely accepted analytical tool for steel plate shear wall analysis, is refined based on phenomena observed during loading of steel plate shear walls in the laboratory. These observations are modelled first in detail and then simplified to provide an accurate prediction of the overall inelastic behaviour, while being efficient to model. The modifications are tested on several test specimens to validate their use. A parametric study examines the effect of varying the angle of inclination of the tension strips on the predicted inelastic behaviour of the model.

ACKNOWLEDGEMENTS

Funding for this research was provided by the Steel Structures Education Foundation and the Natural Sciences and Engineering Research Council of Canada. The first author would like to gratefully acknowledge the financial support from the Alberta Region of the Canadian Institute of Steel Construction through the G.L. Kulak scholarship.

Setup and maintenance of the computer analysis programs were done by D. Lathe and P. Altobelli. Several of the CORELDraw figures were created by Andrew Prince.

TABLE OF CONTENTS

LIST OF TABLES

LIST OF FIGURES

LIST OF SYMBOLS

A	cross-sectional area of equivalent brace (Thorburn *et al.* 1983)
A_b	cross-sectional area of beam
A_c	cross-sectional area of column
A_{CS}	cross-sectional area of compression strut
B	amplification factor applied to seismic loads in columns (CAN/CSA S16-01)
D	dead load
d_b	depth of beam section
d_c	depth of column section
EQ	seismic or earthquake load
F_y	yield strength
F_{yCS}	limiting strength of compression strut
F_{yPL}	yield strength of infill plate
h	storey height
I_b	moment of inertia of beam section
I_c	moment of inertia of column section
L	centre-to-centre distance of columns
LL	live load
M	moment force
M_p	plastic moment

M_{pc} plastic moment adjusted for axial loads

M_y yield moment

P axial force

P_y axial force at yield

Q applied lateral load to steel plate shear wall panel (Mimura and Akiyama 1977)

R seismic force reduction factor (NBCC 1995)

R_d ductility related force modification factor (NBCC 2005)

R_o overstrength related force modification factor (NBCC 2005)

R_y factor applied to yield stress to estimate the probable yield stress (CAN/CSA S16-01)

S snow load (NBCC 1995)

t infill plate thickness

V_{re} probable shear resistance at the base of the steel plate shear wall for the supplied plate thickness

V_s applied shear load (Berman and Bruneau 2003)

Z plastic modulus of wide-flange section

α angle of inclination of the average principle tensile stresses in the infill plate with respect to the boundary column

δ lateral deflection of steel plate shear wall panel (Mimura and Akiyama 1977)

δ_y yield deflection of steel plate shear wall specimen

Δ	elongation of tension strip or shortening of compression strut
Δ_y	elongation of tension strip at yield force; shortening of compression strut at limiting stress
θ	rotation of beam or column element
ϕ	acute angle of equivalent brace with respect to the boundary column
ω_h	column flexibility parameter (CAN/CSA S16-01)
Ω_s	overstrength factor (Berman and Bruneau 2003)

1. INTRODUCTION

1.1 Background

Numerous research programs have confirmed that steel plate shear walls are an effective method of resisting lateral forces on structures such as those due to wind and earthquakes. Moreover, they have been shown to be an economical solution (Timler *et al.* 1998). A conventional steel plate shear wall consists of thin and unstiffened steel plates bounded by steel columns and beams. Steel plate shear walls can be multiple storeys high and can be one or more bays wide with either simple shear or moment–resisting beam-to-column connections. The primary mechanism for resisting storey shears arising from lateral loads comes from the post-buckling inclined tension field that forms in the infill plate. Steel plate shear walls have been shown to possess considerable strength, ductility, redundancy, and robustness (*e.g.*, Timler and Kulak 1983, Driver *et al.* 1997; 1998a).

Modern design codes and standards are increasingly requiring an accurate assessment of inelastic structural response. However, current methods of analysing steel plate shear walls to obtain a reasonable approximation of the complete structural response curve require the use of sophisticated nonlinear finite element software or, alternatively, elastic analyses that must be supplemented with time consuming hand calculations. While research institutions often use powerful and sophisticated software packages, they are not common in industry. Design engineers require the ability to assess inelastic structural response using conventional analysis software that is commonly available and is relatively simple and expeditious to use. Most analysis software used by design engineers are elastic analysis programs that utilise inelastic methods, such as rigid–plastic hinges, to approximate the post-yield behaviour of a structure.

1.2 Objectives and Scope

This research proposes refinements to the strip model, as described by Thorburn *et al.* (1983), to obtain a more accurate prediction of the inelastic behaviour of steel plate shear walls using a conventional structural engineering software package. The refinements are based on observations from laboratory tests on steel plate shear wall specimens. Modelling efficiency is also evaluated against accuracy of the solution. A modified

version of the strip model is proposed, which is shown to be efficient to generate while maintaining a high degree of accuracy. The parameters of the proposed model are generic and can be implemented into any structural analysis program with pushover analysis capabilities. A parametric study is also performed to determine the sensitivity of the predicted nonlinear behaviour to variations in the angle of inclination of the infill plate tension field.

The research focuses on the pushover analysis method to obtain a good prediction of the inelastic behaviour of steel plate shear wall test specimens, which for cyclically loaded specimens is best captured by the envelope of the hysteresis curves. The research is limited to the analysis of unstiffened steel plate shear walls with relatively thin infill plates that contain no openings. While other analytical methods have been proposed to predict the inelastic behaviour of steel plate shear walls, they are not examined in detail in this report.

1.3 Chapter Overview

This section provides an overview of the remaining content of the report.

A chronological summary of previous research on steel plate shear walls, with the main focus being on analytical research, is presented in Chapter 2.

Chapter 3 describes the development of the detailed model, which consists of refinements to the strip model as described in CAN/CSA S16-01 based on observed phenomena during loading of steel plate shear wall specimens. The purpose of these refinements is to provide a more accurate prediction of the inelastic behaviour of steel plate shear walls. A pushover analysis is performed on the detailed model of a large-scale four–story, one–bay specimen to obtain a pushover curve, which is compared to the envelope of the hysteresis curve of the specimen to test the accuracy of the predicted behaviour. The pushover curve of the detailed model is also compared to that of the basic strip model.

Each parameter of the detailed model is examined more closely in Chapter 4, with the purpose of simplifying the modelling process. If the parameter could be simplified, while maintaining good accuracy, then the simpler form was kept. The resulting model was

named the simplified model. The pushover curves of both the detailed and simplified models are compared to the envelope curve of the modelled specimen and the pushover curve of the basic strip model. The model that displays both a high degree of accuracy and modelling efficiency is selected for further research and renamed the modified strip model. A brief sensitivity analysis is performed on the modified strip model to confirm the limiting strength of the diagonal compression strut, one of the parameters of the model, which was selected based on work by Kulak *et al.* (2001). Frame forces from the modified strip model are compared to those obtained from the test specimen and the basic strip model.

The modified strip model is validated by modelling other test specimens in Chapter 5, which consisted of different configurations from the previous specimen. These different configurations include pinned beam-to-column connections rather than moment–resisting ones, flexible columns, and a very thin infill plate. Pushover curves are obtained and compared to the envelope curves of the modelled test specimens. Refinements to the modified strip model are explored based on deviations found during the comparison of the response curves.

Chapter 6 investigates the effect of varying the angle of inclination of the infill plate tension field (*i.e.*, the tension strips) on the nonlinear behaviour of steel plate shear walls as predicted by the modified strip model. Different types of structures are analysed, which include varying aspect ratios, column stiffnesses, and beam-to-column connection types. The number of storeys is also varied to look at the effect that the overturning moment has on the model. The seismic design of the members for each model is based on the current codes and standards (*i.e.*, NBCC 2005, CAN/CSA S16-01). Observations are also made highlighting specific issues that arose from the design process.

Chapter 7 provides a summary of the research conducted and presents conclusions and recommendations for further research.

2. LITERATURE REVIEW

2.1 Introduction

Research on steel plate shear walls began in the early 1970s. Experimental and analytical studies conducted since then have demonstrated that properly designed steel plate shear walls can be an effective and economical design alternative for resisting lateral wind and earthquake loads on buildings. Several buildings have utilised steel plate shear walls of various forms as a lateral load resisting system. Early designs were based on the concept of preventing buckling of the infill plate due to shear. In Japan, this was accomplished by using heavily stiffened thin plates, while in the United States, moderately thick plates were used. However, recently there have been several buildings that have implemented unstiffened thin infill plates for the shear resisting system.

For many years, it has been known that buckling of a plate with a stiff boundary frame does not represent the limit of plate capacity in shear. An in-plane diagonal tension field forms after buckling occurs in a properly designed shear panel. Wagner (1931) demonstrated that a diagonal tension field would form after buckling in thin aluminum aircraft shear panels supported by stiff boundary members. He developed the "pure" tension field theory whereby the diagonal tension field that forms in a thin plate supported by stiff boundary members is the primary mechanism for shear resistance. Kuhn *et al.* (1952) proposed the "incomplete" diagonal tension theory, which assumes plate shear capacity is a combination of pure shear and the inclined tension field. Following the research of Wagner and Kuhn, Basler (1961) developed an incomplete diagonal tension field model to predict the shear capacity of steel plate girders with intermittent transverse stiffeners to anchor the tension field. Basler's work has been widely accepted and can be found as the basis for the design of plate girders in several steel design standards and specifications (*e.g.*, CAN/CSA S16-01, AISC 2005). Takahashi *et al.* (1973), who is believed to have conducted the first extensive research programme on the behaviour of steel plate shear wall panels, found that under cyclic loads heavily stiffened steel panels perform better in shear than unstiffened steel panels, although it is unlikely that they would be economical in most markets.

The following sections describe the primary research developments related to unstiffened steel plate shear walls, with an emphasis on analytical techniques. Since the model developed in this report is based on the strip model originally proposed by Thorburn *et al.* (1983), developments in this analytical technique are also described in some detail.

2.2 Mimura and Akiyama (1977)

In addition to a testing programme, Mimura and Akiyama (1977) developed a model to describe the hysteretic behaviour of a steel plate shear wall panel, as shown in Figure 2.1, assuming the deformation required to form the tension field when loading in the opposite direction is equal to one-half of the plastic deformation of the previous load cycle. In the figure, Q is the lateral load applied to the panel and δ is the resulting lateral deflection. Other notable assumptions included setting the plastic Poisson's ratio of the plate to 0.5 and a constant angle of inclination of the tension field that was set to 45°. The path OAB describes the initial positive loading of the steel plate shear wall. The unloading of the steel plate shear wall, as described by BC′, was assumed to be parallel to the initial loading path, OA. C′C describes the loading of the wall in the opposite direction, or negative loading. Shear buckling of the infill plate was assumed to have occurred at point C and the tension field to have re-formed in the plate at point D. The point where the tension field re-formed was located on a line parallel with OA and starting at point D′, which was set at the halfway point between O and C′, a direct result of setting the Poisson's ratio of the plate to 0.5. Assuming a negative monotonic curve OA′E, the hysteresis model continues down the path DA′E. The removal of the negative load from the wall, as described by EF′, is assumed to be parallel to OA.

2.3 Thorburn *et al.* (1983)

The first comprehensive analytical investigations of conventional unstiffened steel plate shear walls were conducted at the University of Alberta. Thorburn *et al*. (1983) recognised that buckling of the infill plate due to lateral loads does not represent the ultimate capacity of steel plate shear walls and that the inclined tension field dominated the post-buckling behaviour of the infill plates. An analytical model—termed the strip model—was developed to simulate the tension field behaviour, wherein the infill plate is

modelled as a series of tension–only strips oriented at the same angle of inclination, α, as the tension field. A typical panel, representing a one storey "slice" of the shear wall, is shown in Figure 2.2. It was demonstrated that summing the responses of individual storeys gave a good approximation of the response of a strip model of the entire shear wall, resulting in savings in modelling effort where several identical panels are present. The strip model assumes that the boundary beams are infinitely stiff in order to reflect the presence of opposing tension fields above and below the modelled panel. The model studied in this research program used hinged connections at the beam ends (Figure 2.2), although the researchers indicated that frame behaviour could also be included. The tensile yield strength of the plate material was considered to be the limiting stress and the shear resistance of the infill plate prior to buckling was neglected. Thorburn *et al.* (1983) showed that ten strips per panel adequately represent the tension field action developed in the plate. All analyses conducted in this research were elastic. The Canadian steel design standard, CAN/CSA S16-01, recommends the strip model as a design tool for steel plate shear walls.

Using the principle of least work, Thorburn *et al*. (1983) derived an equation for α that takes the following form:

$$\tan\alpha = \sqrt[4]{\frac{1+\frac{Lt}{2A_c}}{1+\frac{ht}{A_b}}} \tag{2.1}$$

where t is the thickness of the infill plate, A_c and A_b are the cross-sectional areas of the column and beam, respectively, and the other parameters are depicted in Figure 2.2. The derivation included the effect of the axial stiffnesses of the boundary members, but not the flexural stiffness.

In order to simplify the iterative process of designing a steel plate shear wall, Thorburn *et al*. (1983) developed a Pratt truss model, known as the equivalent brace model, that is illustrated in Figure 2.3. The infill plate at a single storey is modelled as a single diagonal tension-only brace intersecting the working points of the frame. The diagonal brace

represents the stiffness characteristics of the tension field in the infill plate, assuming rigid boundary elements. The equation for the area of the brace is as follows:

$$A = \frac{tL\sin^2 2\alpha}{2\sin\phi\sin 2\phi} \tag{2.2}$$

where ϕ is the acute angle of the brace with respect to the column and all other parameters are as defined above. CAN/CSA S16-01 (Clause 20.2) recommends the equivalent brace model as a preliminary design tool for steel plate shear walls.

Thorburn *et al.* (1983) conducted a parametric study to assess the effect on the panel stiffness and strength of the plate thickness, the panel height, the panel width, and the column flexural stiffness. It was found that the parameters were closely interdependent with one another and their interaction complex.

2.4 Timler and Kulak (1983)

To verify the analytical method developed by Thorburn *et al.* (1983), Timler and Kulak (1983) tested a full-scale specimen that represented two single–storey, one–bay steel plate shear wall elements. Due to the testing procedure implemented in this research, the columns were the horizontal elements while the beams were vertical. As seen in Figure 2.4, the interior beam of the test specimen incorporated moment–resisting beam-to-column connections, while the exterior beams utilised pin connections. The specimen was loaded in an incremental manner to both service and ultimate levels. A cyclic load test up to the allowable deflection limit was also performed.

The researchers recognised that the flexural stiffness of the columns affects the value of α. Thus, the equation for α, originally developed by Thorburn *et al*. (1983), was modified as follows:

$$\tan\alpha = \sqrt[4]{\frac{1+\dfrac{tL}{2A_c}}{1+th\left(\dfrac{1}{A_b}+\dfrac{h^3}{360I_cL}\right)}} \tag{2.3}$$

where I_c is the moment of inertia of the column about an axis perpendicular to the panel and all other parameters were defined earlier. It was found that for the case of beams that have an infill plate on one side only, and are therefore free to bend, such as the beam at the top of a shear wall (or the edge of the test specimen), the flexural stiffness of the beam affects α. Thus, the equation for α was re-derived for the infill plate at the top of a steel plate shear wall and was presented as follows:

$$\tan\alpha = \sqrt[4]{\frac{1+Lt\left(\frac{1}{2A_c}+\frac{L^3}{120I_b h}\right)}{1+ht\left(\frac{1}{2A_b}+\frac{h^3}{320I_c L}\right)}} \tag{2.4}$$

where I_b is the moment of inertia of the beam about an axis perpendicular to the panel and all other parameters were defined previously. Equations 2.1, 2.3, and 2.4 were all derived assuming pinned beam-to-column connections. The Canadian steel design standard (Clause 20.3.1, CAN/CSA S16-01) specifies the use of Equation 2.3 for the calculation of α.

Timler and Kulak (1983) modelled their test specimen using the strip model. Since an elastic analysis program was utilised, inelastic behaviour was simulated in the boundary members by successive reductions in the cross-sectional properties of the entire length of the members and in the strips by limiting the stress to the static yield stress measured from tension coupons. Good correlation was found between predicted and actual values of the infill plate stresses, axial strains, and the load vs. deflection response. The discrepancies found in using the Thorburn *et al*. (1983) equation for α were minor. However, it was recommended that the revised equation (Equation 2.3) be used to describe more accurately the angle of the tension field.

2.5 Tromposch and Kulak (1987)

Tromposch and Kulak (1987) tested a one–storey, two–panel specimen similar to that tested by Timler and Kulak (1983) except that bolted beam-to-column connections that would be used typically in the field and stiffer columns were used, in addition to a thinner

plate (3.25 mm). Also, the columns were pre-stressed before testing to simulate gravity loads on the structure. The main objectives of the tests were to examine the hysteretic behaviour of the specimen and to verify the analytical strip model proposed by Thorburn *et al* (1983). The specimen displayed ductile behaviour with severely pinched hysteresis curves due to the thin infill plate and flexible boundary frame.

Figure 2.5 shows the hysteresis model developed by Tromposch and Kulak (1987), which was based on previous research by Mimura and Akiyama (1977). Although this model could be used for shear walls with moment–resisting beam-to-column connections, no such tests were performed. Tromposch and Kulak also showed that the strip model (Thorburn *et al.* 1983) gave conservative estimates of both initial stiffness and ultimate capacity of steel plate shear walls. Inelastic behaviour was accounted for in a similar manner to that used by Timler and Kulak (1983). Tromposch and Kulak (1987) investigated models with fixed and pinned beam-to-column connections to assess the ability of the model to predict the behaviour of typical bolted connections and concluded that the behaviour of the test specimen fell between the two extremes. The researchers also found that the eccentricity of the fish plate (see Figure 2.4) with respect to the centre of the boundary members had no noticeable effect on the performance of the steel plate shear wall specimen.

2.6 Elgaaly *et al.* (1993a)

Elgaaly *et al*. (1993a) conducted analyses on three quarter-scale steel plate shear wall test specimens (Caccese *et al.* 1993). All specimens were three storeys high and one bay wide. The thickness of the infill plates was varied from 0.76 mm to 2.65 mm and beam-to-column connections were fixed-type. Two of the three specimens were modelled using a six-by-six mesh of shell elements representing each infill plate and three-node isoparametric beam elements representing the beams and columns. The inelastic behaviour was modelled using the von Mises yield criterion and the flow theory of plasticity. A Newton–Raphson iteration scheme was implemented. The shell element model overestimated both the elastic stiffness and ultimate capacity of the test specimens. This was attributed to the inability to model out-of-plane deformations in the infill plate

and coarseness of the mesh that prohibited the model from accurately representing the multiple buckle wavelengths observed during testing.

Elgaaly *et al.* (1993a) also developed a "truss" model based on the strip model developed by Thorburn *et al*. (1983). Twelve strips were equally spaced for each panel and the material properties for the strips were based on a trilinear stress vs. strain relationship. The initial modulus was based on the nominal modulus of elasticity for steel, while the second modulus was selected to obtain good agreement between analytical and experimental results. A flat line followed, starting at a point defined by the researchers to obtain a good agreement between the analytical and experimental results. Using this trilinear material model on a steel plate shear wall specimen with rigid beam-to-column connections, it was found that there was good agreement with the test results for ultimate capacity, but that the model overestimated the elastic stiffness. Elgaaly *et al.* (1993a) also conducted sensitivity studies to investigate the effect of the angle of inclination of the infill plate tension field, α, and the number of strips per panel on the trilinear truss model. It was found that the model with four truss strips per panel overestimated the ultimate strength by about 2.5% and that the ultimate strengths for the six– and twelve–strip models were practically the same. It was also found that varying α from 38° to 45° had little effect on the initial stiffness and that the difference in ultimate strength was 5.1%.

A second truss model was implemented to study the hysteretic behaviour of the steel plate shear wall specimens. The tension strips were aligned in both diagonal directions and oriented at an angle of 42.8°. Empirical factors determined from the test results were applied to the model to obtain good agreement. While satisfactory agreement was found between the model and the test results, it should be noted that the results are only relevant for the test specimens used by the researchers. Further study is required on the sensitivity of the empirical factors employed.

2.7 Xue and Lu (1994)

Xue and Lu (1994) conducted analytical studies on four twelve-storey three–bay steel plate shear wall configurations. For each case, the exterior bays had moment–resisting beam-to-column connections and the interior bay had steel infill plates at each storey.

The interior bay consisted of either rigid or simple beam-to-column connections and the infill plate was either connected to all the boundary members or to the beams only. For comparison, upper and lower bound cases of the twelve-storey three–bay steel plate shear walls were included in the analyses. The interior bay of the upper bound case had infill plates, which were assumed not to buckle under load, that were connected to all boundary members and the beam-to-column connections at all frame joints were rigid. The lower bound case consisted of a frame with simple beam-to-column connections in the interior bay and no infill plates.

The six frame–wall structures were modelled using elastic line elements for the columns and beams and four-node shell elements with large-deformation capacity for the infill plate. A 6×6 mesh was used for all panels, with the exception of the bottom panel where a 6×8 mesh was used. The structures were loaded monotonically with lateral forces at each floor. Gravity loads were not applied. Based on the analysis results, Xue and Lu (1994) concluded that the beam-to-column connection type had a very small effect on the lateral stiffness of the frame. It was found that the frames with the infill plates connected to all surrounding boundary members had a stiffness that was almost as high as the upper bound case. The frames with infill plates connected only to the beams were found to have a stiffness that was much higher than the lower bound case, but was lower than if the infill plates were connected to all surrounding boundary members. Despite this observation, Xue and Lu (1994) recommended that the infill plate be connected to the beams only. The main factor that led to this conclusion is that the analysis predicted that the columns of the stiffer system would carry a proportionally larger share of the storey shears, which could lead to early failure of the columns. It should be noted that no tests were performed to verify the analytical results.

2.8 Driver *et al.* (1997; 1998a, b)

Driver *et al*. (1997; 1998a) performed tests on a large–scale, four–storey, single bay steel plate shear wall specimen, as shown in Figure 2.6. The specimen had moment–resisting beam-to-column connections and the infill plates were welded to fish plates that were also welded to the boundary members. Gravity loads were applied to the tops of the columns and cyclic lateral loads of equal magnitude were applied at each floor level, as

per the requirements of ATC-24 (Applied Technology Council 1992). The specimen was able to resist increasingly higher loads at each successive cycle until a deflection of five times the yield deflection ($5\delta_y$) was reached. After the ultimate strength (3080 kN) was attained, the deterioration of the load-carrying capacity was gradual and stable. The maximum deflection attained by the lowest storey before failure occurred was nine times the yield deflection ($9\delta_y$). The hysteresis curves were also very stable throughout the test. It was found that the amount of energy dissipated during the loading cycles was significantly greater than that shown by similar specimens, but with shear-type beam-to-column connections (*i.e.*, Tromposch and Kulak 1987). Overall, the test behaviour showed that a properly designed steel plate shear wall system is an excellent lateral load-resisting system for seismic loading.

Driver *et al.* (1997; 1998b) also developed two analytical models to predict the structural behaviour of the steel plate shear wall specimen. The first was a finite element model, which used quadratic beam elements to represent the beams and columns and quadratic plate/shell elements to model the infill plates. As-built dimensions and measured material properties of the test specimen were input into the model. An estimated out-of-flatness of the panels and the experimentally obtained residual stresses were also incorporated. A monotonic analysis that included geometric and material nonlinearities was conducted up to a point where significant yielding occurred and where convergence became difficult to achieve. This nonlinear analysis was found to be in excellent agreement with the experimental data, but was unable to reach the full shear wall capacity. A full response analysis (with geometric nonlinearities excluded) was also performed and provided an excellent prediction of ultimate strength (almost exact, but model curve keeps increasing in capacity), but overestimated the initial stiffness by about 15%. A cyclic finite element analysis using a kinematic hardening rule was performed with the geometric nonlinearities excluded. The load vs. displacement results from this analysis showed good agreement with the test data, but they did not display pinching of the hysteresis curves.

For the second model, Driver *et al*. (1997; 1998b) used as its basis the strip model (Thorburn *et al*. 1983) to predict the envelope of the cyclic curves obtained in the test.

The purpose of this model was to analyse the specimen using structural analysis software that is widely used in the design office. Inelastic behaviour in this case was modelled using discrete plastic hinges, although since no common commercial structural analysis program was available at that time that could account for this behaviour directly, hinging of both the inclined tension strips and the frame members were modelled iteratively using an elastic analysis program. When a column or a beam reached its plastic moment capacity, M_{pc} or M_p, respectively, a true hinge was placed at that point and a constant moment of the magnitude M_{pc} or M_p was applied at the hinged joint. The frame was modelled using member centreline dimensions and only the frame member endpoints were examined for flexural hinging behaviour. When a tension strip reached yield, it was removed from the model and the tensile yield force of the strip was applied in the direction of the strip axis where the ends of the strip had been connected to the frame. After each hinging "event," the revised softened model was reloaded and the process was repeated until a plastic mechanism formed. The gravity loads used in the test and P-Δ effects were included in the analysis. It was found that this model slightly underestimated the elastic stiffness of the test specimen, while providing excellent agreement with the ultimate strength. Driver *et al.* (1997; 1998b) discussed various phenomena that could account for the underestimation of the initial stiffness of the test specimen by the strip model. One is the localised compression field that form in the diagonally opposite corners of the frame that form acute angles in the deformed structure where the compressed length of plate is short. Another factor is the increase in axial stiffness of the tension column arising from the presence of the infill plate connected to it; there will be some region that will be effective in tension in the vertical direction.

Driver *et al.* (1997; 1998b) also demonstrated that for their shear wall specimen, varying the angle of inclination of the tension field from 42º to 50º had little effect on the predicted storey shear vs. storey drift predictions and recommended a parametric study be conducted to examine this observation further. They also found that using twenty strips to model the infill plate did not provide a better prediction of the overall response than did the use of ten strips. Based on the strip model, the researchers also proposed a new hysteresis model that explicitly divides the steel plate shear wall behaviour into two

distinct components—that of the moment–resisting frame and that of the infill panel—that was shown to provide good predictions of cyclic behaviour.

2.9 Elgaaly and Liu (1997)

Elgaaly and Liu (1997) conducted an analytical investigation of steel plate shear walls. Based on test observations made by Caccese *et al*. (1993), it was found that the tension strains in the infill plate were not uniform throughout, but were higher near the boundary members. To reflect this observation, the researchers modified the trilinear material model (Elgaaly *et al*. 1993a) by incorporating square gusset plates at the ends of the tension strips. The gussets resist a combination of pure shear and diagonal tension, which is a different behaviour than that of the tension–only strips. Yielding occurs in the gussets before the tension strips. The dimensions of the gusset plates were determined by equating the buckling shear stress of the square gusset plate to the shear yield stress of the plate material. An angle of inclination of the tension strips was assumed to be 45° and an empirical plastic deformation factor was incorporated into the analysis to obtain good agreement between the analytical model and the quarter–scale test specimens of Caccese *et al*. (1993).

Elgaaly and Liu (1997) analysed two types of steel plate shear walls: with welded connections of the infill plates to the boundary members and with bolted connections. The results from the analyses were compared against the steel plate shear wall specimens with the infill plate welded to the boundary members (Elgaaly *et al.* 1993a) and with the infill plate bolted to the boundary members (Elgaaly *et al.* 1993b). Modifications were made to the trilinear stress vs. strain relationship of the trusses, which include tension strip plus gusset plates, to reflect the different behaviour observed for bolted shear walls, notably bolt slip and the potential for tearing at the bolt holes. Empirical factors employed in the truss model by Elgaaly *et al.* (1993a) were used to obtain good agreement with test data.

2.10 Lubell (1997)

Lubell (1997) conducted experiments on two one–storey steel plate shear wall specimens (SPSW1 and SPSW2), depicted in Figure 2.7, and one four–storey specimen (SPSW4),

depicted in Figure 2.8. In all specimens, the beams were connected to the columns using moment–resisting connections. The top beam of specimen SPSW2 consisted of two S75×8 sections, one on top of the other, with the sections fully welded along the adjacent flange tips. It was found during the fabrication of SPSW1 that out-of-plane deformations in the infill plate, with a maximum of 26 mm measured at the centre of the panel, occurred due to welding distortion. The deformations were corrected in specimens SPSW2 and SPSW4 such that the maximum out-of-plane deformation was less than 5 mm. Steel masses were placed at each storey of specimen SPSW4 to simulate gravity loading. Quasi-static cyclic testing, based on ATC-24 (Applied Technology Council 1992) requirements, was performed on all three specimens. The single-storey specimens were shown to be very ductile, attaining inelastic deformations of about $6\delta_y$. However, Figure 2.9 shows that the initial stiffness of the specimens differed by a considerable amount. This was probably due to the large initial out-of-plane deformations of the infill plate of specimen SPSW1 and the higher beam stiffness in specimen SPSW2. SPSW4 was shown to be more flexible than SPSW2 (Figure 2.9), which was explained by the influence of the overturning moment on the four-storey specimen. It was loaded to a first storey displacement of $1.5\delta_y$ when global out-of-plane buckling of the slender column occurred. Significant "pull-in" of the columns was observed in all specimens due to their low flexural stiffness.

Lubell (1997) conducted analytical studies of the test specimens using a nonlinear frame analysis program, CANNY-E. The beam and column elements were located at the centroid of each member, with the exception of the top beam of SPSW4 in which the beam element was located 37 mm below the top flange in order to have equal aspect ratios (1:1) for each storey. The intermediate beams of the SPSW4 model were modelled as rigid beam sections. Fifteen equally spaced tension–only inclined elements were used to represent the infill plate of each panel and were oriented, with respect to the column, at an angle of 37°, as calculated by Equation 2.3 (Timler and Kulak 1983). Beam and plate elements incorporated trilinear stiffness parameters to account for both yield and post-yield strain hardening and the column elements used multiple bilinear springs to model the inelastic interaction between axial and flexural load effects over an assumed hinge

length of 20% of the column depth. P-Δ effects were also accounted for. Two types of strip models were created. The first used monotonic loading to describe the pushover envelope behaviour of the specimens. The second used reversed cyclic loading to describe the hysteretic behaviour of the models. In the second model, the tension–only strips were inclined in both directions, giving a total of thirty strips per panel. Loading histories for the cyclic model were similar to those of the associated test specimens.

The results for the monotonic SPSW1 model were found to be inconsistent with the test results. The model predicted a higher initial stiffness and ultimate strength (10% above test ultimate strength). Lubell (1997) attributed these deviations to the initial out-of-plane deformations of the infill plate, the changing value of α throughout the test, and inaccurate modelling of the top beam. The cyclic analysis of the SPSW1 model was not pursued due to these numerical inaccuracies.

The monotonic SPSW2 model had good agreement with the initial stiffness of the specimen, but slightly underestimated the ultimate strength. The cyclic model was able to capture the pinching of the hysteresis curves. Overall behaviour of the cyclic model matched that of the test. However, there were a few minor localized differences that were attributed to the numerical modelling simplifications used.

Two monotonic models were created for the SPSW4 specimen. It was found that neither could accurately describe the specimen pushover envelope behaviour completely. Using the value of α calculated according to Equation 2.3 (37°), the model predicted an initial stiffness nearly twice that of the specimen, but good agreement was found with the ultimate strength. A model with a value of α of 22°, based on a partial tension field where the tension field is anchored only by the beams (Thorburn *et al.* 1983), was analysed, although the tension strips were connected to both the columns and beams. This model resulted in a good correlation of the initial stiffness of the specimen, but underestimated the specimen's ultimate strength. For the SPSW4 cyclic model, an α value of 37° was selected since it provided good post-yield results. The model's cyclic behaviour was similar to that of the SPSW2 model, except the reverse loading regions of the SPSW4 model hysteresis loops were more curved than those of the one storey model. The cyclic

model suggested that if the column had not buckled, the specimen could have resisted more loading cycles. A direct comparison between the model and the specimen hysteresis loops was not made.

Lubell (1997) conducted a series of parametric studies, using the SPSW2 monotonic model, to investigate the sensitivity of certain model parameters. It was found that the initial stiffness was not overly sensitive to changes in infill plate thickness, t, but the ultimate strength was found to increase as t increased. It was also found that as α decreases, both the initial stiffness and the ultimate strength of the specimen decreased.

2.11 Timler *et al.* (1998)

Researchers and industry professional engineers collaborated on an analytical study into the design and cost feasibility of steel plate shear walls. Comprehensive designs of medium–sized office buildings with steel plate shear walls of varying ductility ratings for different locations across Canada were conducted and compared with alternative designs using reinforced concrete shear walls. The designs of the steel buildings were based on Appendix M of CAN/CSA S16.1-94 and the 1995 National Building Code of Canada (NBCC 1995) was used to establish the applied seismic loads.

Based on the design exercises, some modelling simplifications were suggested with respect to the steel plate shear wall guidelines of CAN/CSA S16.1-94. These recommendations include appropriate averaging of the tension field, which includes shifting of the tension struts to align to common nodes on the beam for frames with rigid beam-to-column connections, and relaxing the axial load limitation for columns of cores designed for $R = 4$, where R is the seismic force reduction factor from NBCC 1995. However, these issues were determined to be minor and the design procedure for steel plate shear walls was found to be simple to implement using basic analytical tools. It was found that for steel plate shear wall structures, the super- and sub-structure works were less expensive than traditional reinforced concrete shear wall forms. It was also found that a building with steel plate shear walls could be turned over to the owner substantially more quickly than a similar building with a reinforced concrete core. These factors both contribute to the economic feasibility of steel plate shear wall structures.

2.12 Rezai (1999)

Rezai (1999) conducted shake-table testing on a quarter–scale, four–storey steel plate shear wall specimen nearly identical to the one tested by Lubell (1997) to study the dynamic behaviour. This was the first time a test of this kind was conducted on a steel plate shear wall specimen. All beam-to-column connections were moment–resisting. However, no stiffeners (continuity plates) were provided on the columns for these connections. Steel plates were placed on the beams at each storey to provide a mass of 1700 kg at each level. The specimen was subjected to various site-recorded and synthetically generated ground motions at varying intensities. Due to limitations of the shake table, the test results remained mainly in the elastic range. Thus, the nonlinear behaviour of the steel plate shear wall specimen could not be explored in detail.

Rezai (1999) found that the first mode was the primary mode of vibration with very little contribution from higher modes. The top storeys exhibited behaviour that suggested that flexural behaviour dominated, while the bottom storey acted as a shear panel throughout the test sequence. Based on the load vs. deformation plots for all four storeys, it was shown that the first storey dissipated the majority of energy, while the top floors acted as a rigid body rotating about the first floor. Also, it was found that the flexural strains generated in the intermediate level beams could be considered negligible.

Rezai (1999) also conducted sensitivity analyses using Equations 2.3 and 2.4 to assess the effects of various structural properties on the value of the angle of inclination of the infill plate tension field, α. One structural property was changed while the remainder were kept constant. Five different test specimens were used: Timler and Kulak (1983), Tromposch and Kulak (1983), Caccese *et al.* (1993), Driver *et al.* (1998a), and Lubell (1997). It was found that α did not vary significantly for any change in beam and column cross-sectional area and for infill plate thicknesses, t, of 6 mm and greater, where Equation 2.3 was used. It was found that when Equation 2.4 was used, α varied significantly with changes in t.

Rezai (1999) developed a “simplified” strip model for analyzing steel plate shear wall behaviour, as illustrated in Figure 2.10. The tension–only strips for each panel are placed

diagonally between opposite corners and from the corners to the mid-span of the boundary members, for a total of five strips per panel. The strips were set up in this manner to reflect the non-uniformity of α and to reflect the corner stiffness of each panel. Using this model, good agreement was obtained between the predicted and experimental elastic stiffness of the single–storey specimens of Lubell (1997). However, the model was found to be conservative in predicting the ultimate capacity. Rezai (1999) also compared the results from the "simplified" strip model to the results from the original strip model using the specimen tested by Driver *et al*. (1998a) as a basis. The "simplified" model had a higher estimated elastic stiffness and ultimate capacity than that provided by the conventional strip model.

2.13 Astaneh-Asl (2001)

An attempt at compiling a comprehensive document detailing the behaviour and design of steel plate shear walls was made by Astaneh-Asl (2001). Both stiffened and unstiffened panels were examined and it was recommended that unstiffened infill plates be used unless there are openings in the shear wall that require stiffening. Figure 2.11 shows a list of possible failure mechanisms that is organised into a hierarchical order of failure modes. Ductile failure modes are ranked as more desirable than brittle failure modes and are arranged first. This chart can be an effective design aide for checking each member in a steel plate shear wall system.

Astaneh-Asl (2001) recommended the use of equations that describe the behaviour of plate girders (AISC 1999) for the design of unstiffened steel plate shear walls. The author stated that the use of these equations gives results that are more conservative than those based on other means of analysing steel plate shear walls (*i.e.*, Thorburn *et al.* 1983). Berman and Bruneau (2004) emphasised this point in more numerical detail and concluded that the plate-girder analogy is inadequate for the design of steel plate shear walls.

2.14 Kulak *et al.* (2001)

Kulak *et al.* (2001) presented an overview of steel plate shear wall research conducted to date. A design example of a hypothetical eight-storey building in Vancouver, Canada,

using steel plate shear walls as the lateral load resisting system, was also presented. The preliminary design was performed using the equivalent brace method and the detailed design was performed using the strip model (Thorburn *et al.* 1983). Once the members were sized, a free vibration analysis was conducted on the bi-directional tension–only strip model, from which the fundamental natural frequency of the wall was determined to be 1.65 s. A response spectrum analysis was also carried out to estimate the effect of higher modes of vibration on the distribution of lateral forces over the building height. The analysis determined that the drift ratios due to wind and seismic loads were well within the 1995 National Building Code of Canada (NBCC 1995) limits.

The inelastic static and dynamic response of the shear wall was also analysed using a tension-compression strip model, which is an extension of the tension–only strip model and has inclined strips in both directions to resist lateral load in either direction. The compressive capacity of the strips, taken as 8% of the tensile capacity of the infill plate, was determined by calibrating the tension–compression model for both the load sustained and the cumulative energy absorbed with the hysteresis loops from the test by Driver *et al*. (1998a). The material behaviour was taken to be trilinear with linear–elastic behaviour to yield, strain hardening to the tensile strength of 1.4 times the yield strength at a strain of 0.15, and a flat curve afterwards. P-Δ effects were also accounted for. A nonlinear pushover analysis was conducted on the tension–compression strip model and it was found that the shear wall had an overstrength of about two times with respect to the NBCC 1995 design shear. This overstrength resulted largely from using a minimum infill plate thickness of 4.8 mm, which was considerably greater than what was required as determined during the preliminary design. A nonlinear dynamic time history analysis showed that the interstorey drifts were well within the NBCC 1995 seismic limits, which implies that both structural and non-structural elements are protected from damage due to the stiffness of the steel plate shear wall. The data also showed that a soft storey does not manifest itself at the design load levels. Most of the inelastic action was found to have occurred in the third storey. The Class 1 column section was found to be more than sufficient to absorb the maximum extreme fibre strains without the occurrence of local buckling. It was also found that by changing the column sections of the third and fourth

storeys to a more robust section, the inelastic action was forced to occur in the first storey.

2.15 Behbahanifard *et al.* (2003)

Behbahanifard *et al*. (2003) conducted an experimental and numerical investigation of steel plate shear walls. The test specimen was taken directly from the one tested by Driver *et al*. (1998a), with the bottom panel removed due to the damage from the original test, thus creating a large–scale, three-storey, single–bay specimen. The loading sequence followed ATC-24 guidelines. Before the ultimate strength of the specimen was reached, the first–level beam ruptured at the top flange and web of the beam-to-column connection (after 50 cycles of load, including the original test). Since one of the objectives of the test was to observe the ultimate capacity of the wall and behaviour of the boundary members under extreme loading conditions, the fracture was repaired and testing continued. The specimen reached its ultimate capacity at a deflection of seven times the yield deflection ($7\delta_y$), at which point the strength started to deteriorate gradually due to the formation of tears in the lower–storey infill plate. The specimen displayed high elastic stiffness, excellent ductility, the ability to dissipate high amounts of energy, stable hysteresis loops, and a high degree of redundancy.

A finite element model was developed for analysis of steel plate shear walls. Material and geometric nonlinearities were included in the model. A kinematic hardening material model was implemented to simulate the Bauschinger effect for the cyclic analysis of the shear wall. This model was used to simulate the monotonic and cyclic responses of the specimens of both Behbahanifard *et al*. (2003) and Driver *et al*. (1998a). The solution strategy in the dynamic explicit formulation did not involve iteration, but required very small time steps. This allowed the analysis to be completed without encountering numerical instability. Excellent agreement was observed between the test results and the numerical predictions, although the predicted capacity was slightly underestimated by the finite element model (12% for three-storey specimen, and 7.8% for four-storey specimen). The numerical model also predicted the hysteretic behaviour of the two specimens well, including capturing the pinching effect, although to a lesser degree than the test specimens.

Using the validated finite element model, a parametric study was conducted to identify and assess some of the non-dimensional parameters affecting the behaviour of a single panel steel plate shear wall. It was found that altering the aspect ratio of the infill plates within the range of 1.0 to 2.0 had a negligible effect on the behaviour of the shear wall panel. However, for aspect ratios less than 1.0, both the normalised stiffness and the normalised shear capacity of the panel increase. Increasing the ratio of the axial stiffness of the infill plate to that of the columns $\left(\frac{tL}{2A_c}\right)$ led to an increase in the stiffness of the shear wall panel, but had a negligible effect on the normalised shear capacity of the system. An increase in the column flexibility parameter, ω_h, as defined in Clause 20.4.2 of CAN/CSA S16-01, results in increasing bending deformation in the columns. The inward displacement of the columns induced by the tension field action results in a non-uniform tension field. Thus, both the stiffness and capacity of the system decrease as the column flexibility parameter increases. It was also demonstrated that initial out-of-plane imperfections in the infill plate could have a significant influence on the stiffness of the shear panel, but they have little effect on the shear capacity. In fact, it was found that imperfections of less than $0.01\sqrt{Lh}$ have a negligible effect. The effects of overturning moment and applied gravity load were also investigated using the validated finite element model. It was found that increasing either the gravity load or the overturning moment reduces the elastic stiffness of the shear wall panel in an almost linear manner and also significantly reduces the normalised capacity and ductility.

2.16 Berman and Bruneau (2003)

Using plastic analysis theory and the assumption of discrete strips to represent the infill plate, Berman and Bruneau (2003) derived equations to calculate the ultimate strength of single- and multi-storey steel plate shear walls with either simple or rigid beam-to-column connections. For multi-storey shear walls, equations were developed based on two types of failure mechanisms that provide a rough range of ultimate strengths: soft storey failure and uniform yielding of the infill plates in all storeys simultaneously. To provide a lower bound estimate of capacity, the equation derived for single–storey steel plate shear walls with simple beam-to-column connections was used to predict the

capacity of a variety of single- and multi-storey steel plate shear wall specimens from the literature having either pinned or semi-rigid connections. This equation was found to underestimate the experimental capacities by an average of about 6%, although it overestimated the capacity of one case by about 9%. The equation derived for the soft storey mechanism was found to overestimate the capacity of multi-storey test specimens with rigid connections by about 17%. This model provides only the ultimate capacity. The proposed equations do not describe the initial stiffness, the ductility, or the actual failure mechanism, nor do they provide a means of determining the frame forces for use in design.

Berman and Bruneau also looked at the design of steel plate shear walls using CAN/CSA S16-01. The equivalent storey brace method (Thorburn *et al.* 1983) was used as an actual design case along with the traditional strip model. It was found that if the aspect ratio was not equal to one, the equivalent brace method would result in a higher ultimate capacity than the strip model. (It should be noted, however, that the intended use of the equivalent brace method is for preliminary sizing only and not for detailed design.)

The researchers observed that for design of the infill plate, the storey shear, V_s, found using the equivalent lateral force method, should be multiplied by a system overstrength factor, Ω_s, between 1.1 to 1.5. As such, the minimum thickness of the infill plate for each storey is:

$$t = \frac{2V_s\Omega_s}{F_y L \sin 2\alpha} \tag{2.5}$$

where F_y is the nominal yield strength of the infill plate.

2.17 Kharrazi *et al.* (2004)

Kharrazi *et al*. (2004) proposed a numerical model called the Modified Plate-Frame Interaction (M-PFI) model to analyse the shear and bending of ductile steel plate walls. The M-PFI model separates the behaviour of ductile steel plate walls into three parts: elastic buckling, post-buckling, and yielding. Several steps were involved in developing these equations. First, a shear analysis was conducted that looked at the behaviour of the

infill plates and frames separately and then the shear vs. load displacement relationships for each were superimposed to obtain the shear behaviour of the ductile steel plate wall. Second, a bending analysis was conducted assuming the frame and plate act as a single unit. The interaction between shear and bending behaviour completes the analysis. Equations are proposed to obtain certain points on a shear vs. lateral displacement graph that can be used for analysing the behaviour of the shear wall.

Kharrazi *et al.* (2004) used test data from Driver *et al*. (1998a) to evaluate the M-PFI model using an assumed tension field inclination of 45°. The model overestimated the initial stiffness by 5% and underestimated the ultimate capacity of the specimen by about 10%, although it overestimated the specimen capacity slightly at initial yielding (knee of the experimental envelope curve). The model does not describe the ductility of the steel plate shear wall specimen or the actual failure mechanism, nor does it provide a means of determining the frame forces for use in design.

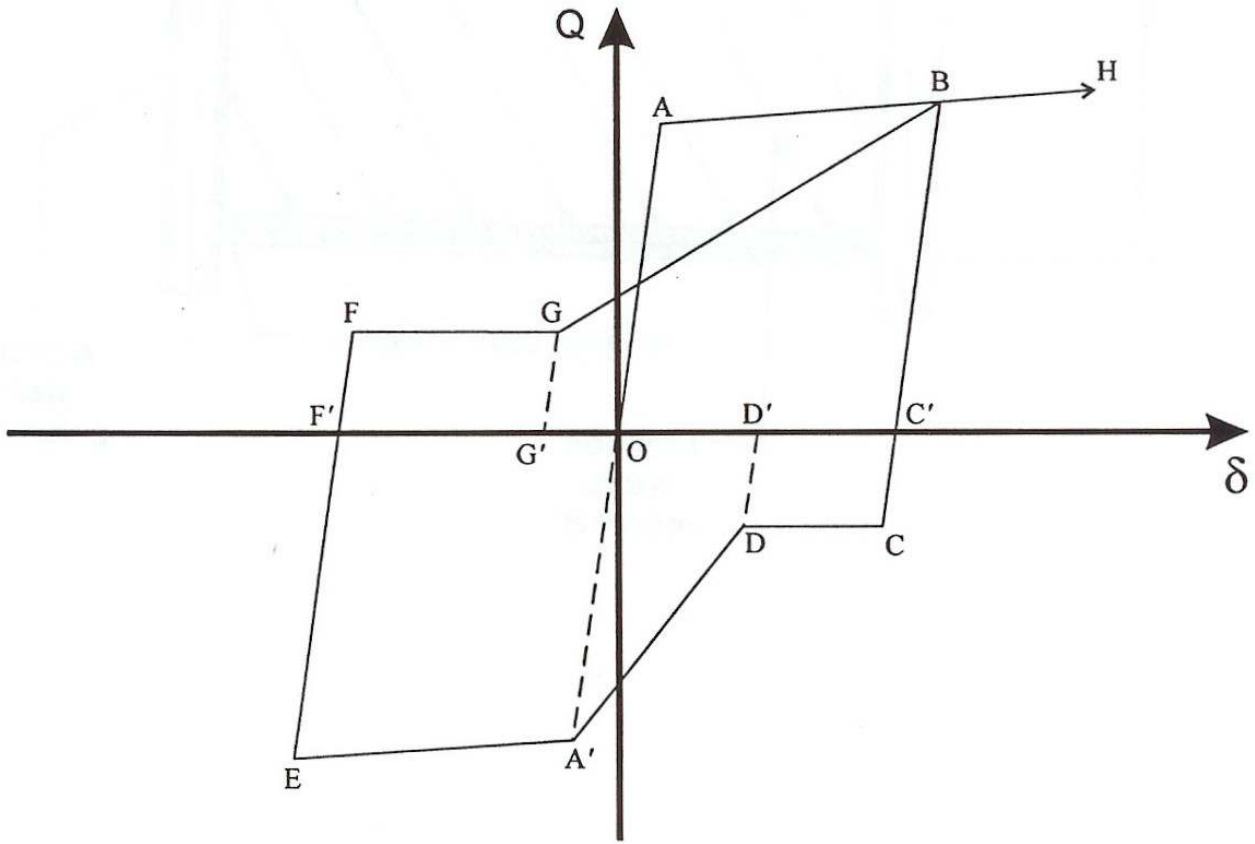

Figure 2.1 - Hysteresis Model (Mimura and Akiyama 1977)

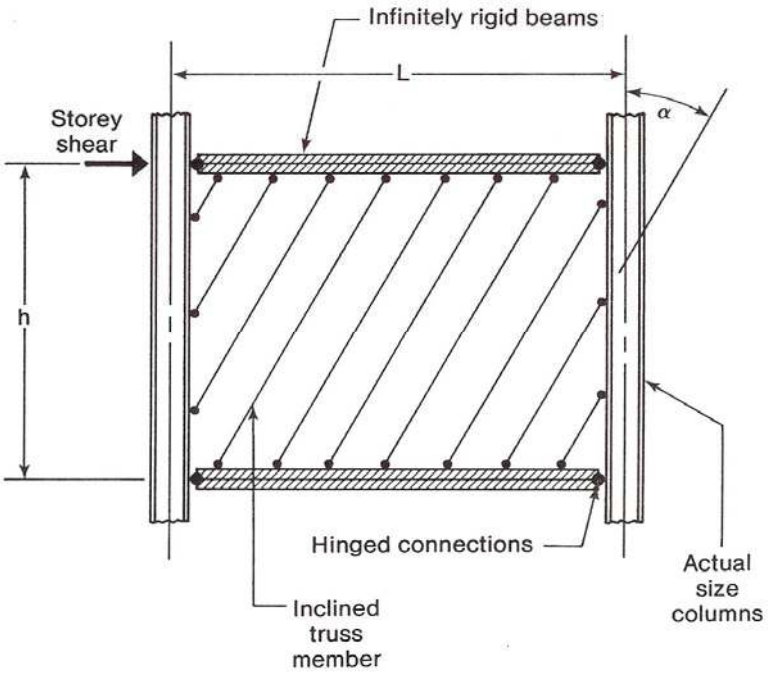

Figure 2.2 - Strip Model (Thorburn *et al.* 1983)

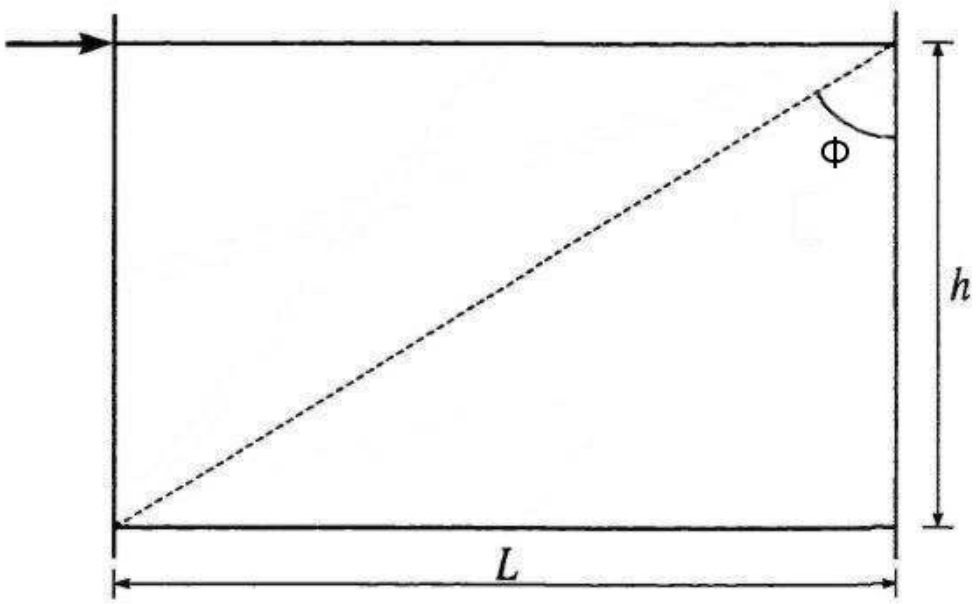

Figure 2.3 - Equivalent Brace Model (Thorburn *et al.* 1983)

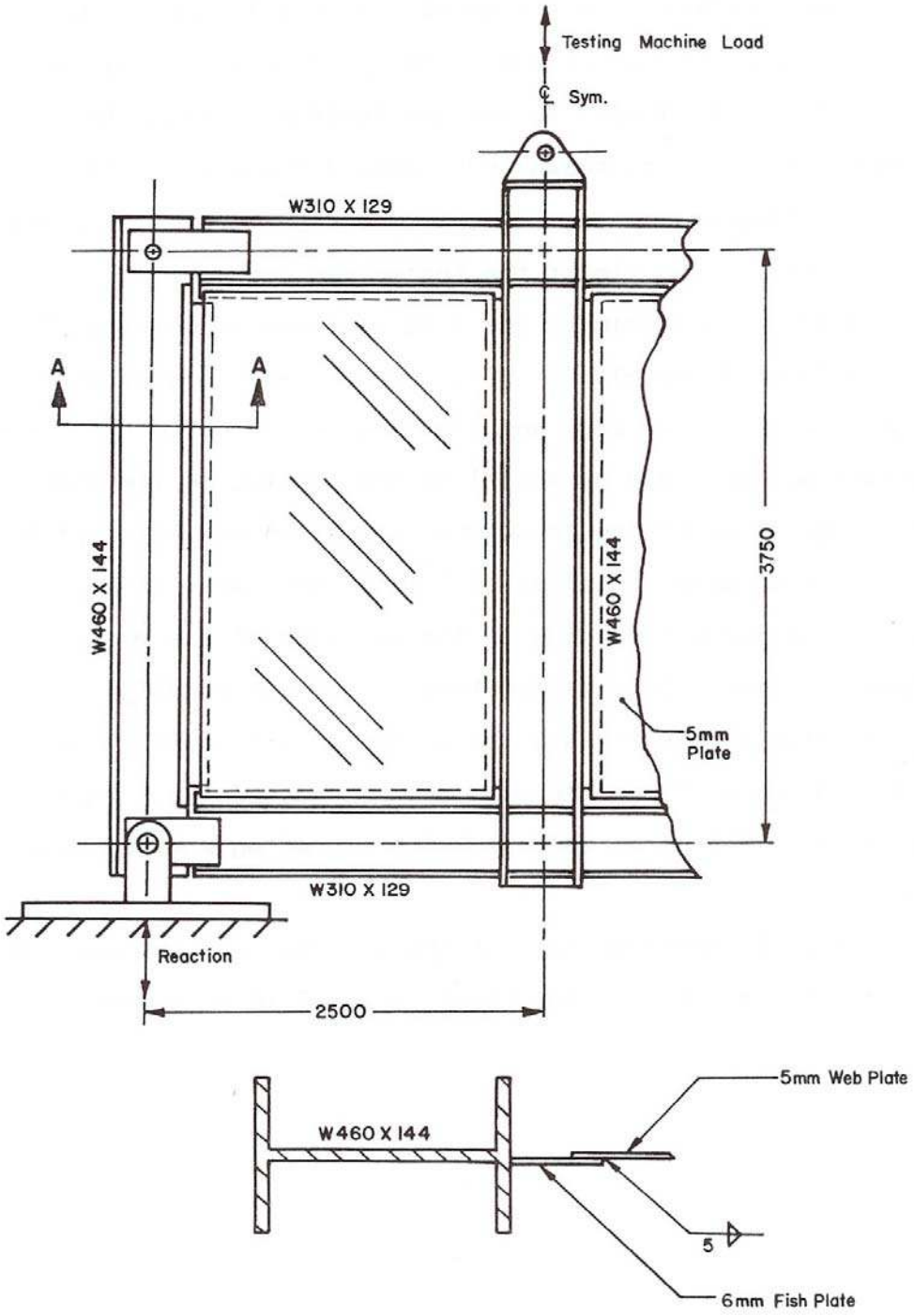

Figure 2.4 - One–Storey Test Specimen (Timler and Kulak 1983)

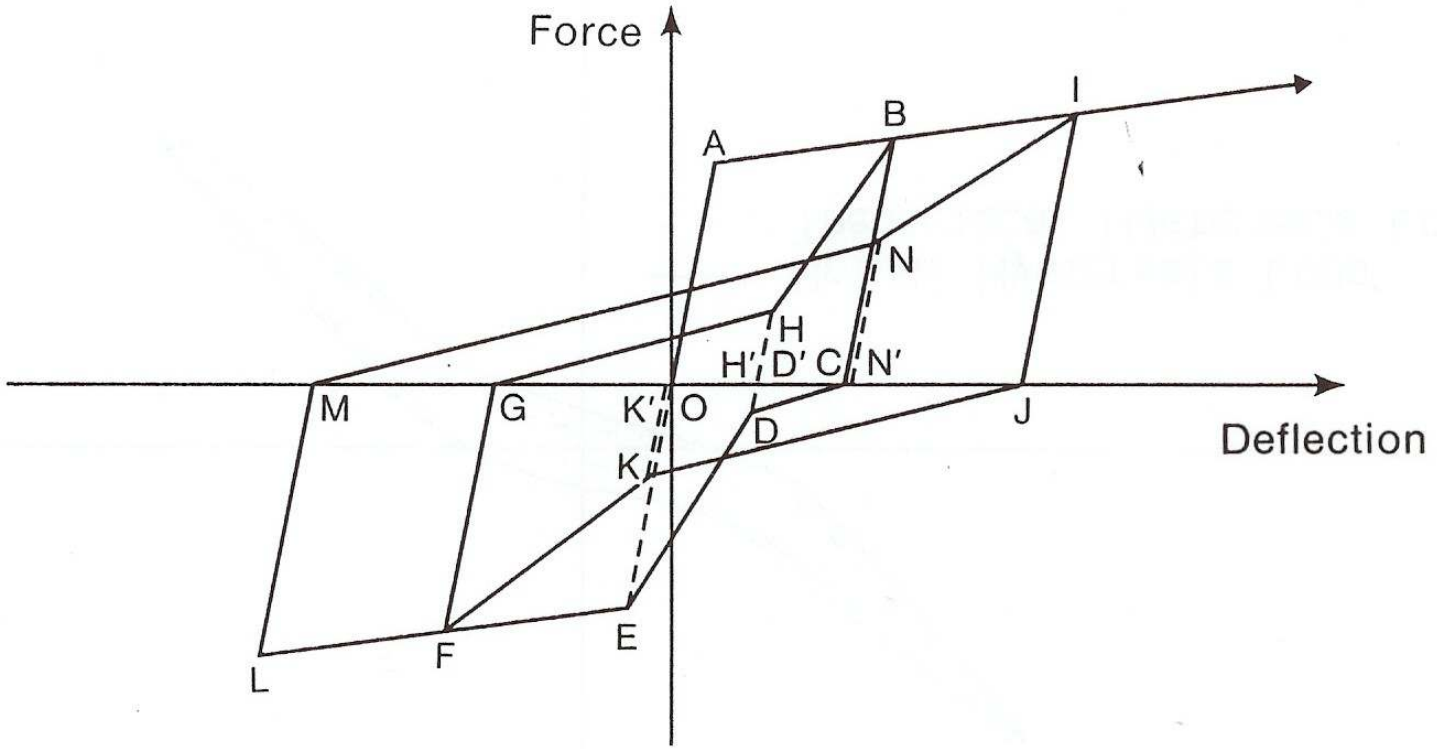

Figure 2.5 - Hysteresis Model proposed by Tromposch and Kulak (1987)

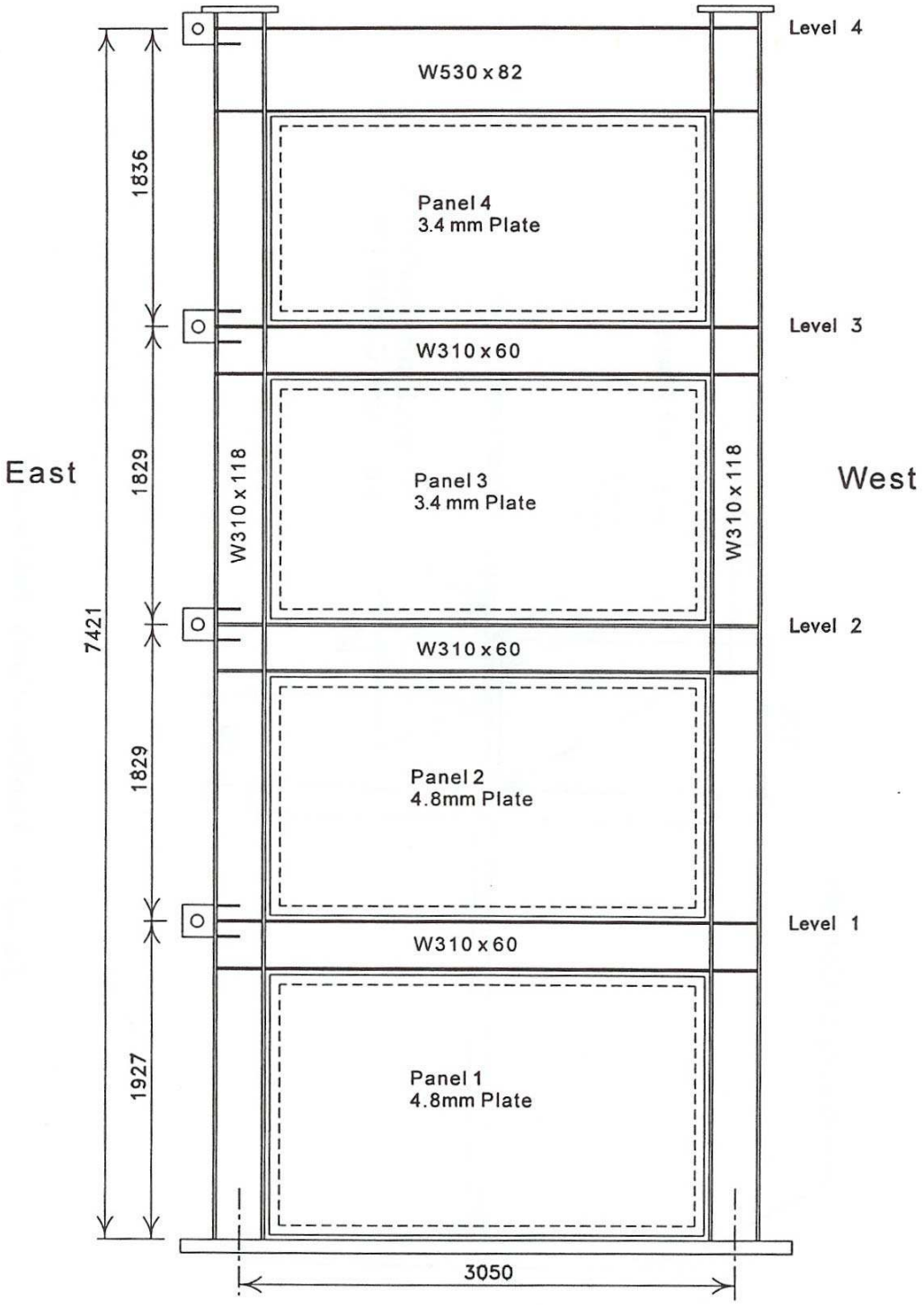

Figure 2.6 - Four–Storey Test Specimen (Driver *et al.* 1997; 1998a)

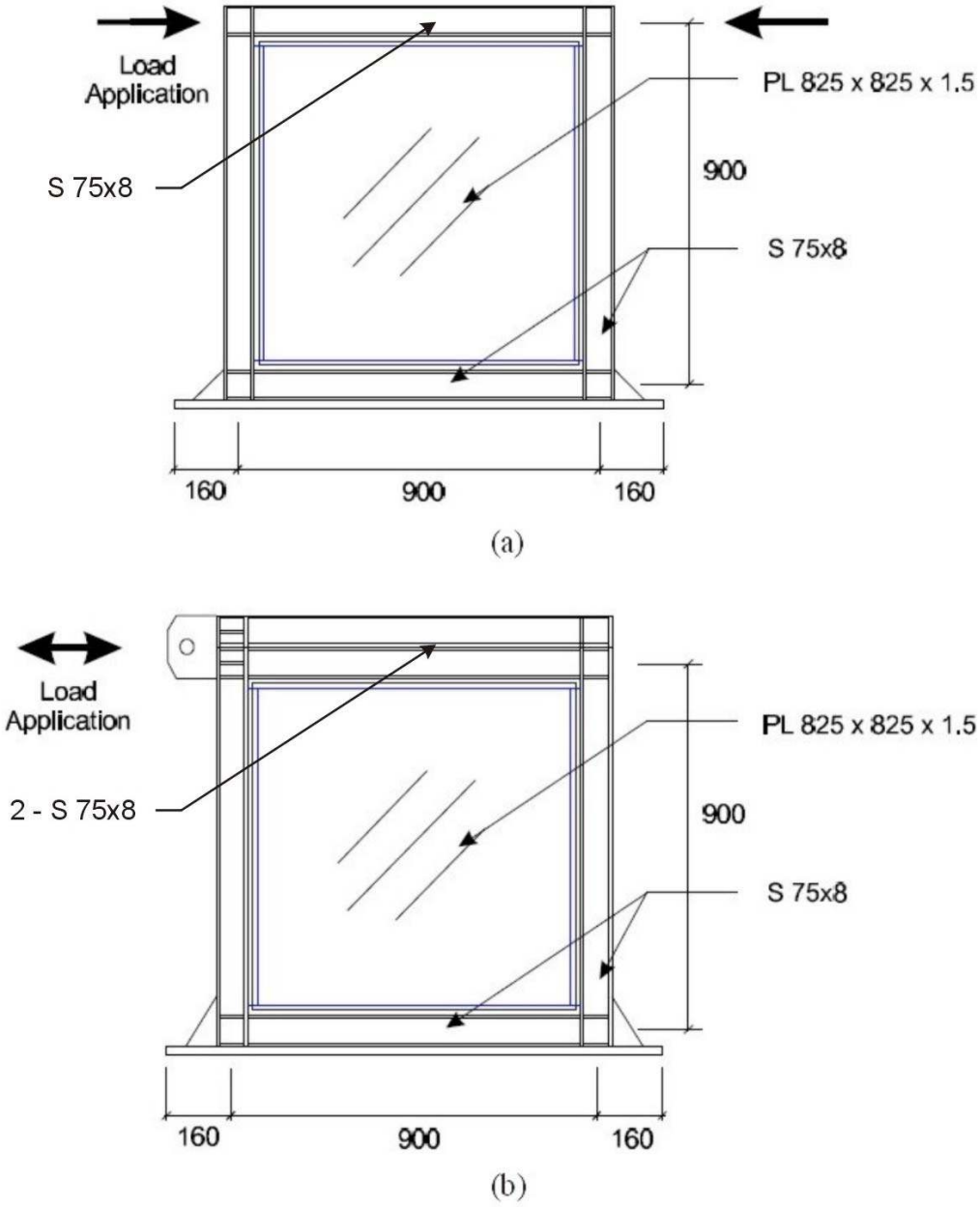

Figure 2.7 - One–Storey Test Specimens (Lubell 1997): (a) SPSW1; and (b) SPSW2

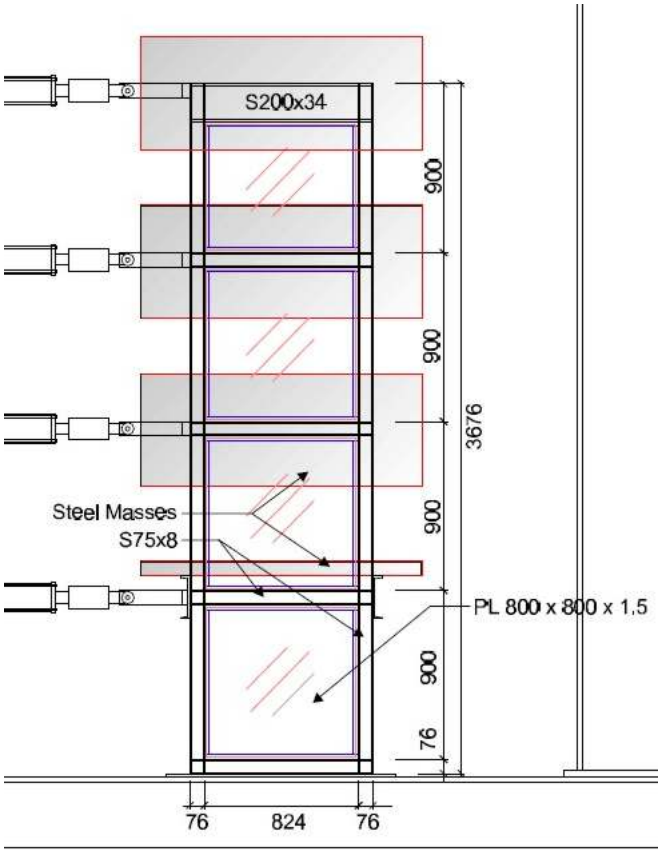

Figure 2.8 - Four–Storey Test Specimen, SPSW4 (Lubell 1997)

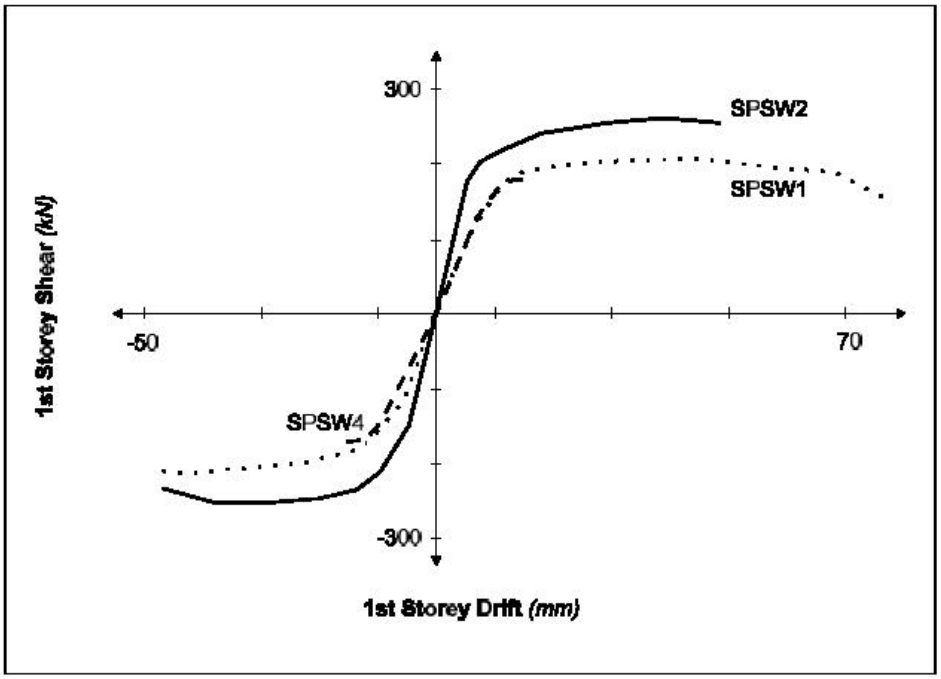

Figure 2.9 - Envelope Curves for One– and Four–Storey Specimens (Lubell 1997)

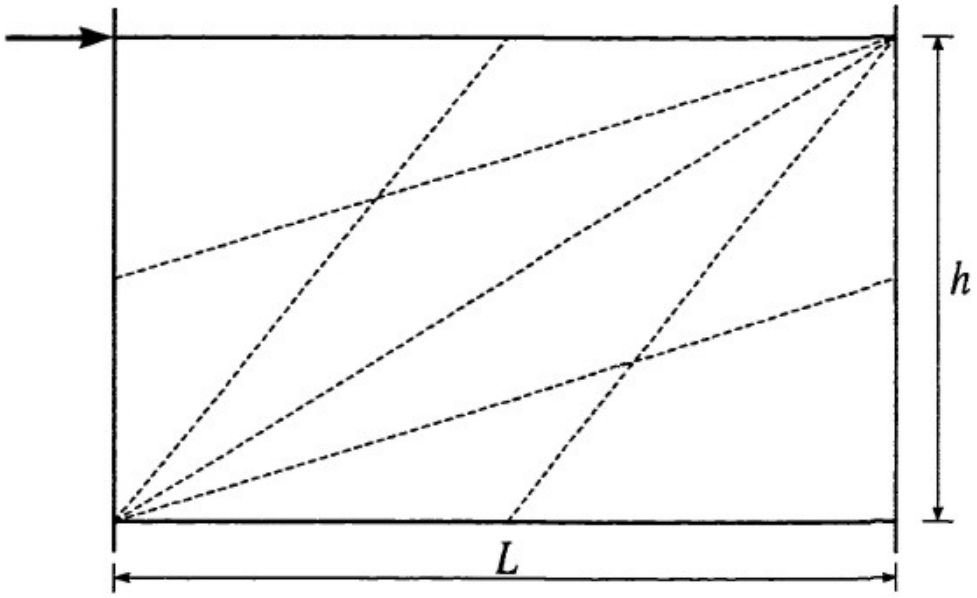

Figure 2.10 - Simplified Strip Model (Rezai 1999)

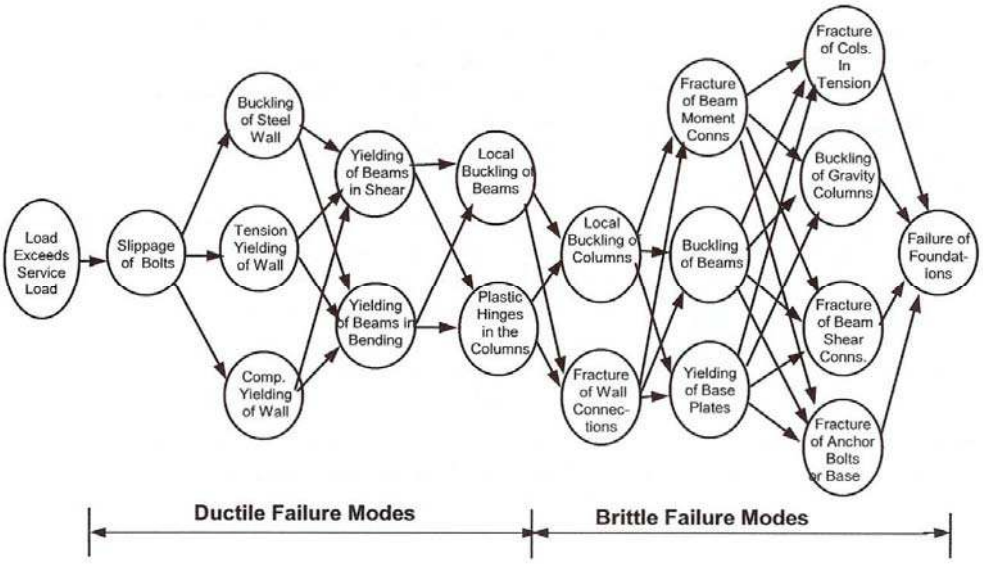

Figure 2.11 - SPSW Failure Mechanism Hierarchy (Astaneh-Asl 2001)

3. DETAILED MODEL

3.1 Introduction

The typical nonlinear behaviour of a properly proportioned steel plate shear wall consists of a high initial elastic stiffness followed by tensile yielding of the infill plates, after which the frame develops localised plastic hinges until the ultimate strength of the wall is obtained. This is followed by a gradual deterioration in strength at large displacements. The inherent ductility of the system contributes to the large energy dissipation capacity of the steel plate shear wall and the load carrying redundancy, particularly in cases where the frame is fabricated with moment–resisting beam-to-column connections, contributes to its robustness. Although hysteresis curves of steel plate shear wall behaviour capture additional information about energy dissipation, in general all of these qualities are reflected in an envelope curve of a cyclically loaded wall, as seen in Figure 3.1. Therefore, it is desirable for the design engineer to be able to model this behaviour both accurately and efficiently.

Several analytical models have been proposed to describe the behaviour of steel plate shear walls. A commonly used model is the strip model (Thorburn *et al.* 1983). In this model, the infill plate of each panel is discretised into a minimum of ten equally spaced tension–only truss elements, which represent the inclined tension field in the infill plates, that are aligned with the average angle of inclination of the major principal stresses that develop under lateral loads. Line elements representing the columns and beams are aligned with the centroidal axis of each member of the steel frame. Vertical and lateral loads are then applied to the model to determine the response of the structure. The strip model can be used conveniently with conventional structural analysis software and is recommended by the Canadian steel design standard, CAN/CSA S16-01.

Driver *et al*. (1998b) reported that the strip model, incorporating elasto-plastic strip and frame hinges to model the inelastic behaviour, provided a reasonable estimate of the response of a large-scale steel plate shear wall but tended to underestimate both the elastic stiffness and the ultimate strength. This chapter proposes and describes several refinements to the strip model that are based on observed phenomena during laboratory

tests of large-scale steel plate shear wall specimens. The primary objective of the refinements is to provide a model, hereafter called the detailed model, that accurately predicts the nonlinear behaviour of a particular steel plate shear wall test specimen while capturing all of the key features of the experimental envelope curve. A static pushover analysis is performed on the detailed model and a pushover curve is obtained from the results. The curve is then compared to the test specimen envelope curve and the accuracy of the detailed model is verified. In the next chapter, the benefits of the individual refinements incorporated into the detailed model will be examined and evaluated in light of the penalty of increased modelling effort.

A structural analysis software package was required for this research that is both widely used in industry and is capable of performing pushover analyses. A survey was conducted to determine the nonlinear capabilities of the various commercial software programs that were available to the design engineer. SAP2000® (CSI 2000) was selected since it is a widely used program, is able to conduct nonlinear pushover analyses, and was readily available to the researchers. However, the development of the detailed model, as presented in subsequent sections, is entirely in generic form and could be implemented in any analysis program with equivalent capabilities.

3.2 Test Specimen and Model Geometry and Loading

A four-storey steel plate shear wall test specimen (Driver *et al.* 1998a), depicted in Figure 2.6, was selected to develop the detailed model. This specimen was selected because it is of a large scale and reasonable proportions and comprehensive experimental data were readily available. Moreover, most of the observed phenomena that contribute to the development of the detailed model were made during the testing of this specimen.

Table 3.1 shows the material properties of the test specimen, based on ancillary tests performed by Driver *et al.* (1997), that were input into the detailed model. Figure 3.2 displays the geometric arrangement of the detailed model based on as-built dimensions of the specimen. The test specimen was analysed as a plane frame. A fixed base support condition was imposed on the model by restraining all the degrees of freedom of the nodes at the base of the columns and restraining the translational degrees of freedom of

the first-panel tension strip nodes that are at the base of the wall. The columns were continuous up to the top beam centroidal axis and all beam-to-column connections were modelled as rigid. The angle of inclination for the tension field of each individual infill plate was calculated as per Clause 20.3.1 of CAN/CSA S16-01 (Equation 2.3). The angles vary from 41.8º to 43.5º, but the mean value of 42.4º is used for all panels. The width and spacing of the pin-ended tension-only strips for each panel, based on ten strips per panel, were also calculated to determine the area of each strip. For the detailed model, each panel is treated separately in distributing the strips. This results in a staggered tension strip formation, as illustrated in Figure 3.2, where the tension strips on either side of an intermediate beam do not necessarily meet at a common node.

Two static load cases were defined based on the test specimen loading patterns. The first was a gravity load case, which consisted of the steel plate shear wall self-weight and vertical loads of 720 kN that were applied to the top of each column of the test specimen. The second load case consisted of horizontal loads of equal magnitude that were applied to one column at the beam top flange at each of the four levels, as in the test. This lateral loading arrangement was selected to simulate the location of the inertial forces induced by floor masses. The pushover analysis implements displacement control for the lateral pushover case, while maintaining equivalent horizontal load magnitudes at each storey. In order to model accurately the location of the lateral force acting at the top flange of the top beam, a stiff "mast" was extended to the top flange of the W530×82 beam, as shown in Figure 3.2.

3.3 Panel Zones

As shown by the shaded region in Figure 3.3, the panel zone is the area of the column that is bounded by the depth of the connecting beam ($d_c \times d_b$) for a moment-resisting connection. It has been demonstrated that the panel zones can provide a ductile fuse for the dissipation of seismic energy in moment frames, thereby reducing the demand on the frame during an earthquake (Krawinkler and Popov 1982, Popov *et al.* 1986). However, Driver *et al.* (1998a) observed that in their steel plate shear wall test specimen inelastic deformations in the panel zones tended to remain small throughout the duration of lateral

loading—and the regions remained essentially elastic up the peak wall capacity—since the primary ductile fuses were the infill plates.

From the node at the connection of the beam and column elements, hereafter referred to as the "connection node," the panel zone extends to half the depth of the column for beam elements and half the depth of the beam, on either side of the connection node, for column elements. The nodes at the periphery of the panel zones have been termed herein the "panel nodes" for convenience of reference, as shown in Figure 3.3. In the strip model, line elements within the panel zones do not accurately represent the rigidity of the connection region, which has a finite depth and width. To approximate the actual behaviour of a panel zone that is expected to remain predominantly elastic, it is reasonable that the beam and column elements within the panel zone be assigned an elastic modulus that is large enough so as to make the elements within the panel zone effectively rigid. A modulus of elasticity of 200 000 GPa, or 1000 times the nominal modulus of elasticity, was found to be sufficient and was used for the line elements within the panel zone in the detailed model.

3.4 Plastic Hinges

Plastic hinges are required to model accurately the inelastic behaviour of steel plate shear walls. Although flexural plastic hinges in frame members have a finite length that is often taken to be approximately equal to the member depth, it is more convenient to model a plastic hinge as occurring at a discrete point. Since the panel zone is assumed to be an effectively rigid area, the nodes representing the flexural plastic hinges are located at a distance of half of the member depth from the boundary of the panel zone. These nodes are referred to herein as "hinge nodes," as illustrated in Figure 3.3. Similarly, a flexural hinge is placed at a distance of half the column depth from each column base support node. To simulate the yielding of the infill plate, an axial hinge is placed at any discrete point along each of the pin-ended tension strips. For the model analysed, the axial hinges were placed at the midpoint of each strip.

User-defined moment vs. rotation curves describe the behaviour of the flexural hinges in the beam and column elements, while force vs. deformation curves describe the

behaviour of the axial hinges in the tension strips. Each hinge is considered to be rigid until yielding commences at that location and up to this point all deformations occur elastically in the line elements between the hinges. Thereafter, the overall behaviour of the wall is influenced by a combination of distributed elastic member deformations and discrete hinge deformations as specified by the hinge behaviour definitions.

For the flexural hinges, moments are calculated for the following extreme–fibre strains, assuming a linear strain gradient through the member cross-section: yield point, onset of strain hardening, strain at ultimate stress, and rupture. (As the members of the frame have stocky webs and flanges, the effects of local buckling were neglected. However, reduced moments could readily be selected at large strains for less stocky sections.) Curvatures associated with each of these strain levels are determined and, assuming a hinge length equal to the member depth and constant curvature within the hinge length, the corresponding discrete hinge rotations are established. Using these calculated values, a quadrilinear moment vs. rotation hinge curve is obtained, as shown in Figure 3.4(a). Table 3.2 shows the flexural hinge values input into the detailed model based on the Driver *et al.* (1998a) specimen with moments normalised by the plastic moment of the cross-section, generally considered to be the peak capacity of a Class 1 or Class 2 cross-section for design. Note that the hinge rotations are zero until point B (corresponding to first yield of the extreme fibre of the cross-section) is reached and the elastic deformations of the member are distributed along its length. All flexural hinges are symmetric under moment reversals. Beam flexural hinges describe the flexural behaviour of the member, which is dominant, and are assumed to be independent of any coincident axial force, while column flexural hinges describe not only the flexural behaviour, but also the interaction between the axial load and moment, thus reducing the specified moments accordingly. There are several methods for describing the axial force–moment interaction. For the detailed model, the interaction is described as follows (FEMA 356):

$$M_{pc} = 1.18ZF_y\left(1-\frac{P}{A_cF_y}\right) \le ZF_y \tag{3.1}$$

where F_y is the column yield stress, P is the axial load, and Z is the column plastic modulus. The axial force vs. deformation curve for the hinge in a tension strip is defined to correspond with a multilinear approximation of the stress vs. strain curve of the plate material using the same reference strains specified above for the flexural hinges. While it is common practice to model the strip material as being elasto-plastic for simplicity, in the case of the detailed model strain hardening is included in an attempt to obtain a more accurate prediction of the nonlinear behaviour of the steel plate shear wall. The generalised axial hinge curve is shown in Figure 3.4(b) and Table 3.3 shows the values that were input into the detailed model, with the axial forces and the hinge elongations normalised, respectively, by the force that causes yielding in the strip and the elongation of the entire member at first yield. Again, it is to be noted that the axial hinge is rigid until Point B is reached, with the elastic deformations of the member being distributed along its length. All axial hinges for the tension strips contain no compressive capacity to simulate the occurrence of buckling of the relatively thin infill plate. That is, for any member experiencing axial shortening, an axial force of zero is assigned.

3.5 Compression Strut

Driver *et al.* (1997) noted that there were certain phenomena present in steel plate shear wall behaviour that are not captured by the strip model. These phenomena could explain, in part, the tendency of the strip model to underestimate both the elastic stiffness and the ultimate capacity. The strip model neglects the small contribution to the stiffness and strength of the infill plate from compressive resistance, which may be significant in the corner regions where the effective length of the plate under compression is small. Moreover, the vertical tension field arising from the overturning moment, which forms in the infill plate near the column on the tension side of the wall is not taken into account. In the detailed model, a pin-ended compression strut is used to account for these observations in an approximate manner with a minimum of modelling effort. The compression strut is a truss element that extends from corner to corner of each panel and is oriented in the opposite diagonal direction to that of the tension strips, as shown in Figure 3.2. Assuming that the whole plate contributes to the compressive resistance, the area of the strut is determined using Equation 2.2 which is based on the equivalent brace

method (Thorburn *et al.* 1983). The use of this approach implies that a full diagonal compression field forms, but it should be emphasised that the compression strut as described above does not physically develop during the lateral loading of a steel plate shear wall. The use of the compression strut is a semi-empirical method of modelling the observed additional contributions to the overall strength of the steel plate shear wall. Although the compression strut not only represents the compression that develops in the corners of the infill plate, but rather a complex array of phenomena that are not captured by the tension–only strip model, these phenomena are referred to in subsequent chapters as the "compression field" for simplicity.

A rigid–plastic axial hinge is placed at a discrete point anywhere along the compression strut to simulate the sudden "buckling" of the strut once its capacity, or limiting stress, has been achieved. For the analyses conducted, the hinge was placed at the midpoint of the strut. The behaviour of the compression strut hinge is described in Table 3.3, where P_y in this case is actually the force at the limiting stress and the values of Δ/Δ_y that occur after Point B are arbitrary since the curve is horizontal. The compression strut axial hinge contains zero tensile capacity. Based on empirical observations of Kulak *et al.* (2001) that consider both the capacity of the wall and energy dissipation characteristics in cyclically loaded models, the limiting stress of the compression strut, F_{yCS}, was set at 8% of the tensile yield strength of the infill plate, F_{yPL}. Although the value of the limiting stress selected is based on the behaviour of the test specimen of Driver *et al.* (1997; 1998a), its use for other test specimens is evaluated in Chapter 5. A sensitivity analysis of F_{yCS} was conducted to determine a valid range of values, the results of which are discussed in Chapter 4.

3.6 Deterioration of Infill Plate

During cyclic loading of a steel plate shear wall test specimen (Driver *et al.* 1998a), tears in the infill plate that arose principally due to kinking of the stretched plate during load reversals were observed to have formed and propagated primarily in the corners of the infill plates. The tearing of the infill plate contributed to the gradual deterioration in the strength of the specimen, which occurred beyond a first-storey displacement of 42.5 mm, as shown in Figure 3.1. A means of modelling this deterioration is desired so that a

maximum strength can be defined, followed by a declining branch of the pushover curve. These features help to characterise the ductility of the steel plate shear wall, a property that is not assessed by previous models.

It was observed (Driver *et al*. 1998a) that the corner tearing by the end of the test extended over a width approximately equal to that of a single strip (when the customary ten strips per panel are used). Therefore, a discrete axial hinge that includes the effects of deterioration is provided only for the two tension strips that intersect the frame closest to the opposite corners of the steel plate shear wall panel, as shown in Figure 3.2. (It should be noted that for certain geometries, the same strip could be closest to the corner at each end, in which case only one strip with a deterioration hinge is provided in the panel.) The deterioration axial hinge was input in these members in place of the typical axial hinge described previously.

Based on empirical observations by Driver *et al.* (1998a), the behaviour of the deterioration axial hinge is defined in Table 3.3. Initially, the behaviour is identical to that of the typical axial hinge. It was found that significant tearing of the bottom infill plate began in the corners at a strip elongation of approximately five times the yield value (*i.e.*, the hinge deformation at Point C is $4\Delta_y$ and the total member deformation at Point C of the deteriorating strip is $5\Delta_y$) and the rate of deterioration was estimated based on the rate of tear propagation observed during the test. By the end of the test, since the tears extended across a width of plate approximately equivalent to the width of one strip in the ten-strip model, the capacity of the deterioration hinge is taken to zero. Although this deterioration behaviour is recognised to be a function of the cyclic loading for this specific specimen, it is considered to be a severe case and therefore would be expected to be conservative for most applications. As in the case of the typical tension strip hinges, the deterioration axial hinge has no compressive capacity.

3.7 Detailed Model Analysis and Results

3.7.1 Pushover Analysis Overview

A pushover analysis is a nonlinear analysis method that loads a structure monotonically to a specific load or displacement level while monitoring aspects of the

response such as the base shear and the deflection of a specified node. A pushover analysis takes into account material nonlinearities, thus enabling the engineer to examine both elastic and post-yield behaviour. Geometric nonlinearities, such as P-Δ behaviour, are generally accounted for due to the large deformations that can arise. Unless a sophisticated finite element analysis package is used, the inelastic behaviour would typically be concentrated in pre-defined locations where plastic hinges are expected to form.

In SAP2000®, the base shear and deflection results are recorded at user-specified increments during a pushover analysis to obtain the inelastic behaviour of the modelled structure during loading. Steps during certain significant events, such as yielding or the unloading of a hinge, that do not necessarily occur at the specified increment are also saved. Defining a small increment size can prevent the occurrence of anomalies, such as load spikes, from appearing in the pushover curve. A load spike, which manifests itself as a vertical rise or drop in load on the pushover curve, may occur when the analysis goes from one specific equilibrium path to another. As well, the input parameters of a pushover analysis should be set to ensure that enough points are saved to represent the important features of the pushover curve adequately.

Some hinge behaviours have sharp drops in load, which can cause numerical instabilities in a pushover analysis. SAP2000® implements three different criteria for unloading hinges in an attempt to solve this potential for instability. “Unload Entire Structure” is the first method. When a hinge reaches a region of negative stiffness, the strains can either increase or decrease. If the strains increase, the load continues to be applied. If the strains decrease, the load is partially removed from the entire structure until the hinge is unloaded to the point on the hinge curve at the end of the negative slope, at which point the load is then reapplied to the structure. “Apply Local Redistribution” is the second method. When a hinge reaches the negative-sloped portion of the curve, a local redistribution of loads is applied to the element containing the hinge and not to the entire structure. A temporary, localised, and self-equilibrating internal load is applied that unloads the element, which in turn causes the hinge to unload. When the hinge has been fully unloaded, the temporary load is

reversed, thus transferring the removed load to the neighbouring elements. "Restart Using Secant Stiffness" is the third method. When a hinge reaches the negative-sloped portion of its response curve, all hinges that have become nonlinear are re-formed using secant stiffness properties and the pushover analysis is restarted. Regardless of the method implemented, when a frame hinge unloads, the pushover analysis may save negative increments in the monitored displacement while the structure is trying to redistribute the load, which results in a jagged pushover curve. A smooth curve can be obtained by saving only the positive increments during the analysis.

3.7.2 Pushover Analysis of the Detailed Model

The parameters of the detailed model described above were applied to the Driver *et al.* (1998a) specimen and a pushover analysis was performed. From this analysis, a pushover curve of the base shear vs. first-storey lateral displacements was obtained and compared to the envelope curve of the test specimen hysteresis behaviour (Figure 3.1). First-storey displacements and shears were monitored since they tend to be the largest in a multi-storey structure under this type of loading. However, deflections from any storey can be recorded and plotted against the base or storey shear.

The pushover analysis for the detailed model consists of two static load cases, as described in Section 3.2. First, the gravity loads and self-weight are fully applied to the modelled structure using load control. Starting from the resulting deflected shape, the lateral load pattern is then applied using deflection control. A node located on the "lee" column at the point of the top flange of the first-storey beam (for consistency with the measurement location in the test) was monitored for deflections in the horizontal direction. The analysis stopped when the first-storey node reached 76 mm, which was the maximum first-storey lateral deflection reached by the test specimen. To account for the sharp drop in load-carrying capacity that is described in the behaviour of the deterioration axial hinge, the "Apply Local Redistribution" hinge unloading option was selected and only the positive increments were saved during the

analysis. A P-Δ analysis was implemented during the pushover analysis to account for geometric nonlinearities.

3.7.3 Pushover Analysis Results

Figure 3.5 shows the comparison between the specimen envelope curve and the detailed model pushover curve. The model provides an excellent representation of the elastic portion of the envelope curve, overestimating the initial stiffness by about 5%. (The initial stiffness of the specimen was determined by selecting a base shear value near the initial yield point and dividing it by the corresponding first-storey lateral deflection, from which a value of 343 kN/mm was calculated.) There is a very small kink in the elastic portion of the detailed model curve at a deflection of 0.7 mm, which is due to the early buckling of the compression strut in the bottom storey. However, this irregularity is barely discernible in the figure is considered negligible. The detailed model pushover curve overestimates the specimen strength slightly at a point just beyond the occurrence of initial yielding and underestimates the ultimate strength of the specimen by 2.9% (2991 kN for the detailed model vs. 3080 kN for the specimen). The peak of the first-storey pushover curve generated by the detailed model occurred at almost the same deflection as the specimen (44.3 mm for the detailed model vs. 42.5 mm for the specimen). The declining curve of the model descends at approximately the same rate as the specimen. At a very large first-storey deflection, the deterioration of the model ceased and was followed by a very slight gain in strength. This is attributed to the fact that only two tension strips deteriorate. Because this occurred at storey deflections far exceeding values that would be considered acceptable for design, further refinement of the deterioration behaviour was considered unwarranted. Despite this slight deviation from the specimen envelope curve, the pushover behaviour of the detailed model is in very good agreement with the test specimen behaviour.

For comparison purposes, a model of the Driver *et al.* (1998a) specimen was generated using the strip model recommended in the Canadian steel design standard, CAN/CSA S16-01. Since specific details about how to implement the strip model—particularly with respect to the incorporation of inelastic behaviour—are not provided

in the standard, methods incorporated in recent models presented in the literature are utilised. The strip model, called the "basic" strip model here to distinguish it from the proposed model, was generated with line elements representing the columns and beams that were located at their respective centroids. Each infill plate was discretised into ten equally spaced strips and oriented at the calculated angle of inclination of the tension field (Clause 20.3.1, CAN/CSA S16-01). To represent inelastic behaviour, all hinges were assumed to behave bilinearly and the flexural hinges were located at the connection nodes or base support nodes for the case of hinges at the column base. Axial hinges for the tension strips were located at the midpoint of each strip. For the case of the basic strip model, the panel zones were not stiffened, no deterioration was modelled, and no compression strut provided. As can be seen in Figure 3.5, the curve from the basic strip model underestimates the initial stiffness by 10% and the peak capacity (*i.e.*, taken at the lateral deflection at which the peak occurs in the test curve) by 12%. Although the basic strip model is conservative for use in design in terms of both elastic stiffness and strength, the detailed model is more accurate in predicting the elastic and inelastic behaviour of the steel plate shear wall and it characterises the ductility of the specimen by means of the descending branch. (It should be noted that the basic strip model curve as presented in Figure 3.5 is not identical to that presented by Driver *et al.* (1998b). Because mainstream commercial pushover software was not available at the time that research was conducted, an elastic structural analysis program was used and inelastic behaviour was implemented in an approximate step-by-step manner. In modelling the column hinges, interaction between the axial load and moment was accounted for in determining the onset of inelastic behaviour (as in the current research), but although this established a limiting hinge moment, the axial force was permitted to increase thereafter.)

3.8 Summary

The strip model for analysis of steel plate shear walls, originally developed by Thorburn *et al*. (1983), was refined to create a detailed model in order to obtain a more accurate prediction of the nonlinear behaviour of steel plate shear walls. The modifications were based largely on experimental observations of test specimens during loading. The panel

zone was stiffened to reflect the small inelastic deformations observed during the loading of a steel plate shear wall specimen. Multilinear rigid-inelastic flexural and axial hinges, generated from the stress vs. strain curves for the material of each member and neglecting local buckling, were used to model the pushover behaviour of steel plate shear walls. The flexural hinges (columns and beam) were located a distance of one-half the member depth from the boundary of the panel zone and the axial hinges were located at a discrete point along the length of the tension–only strip (for the case of this analysis, an axial hinge was located at the midpoint of each strip.) A compression–only diagonal strut was modelled to represent the small contribution of compressive resistance in each infill plate as well as other phenomena not captured by the representation of a continuous plate by a series of discrete tension strips. A bilinear axial hinge, which defines the limiting stress of the strut ($F_{yCS} = 0.08 \times F_{yPL}$), was located at a discrete point along the length of the strut. The tearing of the infill plate corners was modelled using deterioration axial hinges that were located on the strips that came closest to the corners of each panel.

A pushover analysis was performed on the detailed model of the four-storey specimen tested by Driver *et al.* (1998a) using a conventional structural engineering software package. The pushover curve generated by the detailed model was found to be in very good agreement with the test specimen envelope curve, thus demonstrating that the detailed model can be a very accurate tool for predicting the nonlinear behaviour of steel plate shear walls. It is recognised that some of the aspects of the detailed model were developed using observations from the same test specimen. However, the primary features that were calibrated using empirical data—*i.e.*, the compression strut and the deterioration hinge—are included in the validation study of a simplified version of the model, presented in Chapter 5.

Table 3.1 - Material Properties of Test Specimen (Driver *et al.* 1997; 1998a)

Member	Elastic Modulus (MPa)	Static Yield Stress (MPa)	Static Ultimate Stress (MPa)	Rupture Stress (MPa)	Yield Strain (%)	Hardening Strain (%)	Ultimate Strain (%)	Rupture Strain (%)
Panels 1 & 2	208 800	341	456	367	0.175	2.62	20.1	34.2
Panel 3	210 900	257	344	277	0.134	2.44	20.0	42.5
Panel 4	203 100	262	375	303	0.145	1.53	17.7	34.1
W310×118	203 000	313	482	402	0.169	1.41	15.5	26.3
W310×60	203 900	332	478	431	0.191	1.76	16.8	26.2
W530×82	206 100	349	493	421	0.204	1.85	15.5	26.9

Note: 50 mm gauge length used in ancillary tests

Table 3.2 - Flexural Hinge Definitions

Hinge	A*		B		C		D		E	
	M/M_P	θ (rad)	M/M_P	θ (rad)	M/M_P	θ (rad)	M/M_P	θ (rad)	M/M_P	θ (rad)
W310×60 Beam	0	0	0.902	0	0.999	0.035	1.402	0.336	1.402	0.524
W530×82 Beam	0	0	0.874	0	0.999	0.037	1.359	0.310	1.359	0.538
W310×118 Column	0	0	0.897	0	0.999	0.028	1.484	0.310	1.484	0.526

*Refer to Figure 3.4(a)

Table 3.3 - Axial Hinge Definitions

Hinge Type	A*		B		C		D		E	
	P/P_y	Δ/Δ_y	P/P_y	Δ/Δ_y	P/P_y	Δ/Δ_y	P/P_y	Δ/Δ_y	P/P_y	Δ/Δ_y
1st & 2nd Infill Plate	0	0	1.00	0	1.00	15.0	1.34	114.9	1.07	195.4
3rd Infill Plate	0	0	1.00	0	1.00	18.2	1.34	149.2	1.08	317.2
4th Infill Plate	0	0	1.00	0	1.00	10.6	1.44	122.1	1.16	235.2
Compression Strut	0	0	-1.00	0	-1.00	-5.0	-1.00	-20.0	-1.00	-500.0
Deterioration Hinge	0	0	1.00	0	1.00	4.0	0	9.0	0	16.0

*Refer to Figures 3.4(b) and (c)

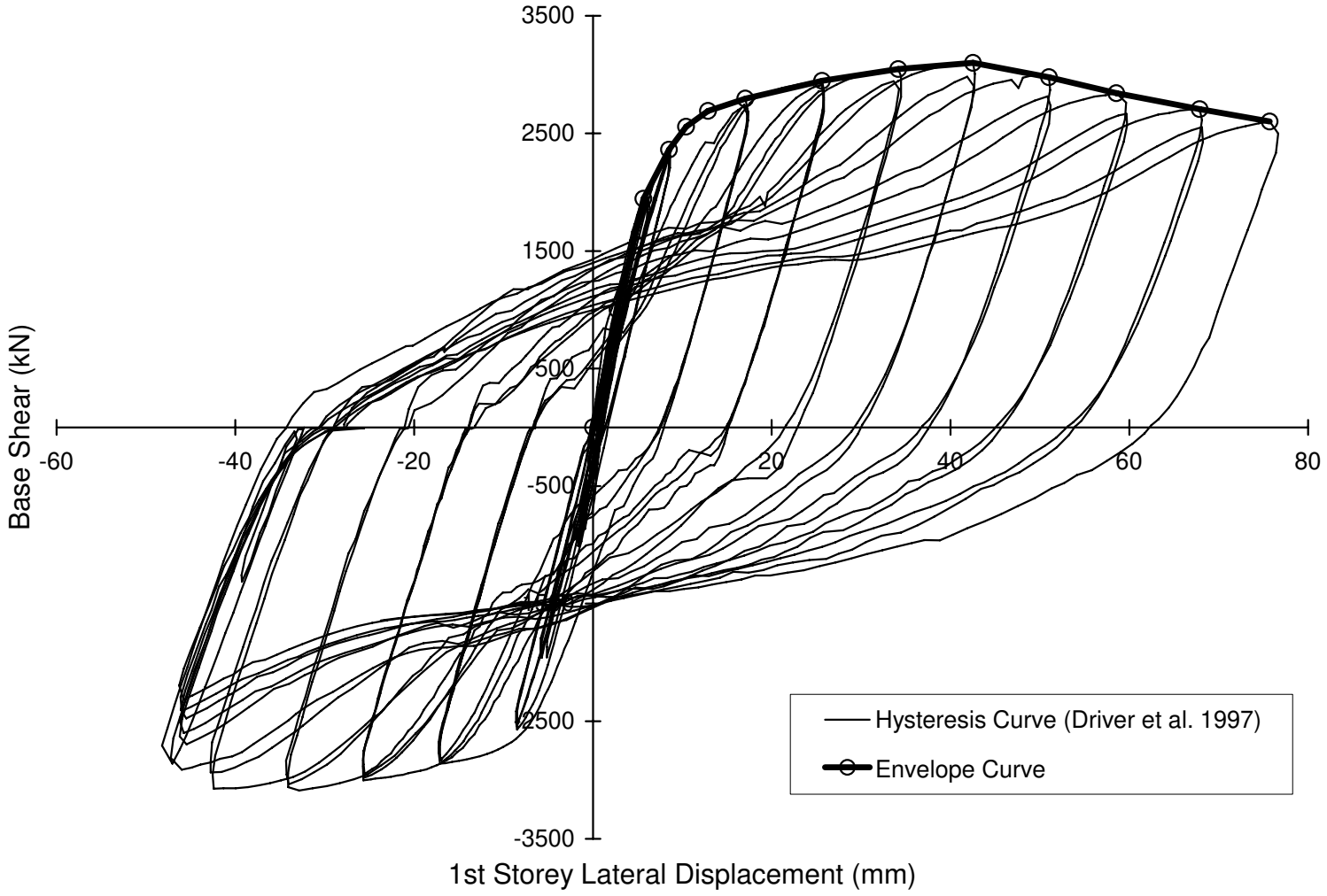

Figure 3.1 - Hysteresis and Envelope Curve for Driver *et al.* (1998a) Specimen

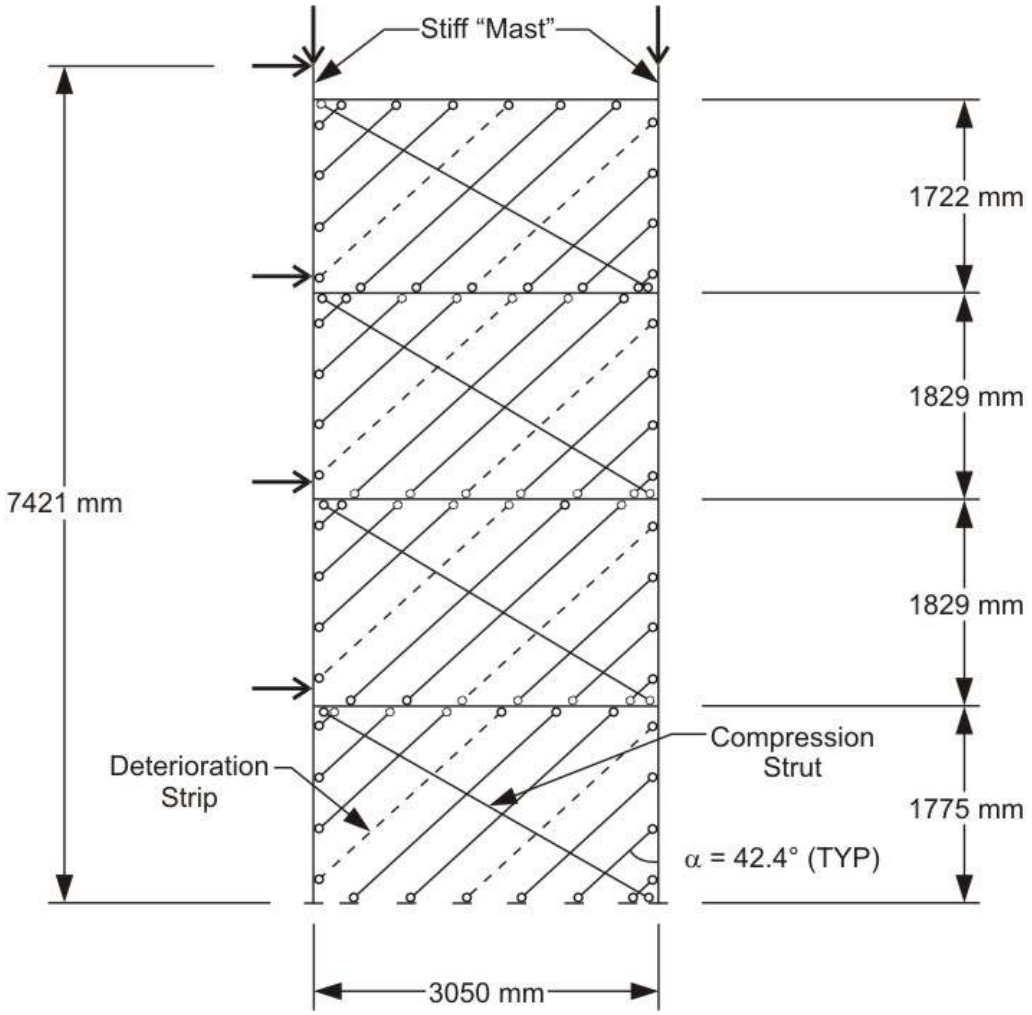

Figure 3.2 - Geometric Arrangement of Detailed Model

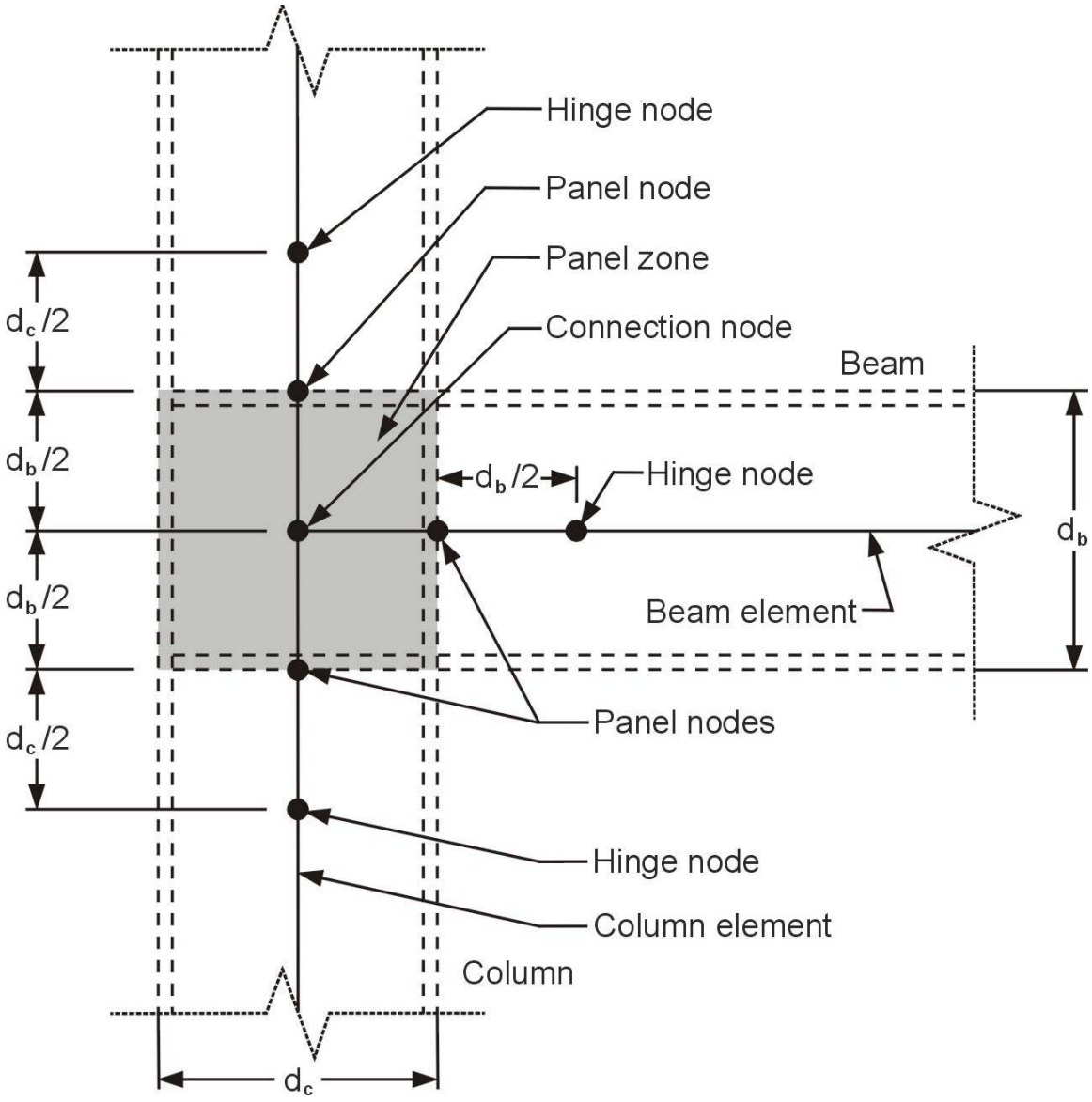

Figure 3.3 - Typical Frame–Joint Model Detail for Rigid Connections

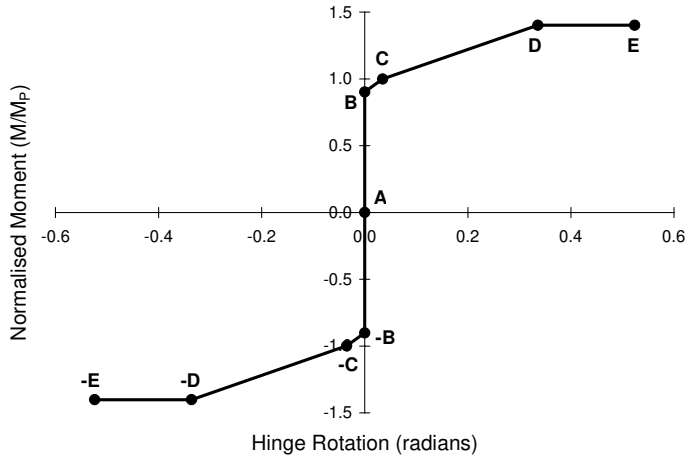

(a)

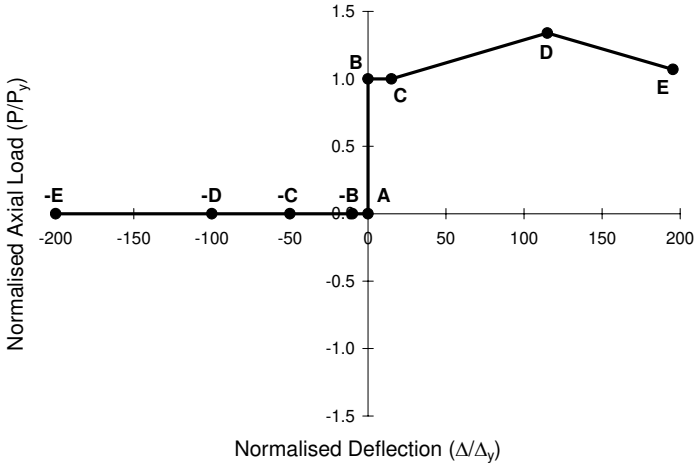

(b)

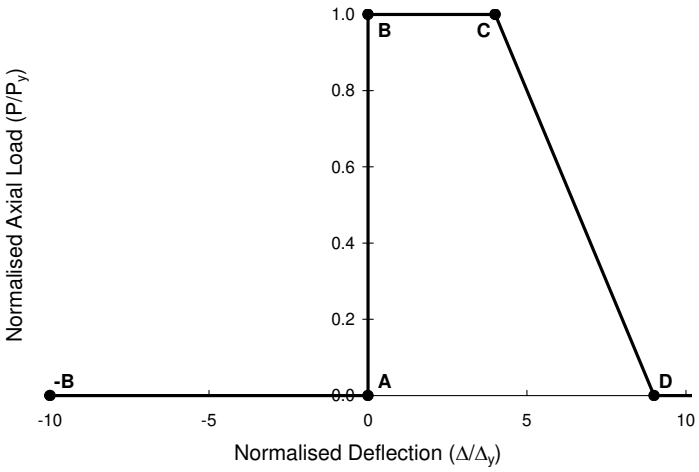

(c)

Figure 3.4 - Typical Behaviour for (a) Flexural Hinges, (b) Axial Tension Strip Hinges, and (c) Deterioration Hinge

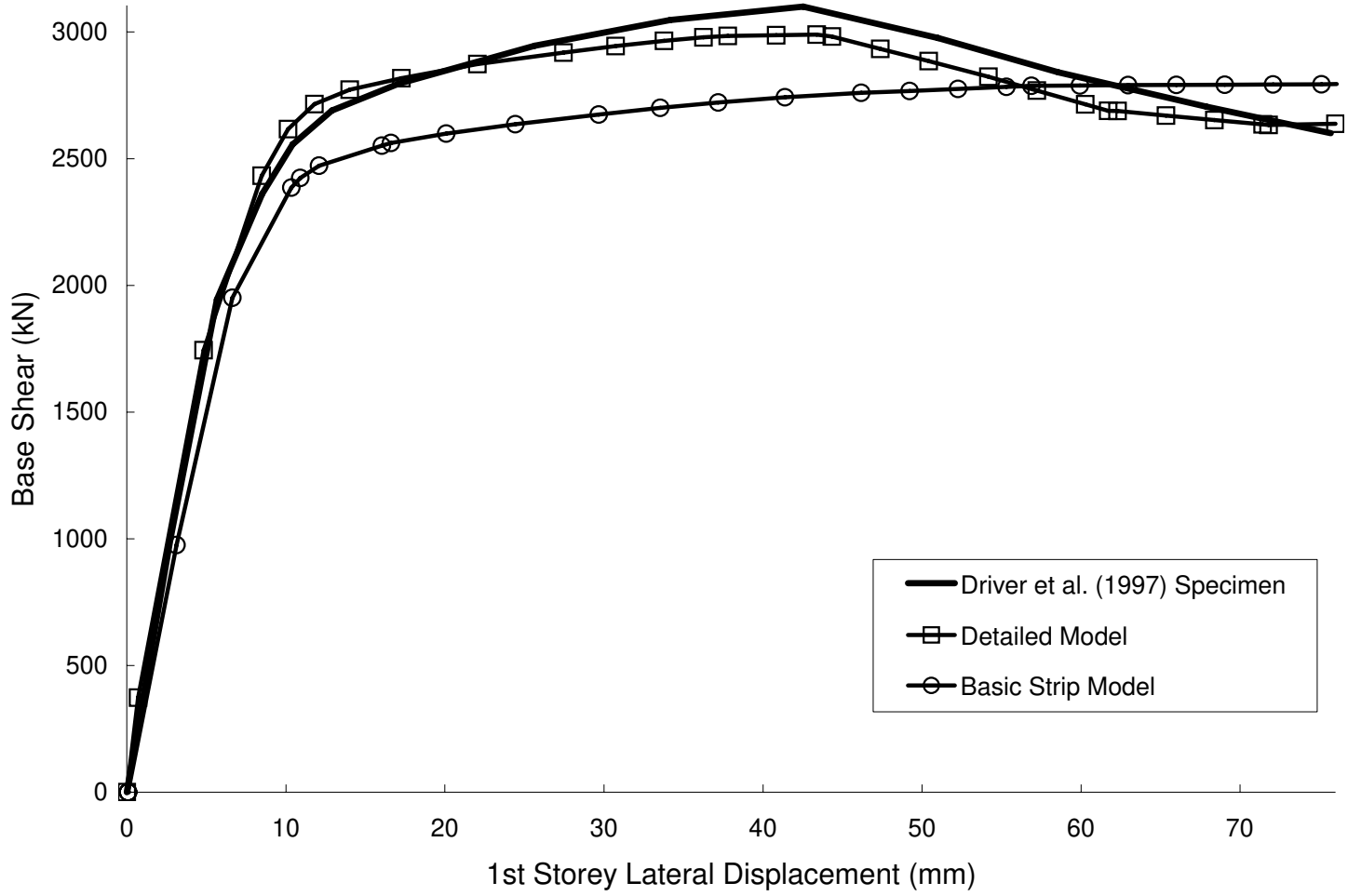

Figure 3.5 - First Storey Response Curves for Detailed Model, Basic Strip Model and Driver *et al.* (1998a) Specimen

4. THE SIMPLIFIED MODEL

4.1 Introduction

It was demonstrated in Chapter 3 that the detailed model predicts the nonlinear behaviour of the Driver *et al.* (1998a) specimen with a high degree of accuracy. However, if the model can be made simpler to generate, while still retaining a good degree of accuracy, then the simplified model would be desirable for use as a design tool. This chapter examines the various parameters of the detailed model more closely to determine their effect on the accuracy of the model as compared with modelling efficiency. The detailed model is the base model from which models with various simplifications are created. Each such model undergoes a pushover analysis and the resulting pushover curve is compared to that of the detailed model and the envelope of the test specimen hysteresis curve. The effect of simplifying each parameter on the accuracy of the solution is then assessed against the accompanying savings in modelling effort. Those simplified parameters that result in a more efficient model to generate, while not adversely affecting the accuracy of the model significantly, are retained as part of the simplified model for design. Therefore, the model that demonstrates the best balance between accuracy and modelling efficiency is selected.

A brief sensitivity analysis is performed on the selected model to determine a range of values for the limiting stress of the compression strut. In addition, frame forces are extracted from the pushover analysis of the selected model and compared to those of the Driver *et al*. (1998a) test specimen to determine the accuracy of predicting the response of the boundary members. The simplified model is validated using the results of other experimental programs and is used for conducting a detailed parametric study in Chapters 5 and 6, respectively.

4.2 Frame–Joint Arrangement

As it pertains to this report, the frame–joint arrangement describes the geometric and material properties of the panel zone region and the locations of the plastic flexural hinges in the model. Modelling the joints as described in the detailed model (Chapter 3)

and illustrated in Figure 4.1(a) can be cumbersome and time consuming. Therefore, three alternative frame–joint arrangements were modelled for comparison. The resulting pushover curves were compared to the Driver *et al.* (1998a) envelope curve and the detailed model pushover curve.

The first revised frame–joint arrangement, as seen in Figure 4.1(b), relocated all the flexural plastic hinges to the panel nodes and the modulus of elasticity of the members within the panel zone remained at 200 000 GPa, representing an effectively rigid panel zone. The modelling benefit as compared to the detailed model is the elimination of one node on each side of each frame joint. For the case of the second revised frame–joint arrangement, shown in Figure 4.1(c), the flexural hinges are relocated as in the first, but the members within the panel zone are assigned the measured moduli of elasticity (listed in Table 3.1) so that the same material model can be used throughout each column or beam. For the third revised frame–joint arrangement, all hinges are relocated to the connection node and the measured moduli of elasticity are input for all frame members, as illustrated in Figure 4.1(d). Thus, for this particular case, no additional nodes are required to bound the panel zone or locate the plastic flexural hinges. For all of the above models, the flexural hinges near the base of the column remain at half the column depth from the base support node since it was found that numerical instabilities occurred when the column hinges were located at the base. It should be noted that usually the measured modulus of elasticity is not available during the design process and the nominal modulus would be used in its place.

Figure 4.2 shows the resulting pushover curves when using the three alternative joint models described above, along with that of the detailed model and the test specimen envelope curve. For the case of the model with plastic hinges located at the edges of the stiffened panel zone (Figure 4.1(b)), the analysis ceased to run right after the ultimate strength was obtained due to numerical instabilities. Although this arrangement provides a good estimation of the capacity of the shear wall and careful refinements to the convergence criteria may have led to a more complete curve, this was not pursued since a further simplification to the joint arrangement provided excellent results. The curve for the model with the plastic hinges located at the connection nodes (Figure 4.1(d)) agrees

very well with the initial stiffness of the specimen envelope curve and underestimates the ultimate strength by 6.7% (2873 kN for the model vs. 3080 kN for the specimen.) The curve for the model with the plastic hinges located at the edges of the panel zone and using the measured moduli of elasticity (Figure 4.1(c)) shows the most favourable results. The pushover curve agrees very well with the initial stiffness of the specimen, underestimates the ultimate capacity by only 4.0% (2957 kN), and deteriorates at almost the same rate as the specimen. Moreover, the ultimate capacity obtained using this model is only 1.1% below that of the detailed model. While the frame–joint arrangement of Figure 4.1(d) is a viable alternative, the curve for Figure 4.1(c) is more accurate in predicting the inelastic behaviour of steel plate shear walls with little additional modelling effort. Therefore, for the case of the simplified model, all frame member elements within the panel zone shall utilise the measured, or nominal, modulus of elasticity and the flexural plastic hinges shall be located at the edges of the panel zone. The only exception to this arrangement is that the flexural column hinges near the base remain at half the column depth from the base support node.

4.3 Crosshatching of Diagonal Tension Strips

In the strip model proposed by Thorburn *et al.* (1983), each panel of a steel plate shear wall is treated separately when calculating both the angle of inclination and the resulting spacing of the tension strips since they are dependent on properties that may vary from storey to storey. This method generally results in a staggered alignment of tension strips in adjacent storeys, as was seen in Figure 3.2 where the detailed model utilised this method with ten equally spaced tension strips for each panel that were oriented at the average angle of inclination of the infill plate tension field. A simplification suggested by Timler *et al.* (1998), herein referred to as "crosshatching," was investigated in an attempt to reduce the number of required nodes further. The crosshatching method uses the average angle of inclination and spaces the tension strips at equal intervals so that strips in panels above and below share common nodes at the beam. Using a spreadsheet, a design engineer can generate the nodes for a steel plate shear wall model rapidly using the crosshatched layout. (Should conditions change drastically in adjacent storeys, the staggered layout can still be used.)

The detailed model was amended using the crosshatching technique, as shown in Figure 4.3. The tension strips were spaced such that ten equally spaced strips would represent the bottom panel. Depending on the geometry of the structure and the value of the average angle of inclination, each panel may have more or fewer than ten tension strips. Cases where some storeys have fewer than ten strips may require reassessment of the selected strip spacing. In some instances, the strips can be very short, as in the case of the top panel.

Figure 4.4 demonstrates that there is little difference in pushover behaviour between the crosshatched and the detailed models. The crosshatched model agrees well with the initial stiffness of the specimen and underestimates the ultimate capacity by about 3% (2989 kN). The peak for the crosshatched model occurs slightly after that for the detailed model (46.5 mm for the crosshatched model vs. 43.4 mm for the detailed model) and deteriorates at almost the same rate as the specimen. Therefore, due to the savings in modelling effort it provides the crosshatching method for defining the tension strip arrangement is incorporated into the simplified model.

4.4 Bilinear Plastic Hinges

The effect of using bilinear hinges instead of multilinear hinges in the beams, columns, and tension strips was also studied as a means of simplifying the modelling process. Since flexural hinge rotations are often defined in terms of chord rotations over the element length, and since the individual element lengths vary in the frame of a steel plate shear wall model depending on the locations of the nodes required at the ends of the tension strips, many different hinge definitions may be needed to achieve the desired model. However, if the plastic hinge behaviour is modelled as rigid–perfectly plastic (with the elastic member behaviour being captured outside the hinge location), only the plastic moment needs to be specified in the hinge definition, resulting in a single hinge definition per member cross-section. Thus, all hinges as described in the detailed model were modified to be bilinear. Although the objective was to incorporate rigid–perfectly plastic hinge behaviour, due to numerical instabilities encountered the column hinges were defined with a very small post-yield slope (0.0002:1) in order to achieve convergence, but the effect of this is considered negligible. In the case of the tension

strips, it was found that strain hardening did not occur during the detailed model pushover analysis, making this simplification for the axial hinges logical. Table 4.1 shows the input values for the bilinear flexural beam and column hinges and Table 4.2 shows those for the bilinear axial hinges used in the tension strips. (Note that although the curves are bilinear, they have still been defined in four segments simply to facilitate interpretation of the output that can indicate the location on the hinge curve at any desired point in the loading history. Different points can be specified on the same curves with identical results.) The flexural hinges are symmetric under moment reversals, while the axial hinges possess no compressive capacity. It was found that although they are simpler to implement, the effect of using bilinear hinges was small and they are therefore included in the simplified model. The impact of this simplification is explored in the simplified model analysis described later.

4.5 Deterioration Hinge and Compression Strut

The effects of the presence of the deterioration hinges in the tension strips that intersect nearest the panel corners and the compression strut were also investigated independently. In one model, all the deterioration hinges in the detailed model were replaced with typical multilinear tension strip hinges, while in another model, the compression struts were removed from the detailed model while maintaining the deterioration behaviour of the tension strips intersecting nearest the corners. Figure 4.5 shows the pushover curves of the above models compared to that of the detailed model and the envelope curve of the specimen. When no deterioration of the tension strips is modelled, as expected the resulting curve follows along the ascending path of the detailed model, but instead of attaining a peak and descending steadily, the curve continues to ascend at a small rate. Since deterioration of the model gives the design engineer an idea of both the ultimate capacity and ductility of the shear wall, the deterioration hinges shall remain part of the simplified model. As discussed in Chapter 3, the deterioration behaviour calibrated to the response of this particular test specimen is considered to be severe and therefore is likely to be conservative for assessing pushover behaviour of typical steel plate shear walls.

The model with no compression strut results in an initial stiffness only slightly lower than that of the test specimen, but it underestimates the ultimate capacity of the specimen by

8.3% (2825 kN). Since applying the compression strut to a model is a relatively simple process and the resulting gain in strength is considerable and improves the accuracy of the model while remaining on the conservative side for design, the compression strut shall also remain a part of the simplified model.

4.6 Pushover Analysis Results for the Simplified Model

The simplifications that were found to reduce modelling effort while maintaining good accuracy in the pushover curve—which include a simpler frame–joint arrangement, crosshatching the tension strips, and bilinear rigid–plastic hinges—were applied to the detailed model to create the simplified model. A pushover analysis was performed using the simplified model with the identical loading details as those described for the detailed model. Figure 4.6 shows the resulting pushover curve and compares it to the pushover curve of the detailed model and the envelope curve of the specimen. The simplified model provides an excellent representation of the initial stiffness of the test specimen—slightly overestimating it by about 1%—and predicts the ascending behaviour of the specimen near the knee of the curve even more accurately than the detailed model (the detailed model curve slightly overestimates the capacity at the initial yield, while the simplified model curve is nearly identical to that of the specimen at this location.) The simplified model underestimates the ultimate strength of the specimen by about 5.3% (2916 kN). The peaks of the first–storey pushover curves generated by the two models occur at almost the same deflection as that of the specimen envelope curve (44.3 mm for the detailed model, 42.5 mm for the simplified model, and 42.5 mm for the test specimen). The declining curve of both models is similar to that of the test specimen, although the simplified model leads to a somewhat more conservative deterioration rate. The pushover curve of the basic strip model, which was described in Chapter 3, is also compared to the simplified model and was found to be less accurate in predicting the nonlinear behaviour of the specimen than the simplified model, as seen in Figure 4.6.

A comparison of the detailed and simplified models indicates that little accuracy is lost with the simplified model, which is significantly more efficient than the detailed model in terms of modelling effort. Moreover, the simplified model provides a somewhat more conservative evaluation of the steel plate shear wall behaviour in terms of both capacity

and rate of deterioration. Therefore, the simplified model will be utilised for further research and is hereafter referred to as the modified strip model.

4.7 Sensitivity Analysis on the Compression Strut Limiting Stress

The compression strut limiting stress, F_{yCS}, was selected empirically using the behaviour of the four storey test specimen, as described in Chapter 3. Therefore, a sensitivity analysis was performed on the modified strip model to determine its sensitivity to varying this parameter. The compression strut selected for the modified strip model has a limiting stress of $0.08\times F_{yPL}$, where F_{yPL} is the static yield strength of the infill plate. Pushover curves were also obtained for three other limiting stress values—$0.05\times F_{yPL}$, $0.10\times F_{yPL}$, and $0.15\times F_{yPL}$—and compared to the pushover curve of the modified strip model and the envelope curve of the test specimen, as illustrated in Figure 4.7. There is little difference in the inelastic behaviour of models with F_{yCS} of $0.05\times F_{yPL}$, $0.10\times F_{yPL}$, and the modified strip model. However, the pushover curve for F_{yCS} of $0.15\times F_{yPL}$ exceeds the specimen envelope curve in the region where limited yielding had taken place. Therefore, a value in the range of 5% to 10% of the infill plate yield stress is likely adequate for the compression strut limiting stress and the use of 8% is considered suitable for the modified strip model.

4.8 Modified Strip Model Frame Force Results

Although the modelling of steel plate shear walls found in the literature has focussed almost exclusively on the pushover or hysteresis behaviour of the system, the need to estimate the frame forces for design purposes cannot be overlooked. Driver *et al*. (1997) compared the frame forces obtained from the basic strip model to those derived from strain measurements in the four storey test specimen and found that the predictions were generally good, although some significant differences were discovered. Therefore, frame forces (moments and axial forces) were extracted from the pushover analysis of the modified strip model and compared to those in the Driver *et al.* (1997) specimen. The frame forces in the specimen were evaluated at specific base shears for each first– and second–storey member. Driver *et al.* (1997) evaluated moments and axial forces for the first–storey columns and beam at a total base shear of 2021 kN, while for the second–

storey columns and beam, moments and axial forces were recorded at a total base shear of 2570 kN. During the pushover analysis of the modified strip model, frame forces were recorded at each increment that the base shear and first–storey deflection were recorded. At one such increment, a total base shear of 2015 kN was recorded, which is 0.3% below the base shear for the first–storey frame forces of the specimen. At a subsequent increment, a total base shear of 2572 kN was recorded, which is 0.08% above the base shear for the second–storey frame forces of the specimen. These differences are considered negligible and the frame forces extracted from the modified strip model at these increments are directly compared to those from the Driver *et al.* (1997) specimen.

Figures 4.8 through 4.19 show the frame forces obtained from the modified strip model and the test specimen. The modified strip model overestimates by a considerable margin the first–storey column moment near the base of the east column, but provides a good estimate near the top of that column and in the west column throughout, as illustrated in Figures 4.8 and 4.9, respectively. The remaining figures show that the modified strip model generally provided conservative results of the frame forces, with the exception of the east column axial forces, where the model underestimated the test results as seen Figures 4.14 and 4.16. (The east columns experience tensile forces due to the applied overturning moment.) Since in most cases compression forces govern for column design, the underestimated tensile forces may not cause the column sections to be inadequately designed. The test results from the second–storey columns, as illustrated in Figures 4.10 and 4.11, suggest that the moments at this level are very small; however, the modified strip model predicts otherwise. As shown in Figures 4.18 and 4.19, the modified strip model, while providing conservative results, did not accurately predict the axial forces of the first– and second–storey beams. It is evident from the results presented in Figures 4.8 though 4.19 that more research is needed to provide a model that can accurately predict both the overall inelastic behaviour and the internal frame forces of a steel plate shear wall. Nevertheless, the modified strip model produces an excellent representation of the pushover behaviour and provides generally conservative frame forces.

Figures 4.8 through 4.19 also include the frame forces from the basic strip model that was described in Chapter 3 for comparison with the results of the modified strip model. In all

cases, the modified strip model provided either equivalent or improved estimates of the frame forces, and significant improvements are revealed in several locations. For example, the modified strip model is more accurate than the basic strip model in predicting the first–and second–level beam axial forces, although they are still overestimated. Significant improvements of the moments of the east column near the bottom of both the first and second storey were achieved, but again they remain overestimated. Therefore, while still giving generally conservative results, the modified strip model is a better tool for predicting frame forces than the basic strip model.

The Driver *et al.* (1997) specimen was also modelled using twenty strips per panel to represent the tension field of the infill plate instead of ten to determine if increased accuracy in either overall inelastic behaviour or frame force prediction would be achieved. It was found that in both cases, utilising twenty strips per panel has little or no benefit in accuracy over using ten, as shown in Appendix A.

4.9 Summary

The parameters of the detailed model were examined more closely to determine if they could be simplified in order to obtain better modelling efficiency, while maintaining a high degree of accuracy in the prediction of nonlinear behaviour of steel plate shear walls. The frame–joint behaviour was altered such that the nominal or measured modulus of elasticity for each member is used within the panel zone instead of a substantially larger modulus used in the detailed model to reflect the true geometry of the joint and the lack of panel zone yielding observed in experiments. Also, the flexural plastic hinge locations were moved to the edges of the panel zone, except at the bases of the columns where the hinges remained at one-half of the column depth from the base support nodes. A method for spacing the tension strips, termed crosshatching, was implemented to reduce the number of nodes at the beam level by having the strips above and below the beam share a common node. All plastic hinge behaviour was modelled as rigid–perfectly plastic (although for the case of the column hinges, a very small plastic slope was required to avoid numerical instabilities that occurred with a flat slope). It was found that each of the above simplifications had a small or negligible effect when compared with the

results of the detailed model and therefore was implemented into the simplified model, which is considered a more efficient model for design purposes.

A pushover analysis was performed on the simplified model to analyse the same specimen that was analysed in Chapter 3 using the detailed model. Comparing the pushover curves obtained from the detailed and simplified models to the envelope curve of the test specimen showed that the simplified model is a good model, and in some ways a better model than even the detailed model, for describing the specimen pushover behaviour. Since very little accuracy was lost, while a more efficient model was obtained, the simplified model was selected for validation with the behaviour of other test specimens and further research and was renamed the modified strip model.

A limited sensitivity analysis was performed on the modified strip model to determine if varying the limiting stress of the compression strut had a significant effect on the predicted nonlinear behaviour of the steel plate shear wall. From this analysis, a range of 5% to 10% of the infill plate yield strength was considered reasonable and the value of 8%, selected using empirical calibration, was recommended.

The frame bending moments and axial forces obtained using the modified strip model were compared to those of the basic strip model (as described in Chapter 3) and the test specimen. While it was found that the modified strip model gave generally conservative estimates of the specimen frame forces (with the exception of columns in tension where the axial forces were underestimated), the model proved to be more accurate in predicting frame force behaviour than the basic strip model. More research is required to obtain a model that is more accurate in predicting frame forces of the boundary members, while still maintaining a high degree of accuracy in overall inelastic behaviour.

Table 4.1 - Bilinear Flexural Hinge Values

Hinge	A		B		C		D		E	
	M/M_P	θ (rad)	M/M_P	θ (rad)	M/M_P	θ (rad)	M/M_P	θ (rad)	M/M_P	θ (rad)
Beam	0	0	1.00	0	1.00	0.01	1.00	0.10	1.00	1.00
Column	0	0	1.00	0	1.02	0.10	1.10	0.50	1.20	1.00

Table 4.2 - Bilinear Axial Hinge Values

Hinge	A		B		C		D		E	
	P/P_y	Δ/Δ_y	P/P_y	Δ/Δ_y	P/P_y	Δ/Δ_y	P/P_y	Δ/Δ_y	P/P_y	Δ/Δ_y
Tension Strip	0	0	1.0	0	1.0	16.4	1.0	50.0	1.0	100.0

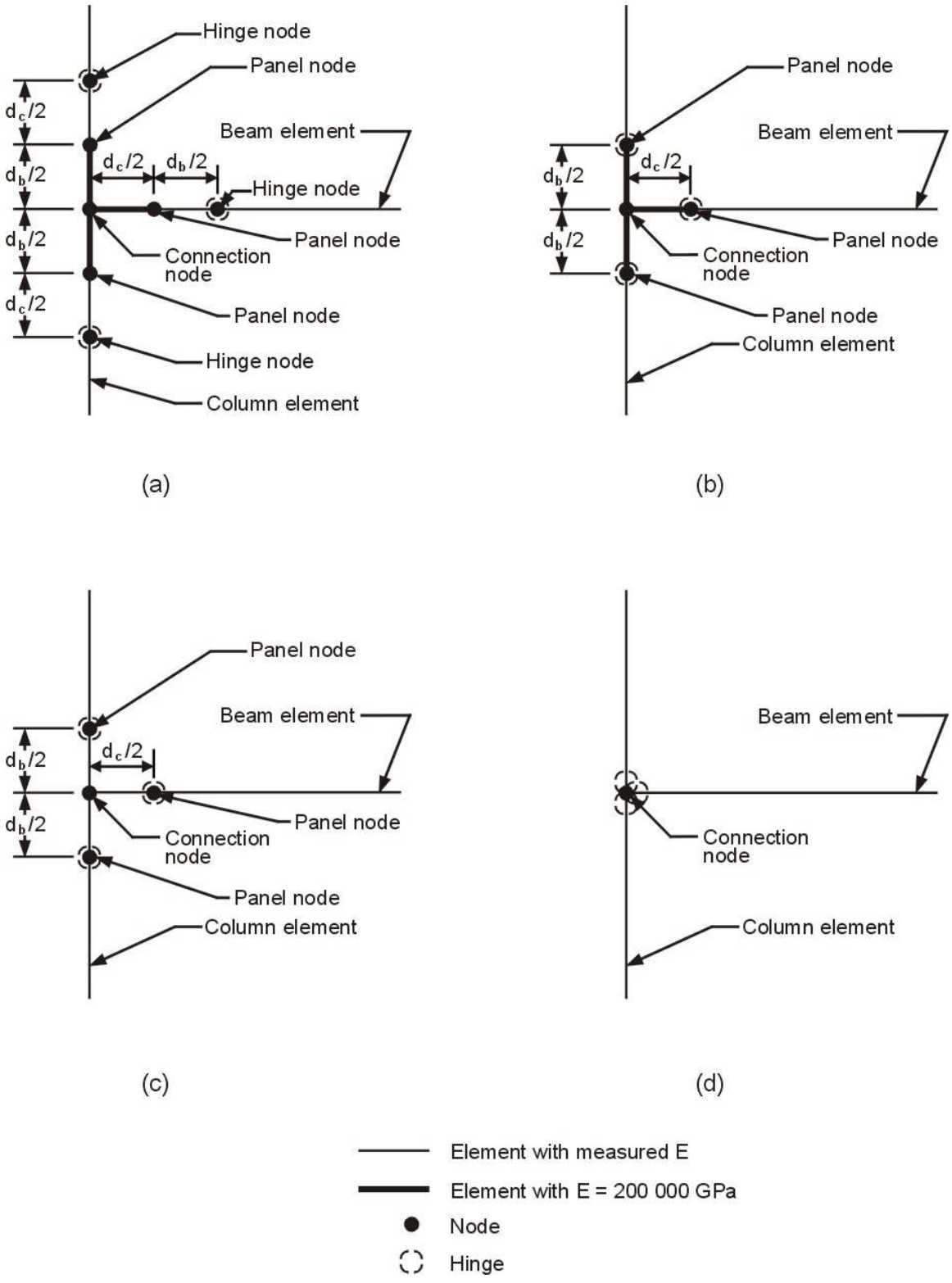

Figure 4.1 - Frame–Joint Arrangements of (a) Detailed Model, (b) Hinges at Edge of Stiffened Panel Zone, (c) Hinges at Panel Node and Nominal Panel Zone Stiffness, and (d) Hinges at Connection Node and No Panel Nodes

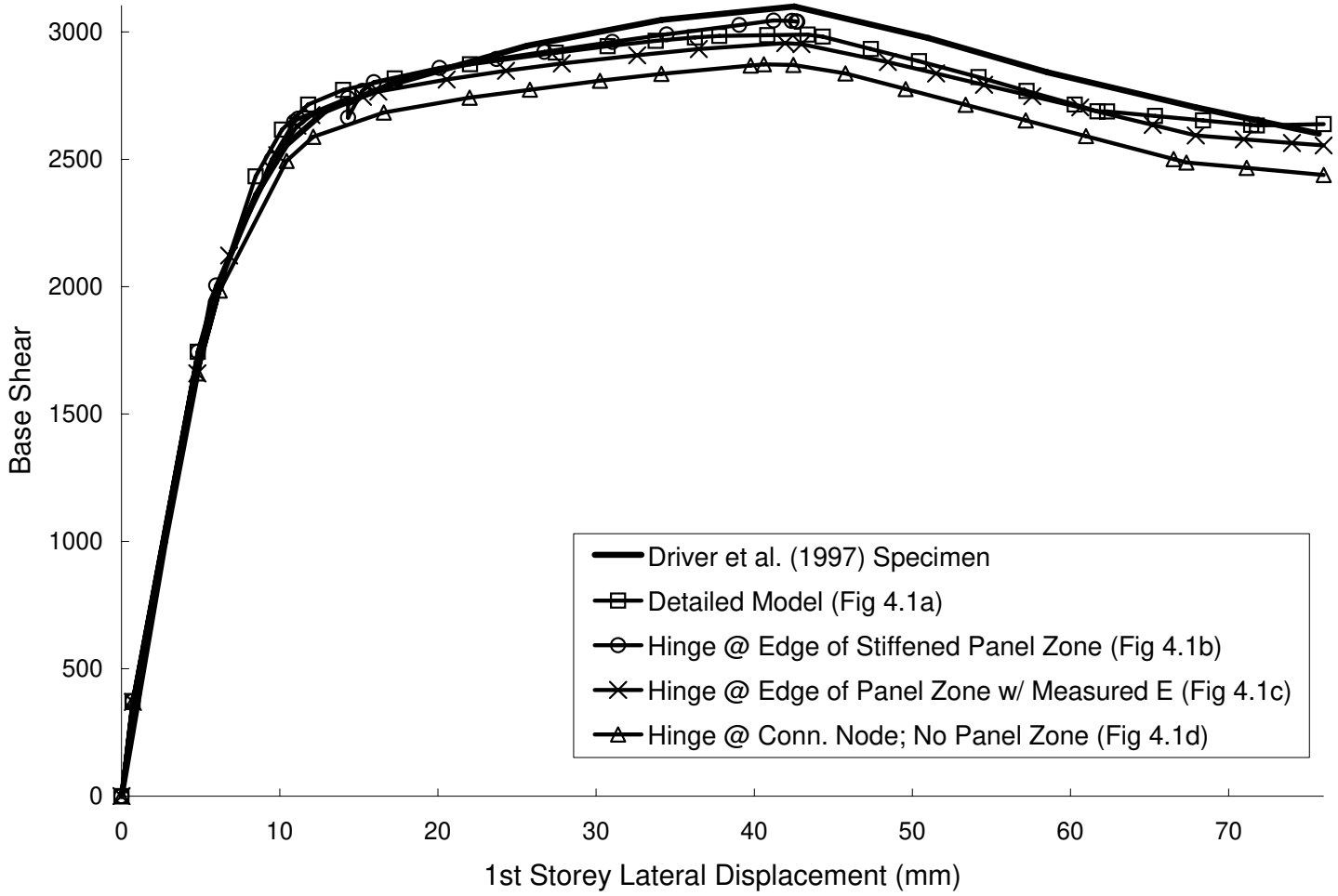

Figure 4.2 - First–Storey Response Curves for Alternative Frame–Joint Arrangements, Detailed Model, and Driver *et al.* (1998a) Specimen

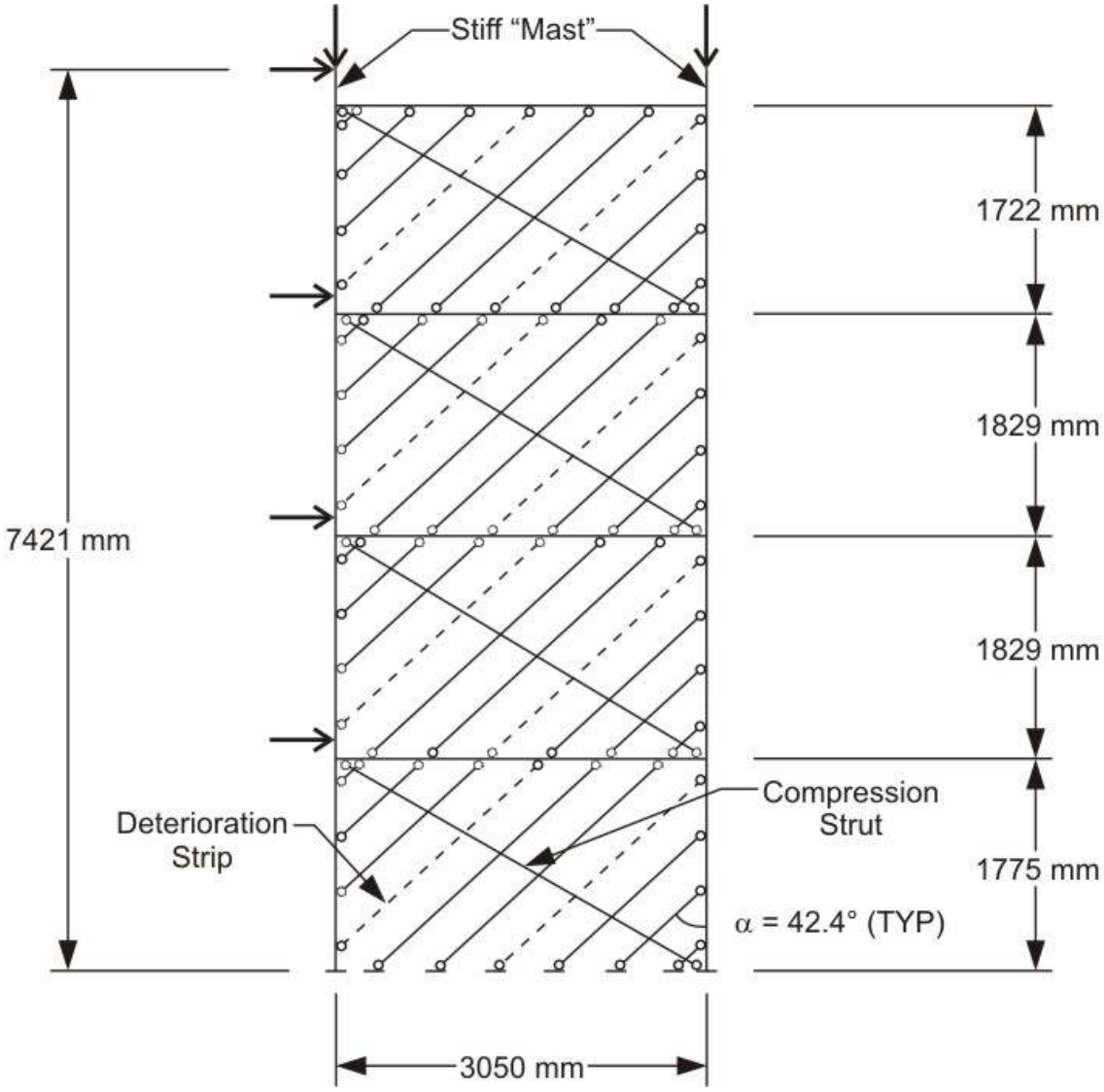

Figure 4.3 - Geometric Arrangement of Crosshatched Model

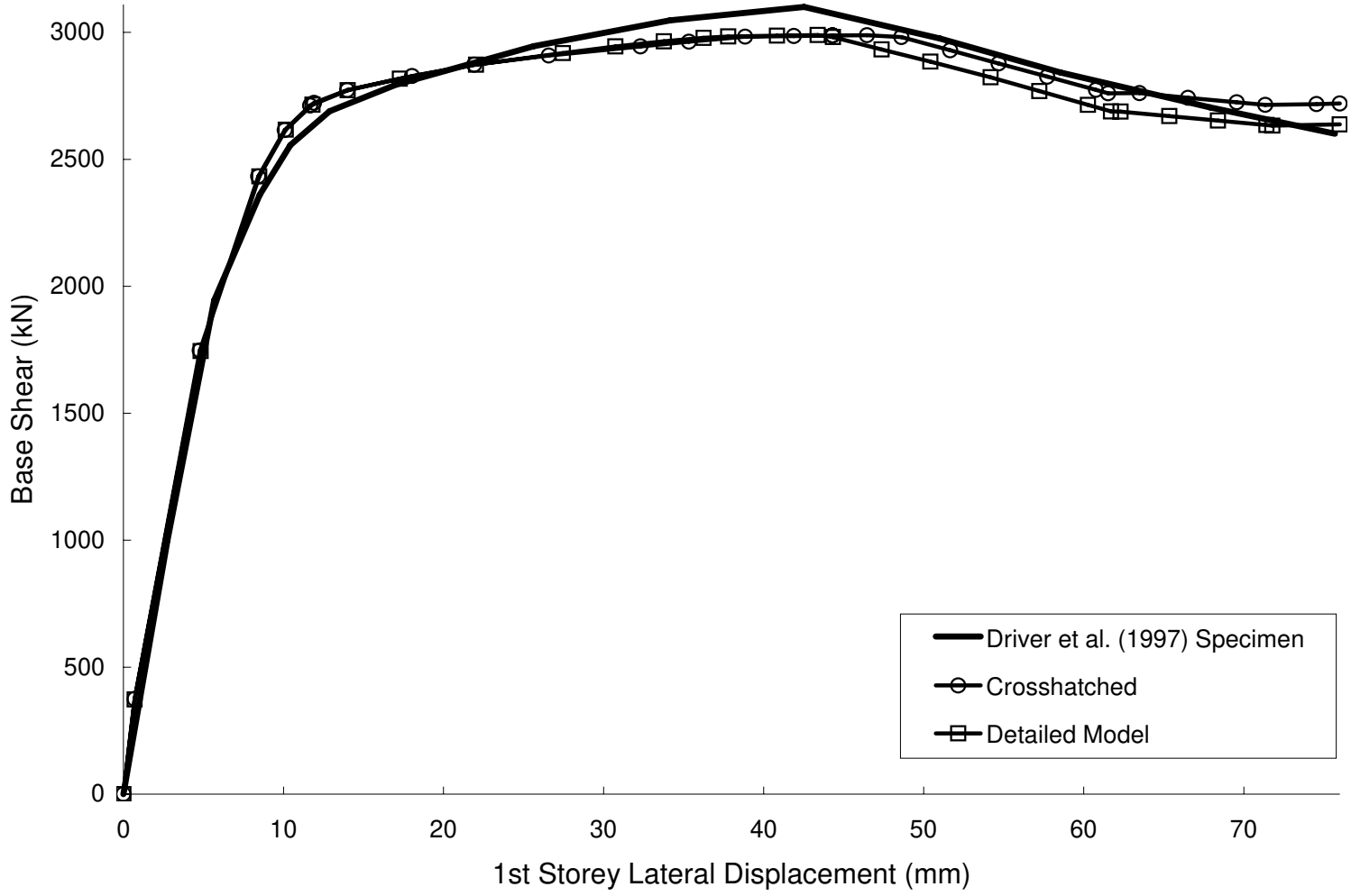

Figure 4.4 - First–Storey Response Curves for Crosshatched Model, Detailed Model, and Driver *et al.* (1998a) Specimen

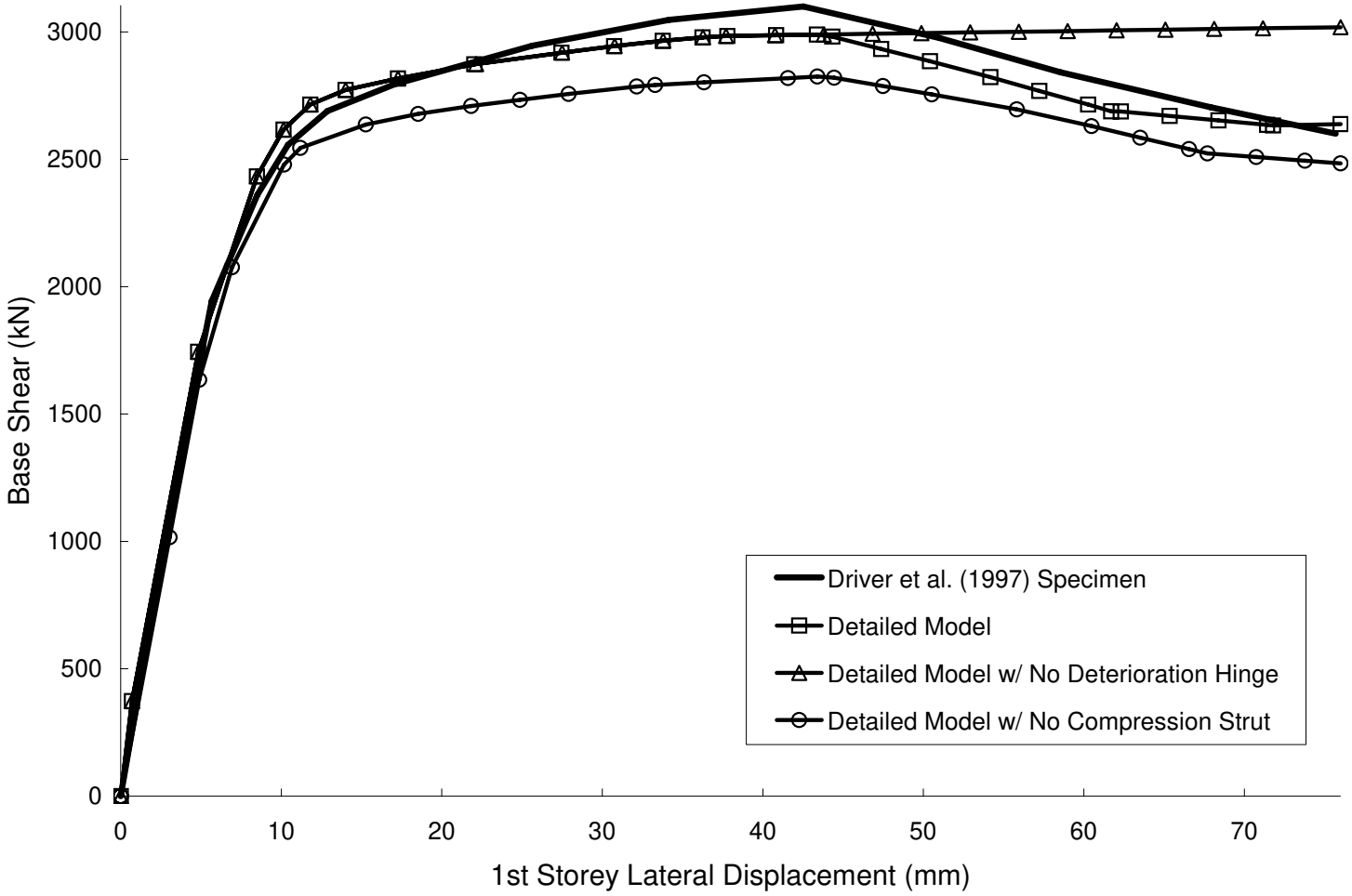

Figure 4.5 - First–Storey Response Curves for Detailed Model, Detailed Model with No Deteriorating Strips, Detailed Model with No Compression Strut, and Driver *et al.* (1998a) Specimen

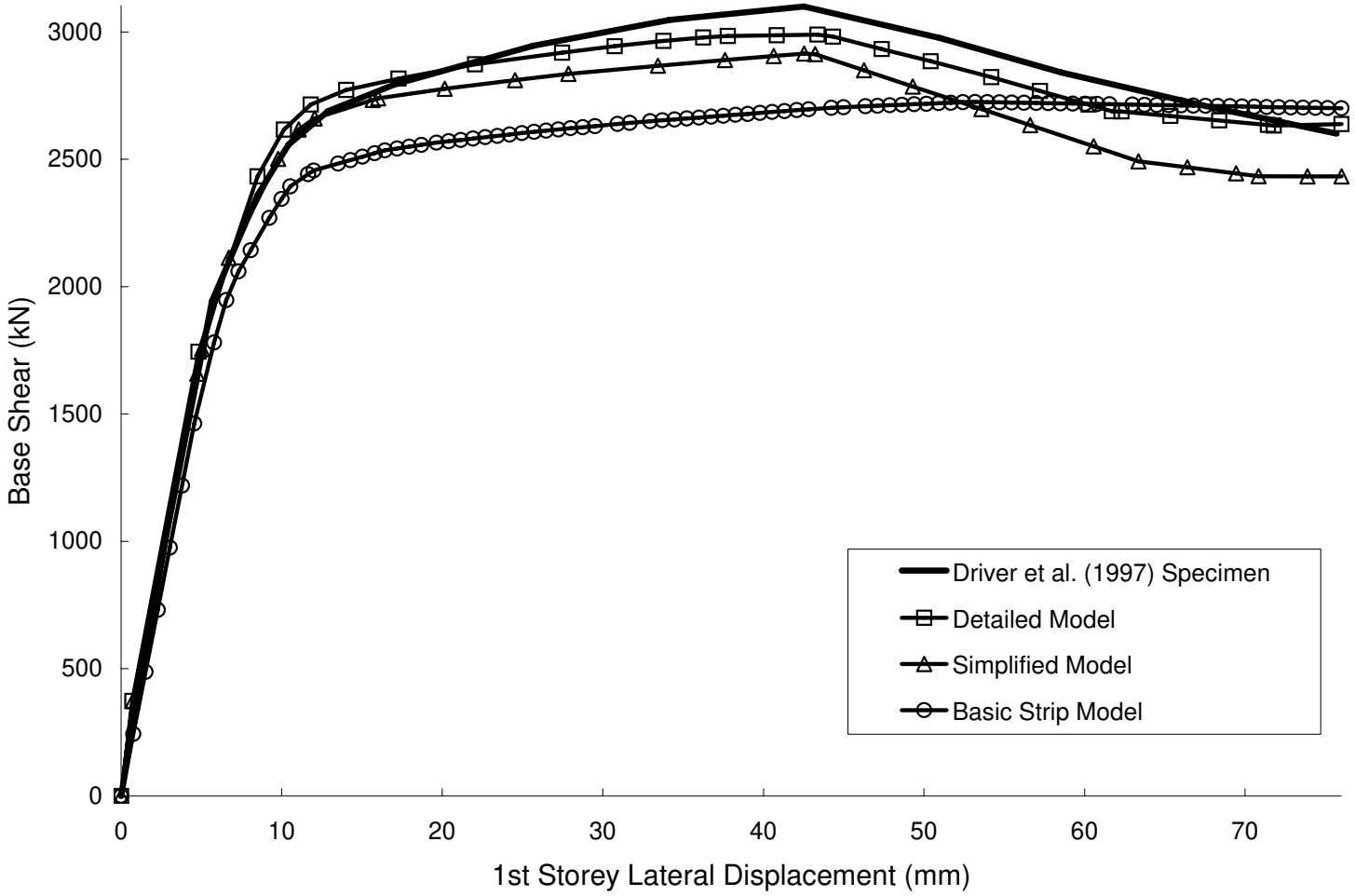

Figure 4.6 - First–Storey Response Curves for Detailed Model, Simplified Model, Basic Strip Model, and Driver *et al.* (1998a) Specimen

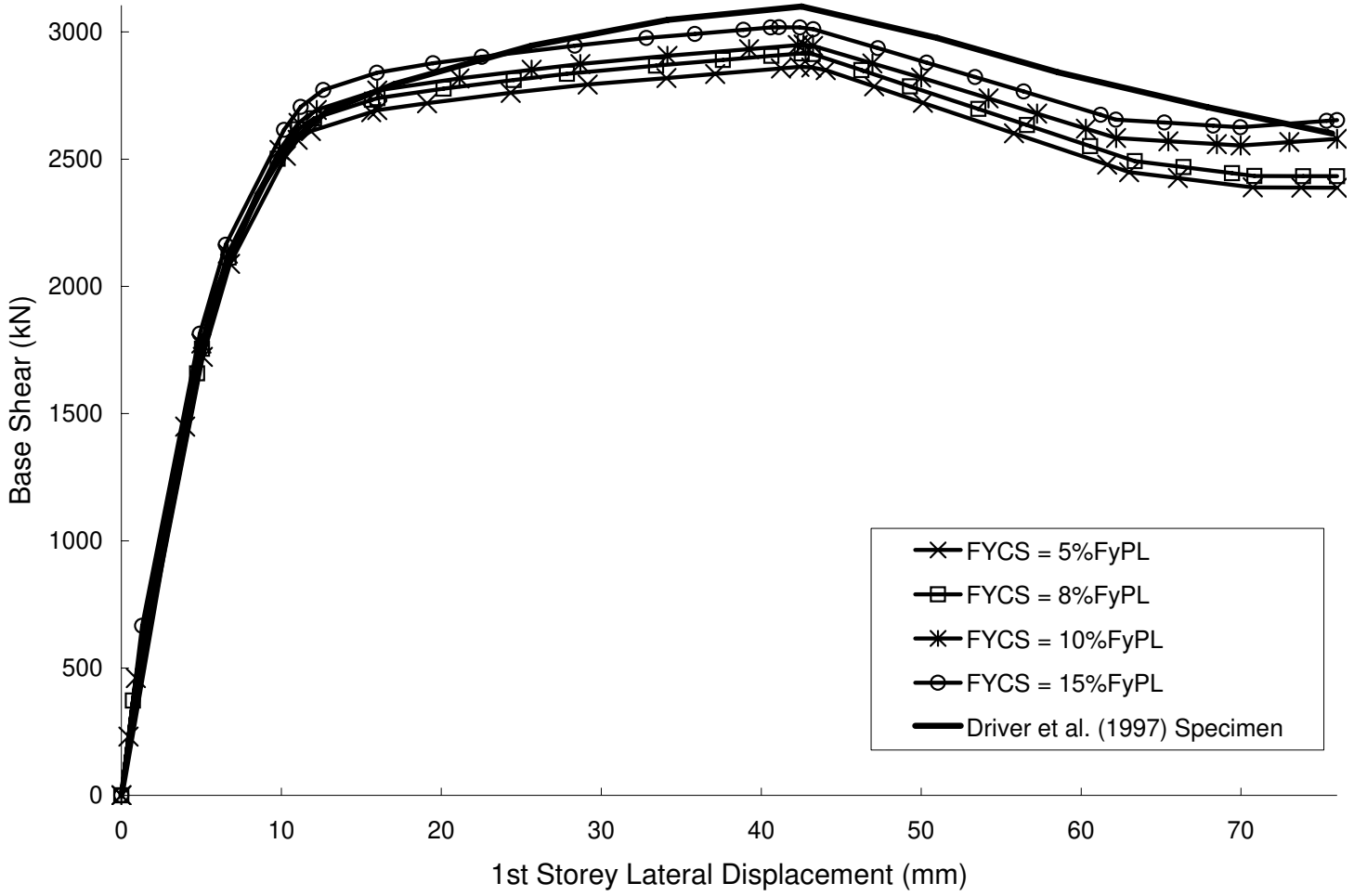

Figure 4.7 - First–Storey Response Curves for Detailed Model with Different Values of F_{yCS} and Driver *et al.* (1998a) Specimen

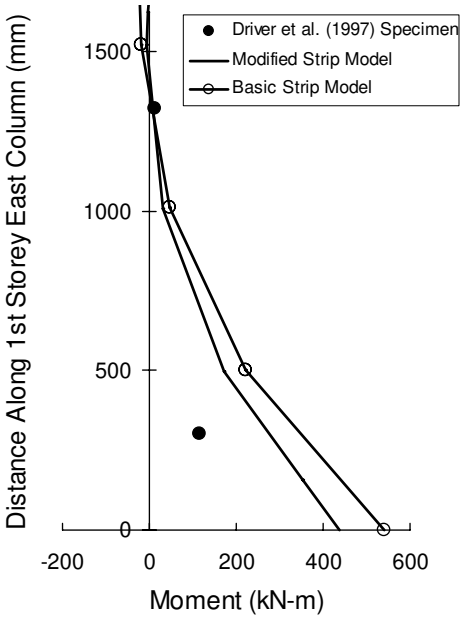

Figure 4.8 - First–Storey East Column Moments

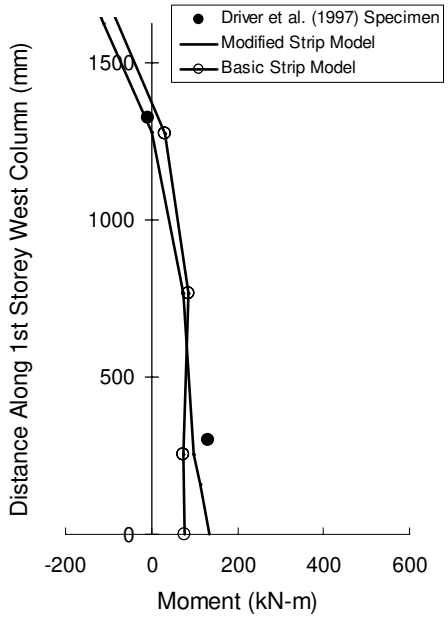

Figure 4.9 - First–Storey West Column Moments

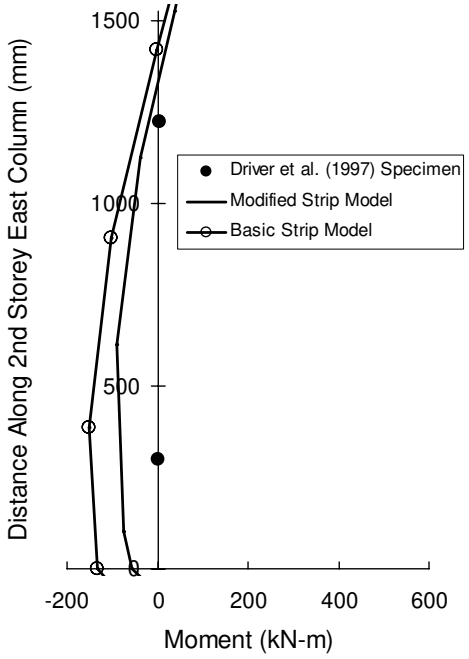

Figure 4.10 - Second–Storey East Column Moments

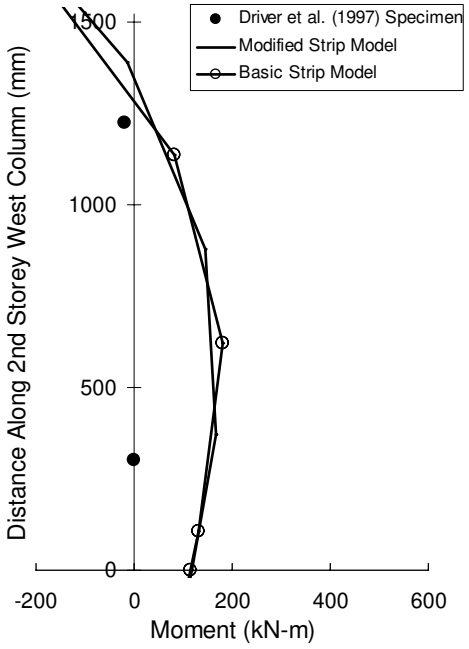

Figure 4.11 - Second–Storey West Column Moments

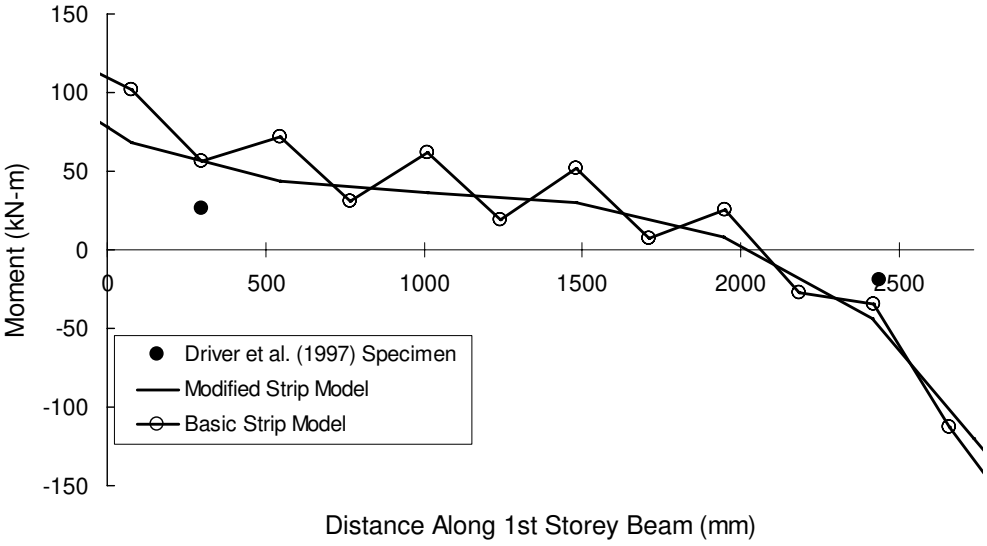

Figure 4.12 - First–Storey Beam Moments

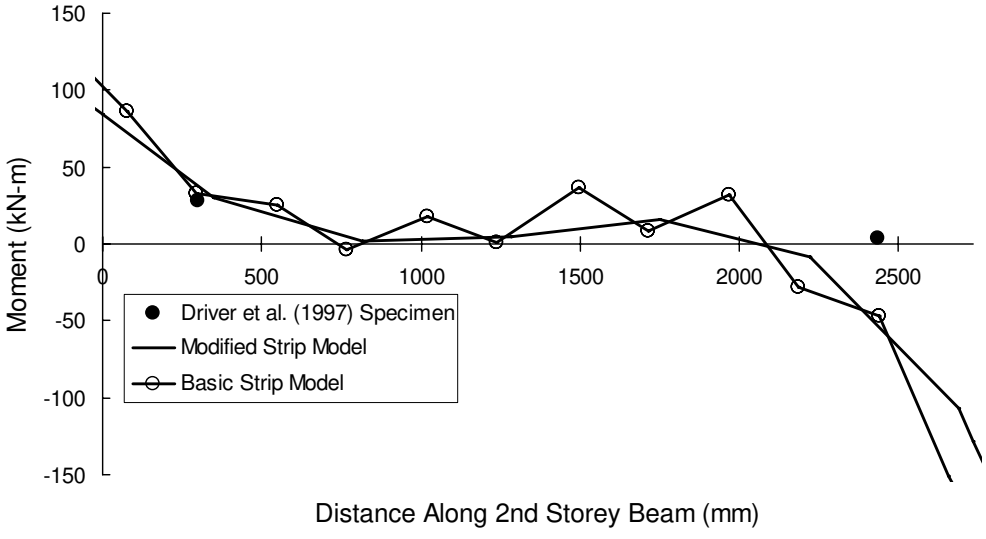

Figure 4.13 - Second–Storey Beam Moments

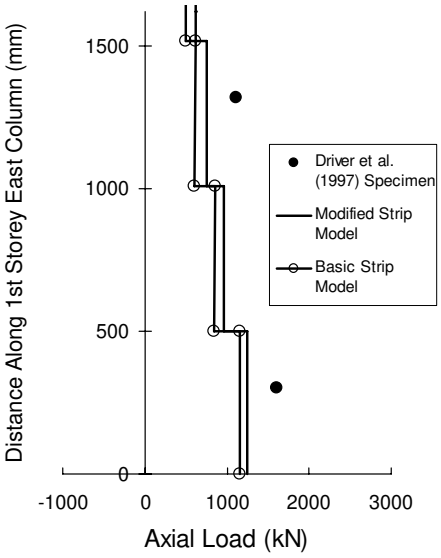

Figure 4.14 - First–Storey East Column Axial Forces

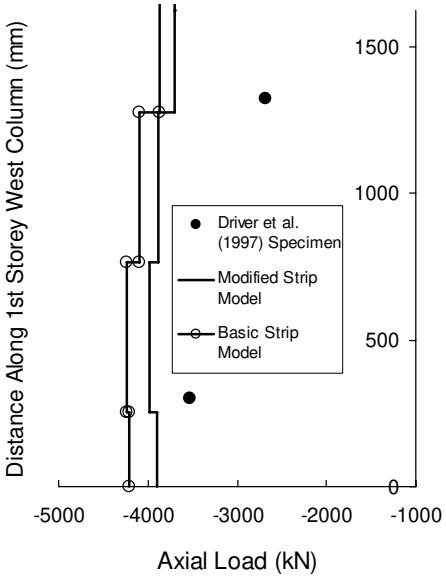

Figure 4.15 - First–Storey West Column Axial Forces

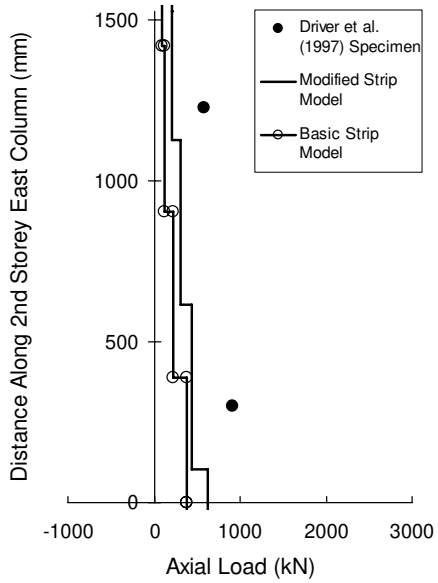

Figure 4.16 - Second–Storey East Column Axial Forces

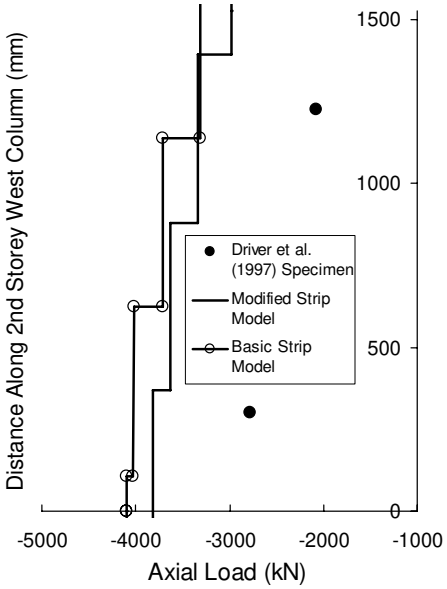

Figure 4.17 - Second–Storey West Column Axial Forces

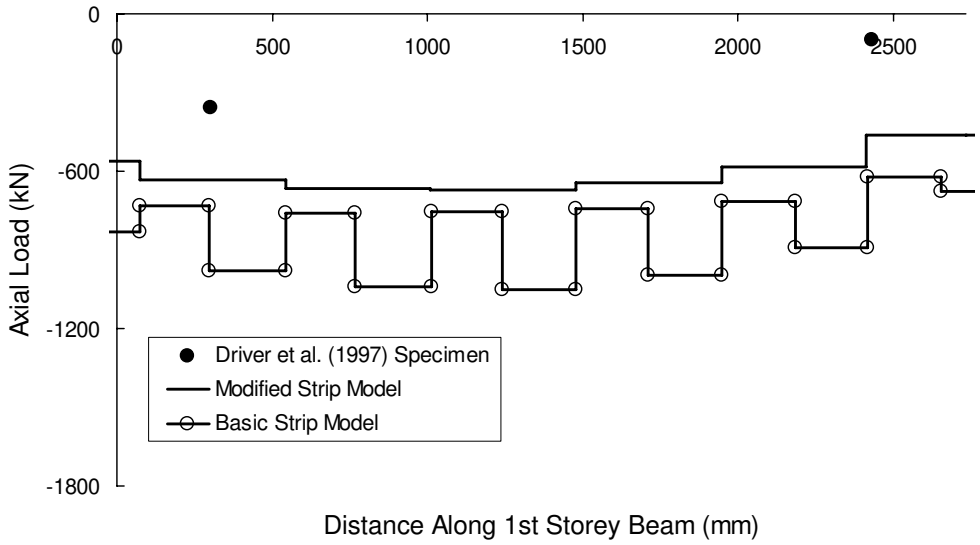

Figure 4.18 - First–Storey Beam Axial Forces

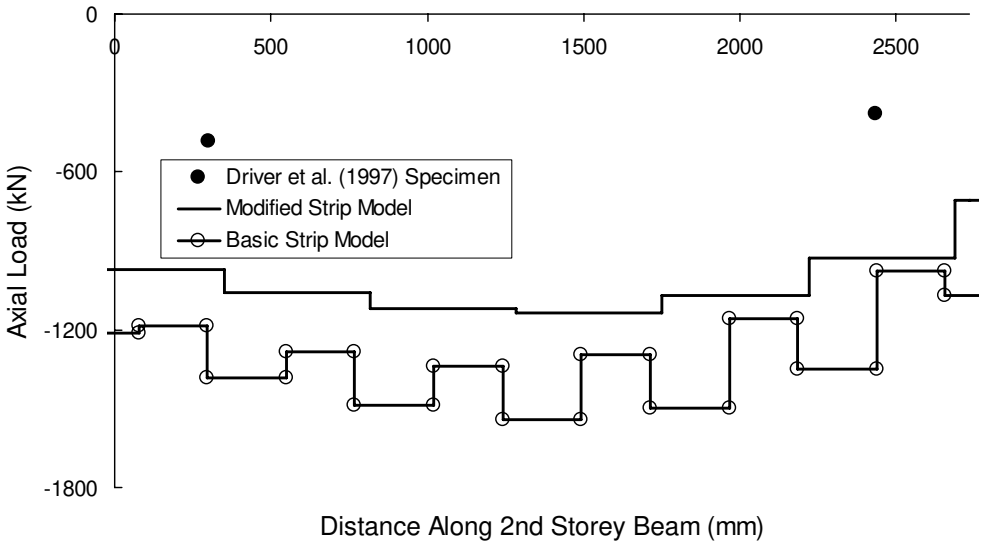

Figure 4.19 - Second–Storey Beam Axial Forces

5. VALIDATION OF THE MODIFIED STRIP MODEL

5.1 Introduction

Chapter 4 demonstrated that the modified strip model predicts the inelastic behaviour of the four–storey steel plate shear wall specimen tested by Driver *et al.* (1998a) with good accuracy. However, there are other specimens discussed in the literature with different geometric properties and configurations that can be used to validate the model further. These specimens permit an evaluation of the ability of the model to simulate specimens with different beam-to-column connection types, column flexibilities, and infill plate thicknesses, all of which have the potential to influence the pushover behaviour of a steel plate shear wall. Therefore, modelling and comparing the predicted inelastic behaviour to such specimens will assist in validating the accuracy of the modified strip model.

This chapter investigates three steel plate shear wall specimens that have different geometries and configurations from that of the Driver *et al.* (1998a) specimen in order to observe how the modified strip model predicts the inelastic behaviour of each specimen. The parameters of the modified strip model, as described in Chapter 4, are applied to each specimen and a pushover analysis is performed. Each resulting pushover curve is compared to the corresponding inelastic envelope response curve of the modelled specimen. Means of adapting the modified strip model are proposed for cases with pinned beam-to-column connections, highly flexible columns, or very thin infill plates.

5.2 Timler and Kulak (1983) Specimen

5.2.1 Model Geometry and Loading

The Timler and Kulak (1983) specimen, described in Section 2.4 and Figure 2.4, utilised a pinned beam-to-column connection, which provided an opportunity to validate the modified strip model on a specimen with beam-to-column connections at the other extreme. Due to symmetry of the specimen and to simplify the modelling process, the modified strip model represented the Timler and Kulak (1983) specimen as a single one–storey, one–bay specimen with the columns and beams in their customary orientation, as illustrated in Figure 5.1. The base of the model was taken to be at the neutral axis of the interior continuously–connected beam where a fixed

support condition was imposed. The column base flexural hinge was located at one-half the column depth from the top flange of the interior beam, which constituted a distance of $\frac{d_c + d_b}{2}$ from the base node of the model, where d_c and d_b are the depths of the column and beam cross-sections, respectively. The interior beam was not modelled since in the analysis the region of the column that would be bounded by the interior beam remains elastic and deforms a negligible amount compared to the hinge. No flexural hinges or panel zone nodes were input at the top of the columns or on the beam. Instead, the strong–axis moment was released at each end of the top beam to represent the pinned beam-to-column connection of the specimen. (For multi-storey structures, the column flexural hinges would remain at the panel nodes at intermediate levels.)

The columns and beams of the specimen consisted of sections built-up from plates that resulted in cross-sectional dimensions similar to those of W310×129 and W460×144 sections, respectively. Timler and Kulak (1983) calculated the cross-sectional properties to be as follows: $A_c = 15\,656$ mm^2, $I_c = 295.4\times10^6$ mm^4, $A_b = 20\,952$ mm^2, and $I_b = 810.3\times10^6$ mm^4. For the case of the modified strip model, the beam and column elements were modelled using W310×129 and W460×144 properties from a standard database, but a modification factor was incorporated to represent accurately the cross-sectional area and moment of inertia of the specimen members. The built-up sections were fabricated from grade 300W steel plate. Although no ancillary tests were performed on the material, the plates were assumed to be hot-rolled with a tensile yield strength of 350 MPa, which was seen as a reasonable estimate of the actual yield strength for 300W steel produced at that time.

The infill plate consisted of a 4.76 mm (3/16″) thick plate that exhibited tensile properties described by Timler and Kulak (1983) as being similar to those of cold-formed steel. The stress vs. strain curve included elastic behaviour up to a proportional limit, followed by a smooth transition-curve up to the static yield stress. Since this behaviour cannot be captured accurately by a bilinear curve, the tension strip axial hinge behaviour was modelled in four segments, as described in Table 5.1.

Based on the ancillary test data, a proportional limit of 129 MPa at a strain of 0.0643% was assumed. The yield stress was determined to be 271 MPa by Timler and Kulak (1983) and the strain at which this stress was achieved was taken as 0.3%. The intermediate stress and strain (*i.e.*, between the proportional limit and yield point) were assumed to be 229 MPa and 0.15%, respectively, to produce a good representation of the measured material curve. Consistent with the modified strip model, the tension strip axial hinge curve was flat after the yield stress was reached. It should be noted that the tension strip axial hinge elongations are normalised in Table 5.1 using the elongation at the proportional limit instead of at the yield stress. Since there is a limit of four segments to describe hinge behaviour in the software used, the deterioration of the infill plates could not be modelled. Therefore, all tension strips were modelled identically.

The measured cross-sectional properties of the beam and columns were used to calculate the angle of inclination of the infill plate tension field, α. Since the infill plate is only on one side of the beam section and the beam is free to bend, Equation 2.4, derived by Timler and Kulak (1983) for the specific properties of the specimen, was used to calculate a value of $\alpha = 52.8°$. The area of the compression strut was calculated using Equation 2.2 and the limiting stress was taken to be 8% of the infill plate yield stress, or 21.7 MPa.

After three cycles to approximately the service load level, Timler and Kulak (1983) applied a load monotonically to the specimen up to the ultimate level. Failure of the test specimen occurred by buckling of the connection plates at one of the pinned connections and weld tearing in that region. According to Timler and Kulak (1983), had localized failure of the detail not taken place, a higher capacity (and larger deflection) would have been attained by the steel plate shear wall specimen. From the data, a monotonic pushover curve was obtained. A lateral load was applied to the column at the elevation of the centreline of the top beam of the modified strip model, which coincided with the point of the pinned support for the specimen that was located at the centreline of the exterior beam. Lateral deflections were monitored at a node on the other column at the top beam, as shown in Figure 5.1, up to 28 mm, the

maximum deflection of the specimen. To obtain a pushover curve that would be comparable to the monotonic curve of the specimen, the base shears as predicted by the modified strip model were doubled (Timler and Kulak 1983 reported the total applied load to the specimen, not the reaction load at each support.)

5.2.2 Analysis Results and Model Refinements

The pushover curve of the modified strip model was compared to the monotonic curve of the specimen, as illustrated in Figure 5.2. It can be seen that a kink forms in the model curve early in the analysis (at a load of 550 kN and lateral deflection of 0.5 mm) due to the yielding of the compression strut. After the formation of the kink, the model curve lies above that of the specimen, although the stiffnesses of the model and specimen are approximately equal. This suggests that had the compression strut not been present, the initial stiffness of the model would be closer to that of the specimen. Despite this deviation, the modified strip model accurately predicts the strength of the specimen at the maximum displacement, slightly overestimating it by 2.1% (5506 kN for the model vs. 5395 kN for the specimen). This small discrepancy may be due to the failure mode of the specimen, described in the previous section. Although it enables the model to predict the strength of the specimen at the maximum deflection in the test quite accurately, it is apparent that the compression strut provides too much stiffness to the modified strip model during the early stages of loading. The reason for this is attributed to the pinned connections used in this specimen that tend to pinch the infill plate, causing buckling to occur early during the load history. Nevertheless, the effect of the compression strut does develop at higher load levels.

To assess the contribution of the compression strut, the model of the Timler and Kulak (1983) specimen was also analysed with the compression strut removed. As can be seen in Figure 5.2, this curve contains no kink and agrees well with the initial stiffness of the specimen, while underestimating the strength at the maximum deflection by 4.5% (5151 kN). The pushover curves from the two models (with and without the compression strut) suggest the compression field for steel plate shear walls with pinned beam-to-column connections does not form during the early stages

of loading. As loading progresses, however, the corners of the panels become pinched and a compression field starts to form there at approximately the initial yield of the specimen (or $11\Delta_y$ of the compression strut). The full strength of the compression field is soon realised, thus contributing to the overall strength of the specimen.

To account for the behaviour described above, a model of the Timler and Kulak (1983) specimen was created that contains a compression strut axial hinge that engages more gradually than the strut developed originally. Table 5.1 shows the normalised load and deflection values for this "calibrated" axial hinge. It should be noted that during the early stages of loading, where the compression strut does not contribute to the stiffness of the model (from Point B to Point C), the slope would normally be flat. However, due to numerical instabilities, a slight slope (0.0001:1) was applied in order to achieve convergence, but the effect of this is considered negligible. It should also be noted that where the strength of the compression strut is introduced to the model (Point C to Point D), the stiffness of the compression strut is five times softer than would normally be. As illustrated in Figure 5.2, the pushover curve of the model with the calibrated strut agrees well with both the initial stiffness and the strength at maximum deflection of the specimen monotonic curve. Due to the calibrated compression strut axial hinge, this model has the same initial stiffness as the model with no compression strut and the same the post-yield curve as the model with the original compression strut having a bilinear axial hinge. It should be noted that although no declining branch could be included in the deterioration hinges due to software limitations, as discussed previously, it was determined that had it been included, deterioration would not have taken place until well past the maximum deflection achieved in the test. Because of this, and the localized connection failure observed in the test specimen, further research is required to assess the deterioration behaviour of steel plate shear walls with pinned frame connections.

Due to a lack of data for steel plate shear wall specimens with pinned beam-to-column connections (there are specimens with shear-type connections, but no other specimens with pinned connections as in the Timler and Kulak (1983) specimen), the calibrated hinge as described above cannot be validated. However, the design

engineer can easily create two models—one with a bilinear compression strut and one without. If required, the initial slope of the curve of the model with no compression strut can simply be extended to intersect the curve of the model that includes the compression strut to obtain a good estimate of the overall steel plate shear wall response.

5.3 Lubell (1997) One–Storey Specimen (SPSW2)

5.3.1 Model Geometry and Loading

Lubell (1997) tested a small scale one–storey specimen, designated SPSW2, as described in Section 2.10 and Figure 2.7(b). Of note, the infill plate thickness was only 1.5 mm and the S75×8 section did not meet the column flexibility limit requirements prescribed in Clause 20.4.2 of CAN/CSA S16-01 ($\omega_h = 3.4$ for the S75×8 vs. $\omega_h = 2.5$ for the CAN/CSA S16-01 limit).

Figure 5.3 shows the geometric and loading arrangement for the modified strip model of the SPSW2 specimen. The base of the model was located at the base of the specimen (*i.e.*, the bottom of the lowest S75×8 beam) and a fixed base support condition was imposed. The base hinge of the columns was located at one-half of the column depth above the top flange of the bottom beam for a total distance from the base node of 114 mm ($d_b + 0.5\ d_c = 1.5\ d_c$). The bottom beam of the specimen was omitted from the model for similar reasons to those described for the Timler and Kulak (1983) model. The height of the model extended to the centreline of the top beam for a total storey height, h, of 976 mm.

The built-up beam section (2–S75×8) was modelled as a typical S75×8 section with A_b and I_b modified to match the cross-sectional properties of the specimen top beam, 2 140 mm^2 and 5.17×10^6 mm^4, respectively. Since the SPSW2 specimen utilised moment–resisting beam-to-column connections, the model represented the connections as rigid and the panel node and flexural hinges are located as described in Chapter 4. The modified strip model of the SPSW2 specimen used the equation in Clause 20.3.1 of CAN/CSA S16-01 (Equation 2.3) to calculate α, despite the fact the

infill plate is on one side of the beam section only and the beam is therefore free to bend under the action of the tension field, which implies that the equation used for the Timler and Kulak (1983) specimen—Equation 2.4—should be used instead. However, the values of α as calculated by the two equations are so close that the effect of using the CAN/CSA S16-01 equation was considered negligible (36.2° for CAN/CSA S16-01 equation vs. 36.8° for Equation 2.4).

Based on the material test data presented by Lubell (1997), a static yield strength of 400 MPa was selected for the columns and beams in the model, while the infill plate yield strength was taken as 320 MPa. The area of the compression strut was calculated using Equation 2.2 and the limiting stress was taken to be 8% of the infill plate yield stress, or 25.6 MPa. The deterioration behaviour of the model was taken to be that as described in Chapter 3, since it is considered to be conservative for most cases.

As in the test, no gravity load was applied. The lateral load was applied from one side of the wall at the level of the centreline of the top beam. A node on the other column at that level was monitored while the model was pushed until the node reached the maximum lateral deflection of the specimen of 50 mm. The contribution of self-weight during the pushover analysis was considered negligible.

5.3.2 Analysis Results and Model Refinements

The pushover curve of the modified strip model was compared to the envelope of the SPSW2 specimen hysteresis curve, as illustrated in Figure 5.4. The model predicts the peak capacity to occur at a considerably smaller deflection than what occurred with the specimen, which suggests that the deterioration axial hinge behaviour as described in Chapter 3 does not accurately reflect the deterioration of the SPSW2 specimen. This is likely due to the very thin infill plate that would be less susceptible to local kinking leading to the formation of cracks. To assess the wall response without the plate tearing that is represented by the deteriorating axial hinges, the deterioration behaviour of the strips was omitted and bilinear tension–only axial hinges were used for all of the inclined tension strips. The pushover curve from this model is also

shown in Figure 5.4 and provides an improved representation of the latter part of the curve.

Similar to the modified strip model of the Timler and Kulak (1983) specimen, a small kink forms in the model curve early in the analysis (at a load of 23 kN and a lateral deflection of 0.3 mm) due to the buckling of the compression strut, as seen in Figure 5.4. After the formation of the kink, the stiffness of the model is almost equal to that of the specimen, but the model curve lies slightly above that of the specimen. Despite this deviation, the model without the deterioration hinge accurately predicts the ultimate strength of the specimen, underestimating it by 0.4% (260 kN for the model vs. 261 kN for the SPSW2 specimen). Since the deterioration of the strips was not being modelled and, thus, no peak of the pushover curve could be established, the ultimate strength of the model was taken at the same deflection as the ultimate strength of the specimen. Nevertheless, the slope of the curve at this point is nearly zero.

The model of the SPSW2 specimen without the deterioration hinges was also run with the compression strut removed. As can be seen in Figure 5.4, the pushover curve of this model agrees very well with the initial stiffness of the specimen, while underestimating the ultimate strength of the specimen by 6.1% (245 kN). The pushover curves of the models with and without the compression strut suggest that early in the loading stage, the compression field does not form in the very thin infill plate. However, at a point approximately halfway through the initial yield portion of the envelope curve (about 11 mm total storey displacement), the full strength of the compression field starts to be realised. Therefore, similar to the case of the Timler and Kulak (1983) modified strip model, the compression strut axial hinge requires calibration to obtain a single pushover curve that agrees well with the envelope curve of the specimen. Another model of the SPSW2 specimen was therefore created with a compression strut axial hinge that mimicked the behaviour described above. Table 5.1 shows the normalised load and deflection values for this calibrated hinge. As in the case of the Timler and Kulak (1983) model, a slight slope (0.0001:1) was required from Point B to Point C for the analysis to converge. To obtain good agreement with

the envelope curve, the stiffness of the compression strut (Point C to Point D) was much lower than it would normally be. As can be seen in Figure 5.5, the pushover curve of the model with the calibrated compression strut agrees very well with the SPSW2 specimen envelope curve. Due to the calibrated compression strut axial hinge, this model has the same initial stiffness as the one with no compression strut and the same characteristics near the ultimate strength as the model with the bilinear compression strut. As described for the Timler and Kulak (1983) specimen, a design engineer can readily create two models—one with a bilinear compression strut and one without—and obtain a good estimate of the complete steel plate shear wall response.

5.4 Lubell (1997) Four–Storey Model (SPSW4)

5.4.1 Model Geometry and Loading

The modified strip model was also applied to the four–storey specimen (SPSW4) tested by Lubell (1997), as described in Section 2.10 and Figure 2.8. The SPSW4 model, shown in Figure 5.6, had similar material properties to that of the SPSW2 model. The average value of α was calculated to be 37.5° using the CAN/CSA S16-01 equation for each panel. The area of the compression strut at each level was calculated using Equation 2.2. Using load control, gravity loads of 6.5 kN were applied to each column at every storey level as in the test. The self-weight of the specimen was neglected during the analysis since it was low in comparison to the gravity loads. After the gravity loads were applied to the model, equivalent lateral loads were introduced to one column using deflection control with the loads located at the elevation of the centreline of each interior beam and at 36 mm from the top of the S200×34 beam. To model accurately the loading at the top of the specimen, a stiff "mast" was placed at the top of each column that extended 64 mm from the centreline of the S200×34 beam. The deflections were monitored on the "lee" column at the point of the first–storey beam until the maximum first–storey deflection of the specimen—15 mm—was obtained.

5.4.2 Analysis Results and Model Refinements

The pushover curve of the modified strip model was obtained and compared to the envelope curve of the SPSW4 specimen, as illustrated in Figure 5.7. A kink in the model curve formed early in the analysis due to the compression strut buckling, which caused the model to overestimate both the initial stiffness and the ultimate strength of the specimen. For comparison, a model with the compression strut removed was also created, as seen in Figure 5.7. Even though no kink was present in the response curve of this model, the initial stiffness of the specimen was still overestimated by a significant margin. The model overestimated the ultimate strength of the specimen by 2.8% (181 kN for the model vs. 176 kN for the specimen).

Similar inconsistencies to those described above were observed by Lubell (1997) from their strip model analysis and they suggested that a partial tension field might have formed between the beams only due to the highly flexible columns. Therefore, they proposed an α of 22° calculated using an equation by Thorburn *et al.* (1983) derived based on that assumption. However, Lubell (1997) continued to have the tension strips connected to the column members, as well as the beam members, in the analytical model. Therefore, two additional models of the SPSW4 specimen were also created—one with a compression strut and one without—with the crosshatched tension–only strips oriented at 22° to the vertical and connected to both the columns and beams, and the resulting pushover curves are shown in Figure 5.7. It was found that the model with no compression strut and the reduced angle of inclination of the tensions strips agreed very well with the initial stiffness of the specimen, while underestimating the ultimate strength by 14.8% (150 kN).

These results suggest that during the early stages of loading the SPSW4 specimen, a partial tension field formed with an angle α of 22°. Lubell (1997) observed that as the loading of the specimen progressed, the tension field developed more fully, thus forcing α to increase. Due to the complex nature of the described behaviour—with α changing throughout the load history—and the fact that the columns do not meet the stiffness requirements of CAN/CSA S16-01, no single modified strip model of the

SPSW4 specimen was created to fully describe the inelastic behaviour. It should be noted that even though the deterioration of the tension strips was included in the models (as per Chapter 3), the pushover curves displayed no deterioration effects within the deflection range.

5.5 Summary

The modified strip model was validated using three steel plate shear wall specimens with different properties and configurations than the Driver *et al.* (1998a) specimen. When the modified strip model was applied to the Timler and Kulak (1983) specimen, which used pinned beam-to-column connections, it was found that while the compression field does not form until initial yielding commences, it does contribute significantly to the overall capacity of the specimen. Once the compression strut axial hinge was calibrated so a single model could capture the inelastic behaviour of the specimen, there was good agreement between the model and specimen curves, even though the model did not start deteriorating until a larger deflection. The modified strip model was also applied to the SPSW2 specimen (Lubell 1997), which used flexible columns, a very thin infill plate, and moment–resisting connections. It was found that while the compression field does not form until initial yield of the specimen occurs, it does contribute to the overall capacity of the specimen. The compression strut axial hinge was calibrated so a single model would suffice for steel plate shear walls with very thin infill plates with moment–resisting beam-to-column connections. In both cases, an "eyeball" method using two models—one with a compression strut and one without—could be used easily by a design engineer to estimate the complete response of the steel plate shear wall. For multi-storey steel plate shear wall specimens with very thin infill plates, flexible columns, and moment–resisting connections (SPSW4 from Lubell (1997)), it was found that one model cannot capture the inelastic behaviour of the specimen since the value of α increases as the load is applied.

It was observed that the deterioration axial hinge described by the modified strip model did not accurately describe the deterioration behaviour of the specimens discussed in this chapter. This suggests that further research is required to assess the deterioration behaviour of various steel plate shear wall configurations. However, it is believed that the

deterioration behaviour described in the modified strip model would be generally conservative.

The results presented in this chapter support the use of the compression strut described in Chapter 3 for estimating the capacity of steel plate shear walls. However, for cases with pinned beam-to-column connections or with very thin infill plates, it is suggested that the strut be omitted for estimating the initial stiffness of the steel plate shear wall.

Table 5.1 - Axial Hinge Definitions

Hinge	A		B		C		D		E	
	P/P_y	Δ/Δ_y	P/P_y	Δ/Δ_y	P/P_y	Δ/Δ_y	P/P_y	Δ/Δ_y	P/P_y	Δ/Δ_y
Tension Strip (Timler and Kulak 1983)	0	0	0.476	0	0.845	1.4	1.0	3.7	1.0	100.0
Deterioration Strip (Timler and Kulak 1983)	0	0	0.476	0	0.845	1.4	1.0	3.7	1.0	100.0
Calibrated Compression Strut (Timler and Kulak 1983)	0	0	0	0	-0.001	-10.0	-1.0	-15.0	-1.0	-500.0
Calibrated Compression Strut (SPSW2 – Lubell 1997)	0	0	0	0	-0.0055	-54.6	-1.0	-99.0	-1.0	-500.0

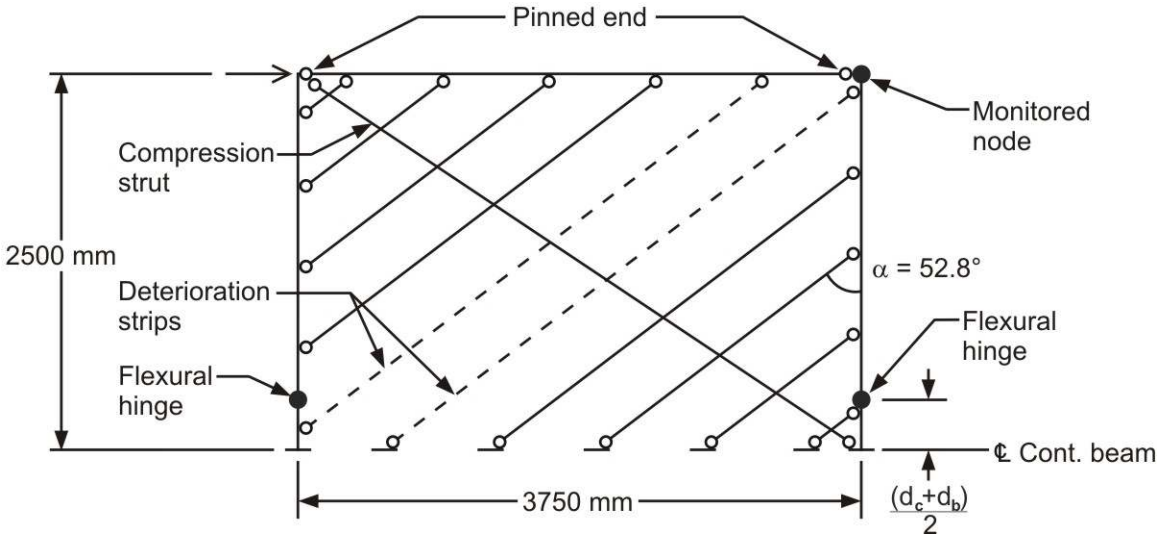

Figure 5.1 - Geometric Arrangement of Timler and Kulak (1983) Specimen Using the Modified Strip Model

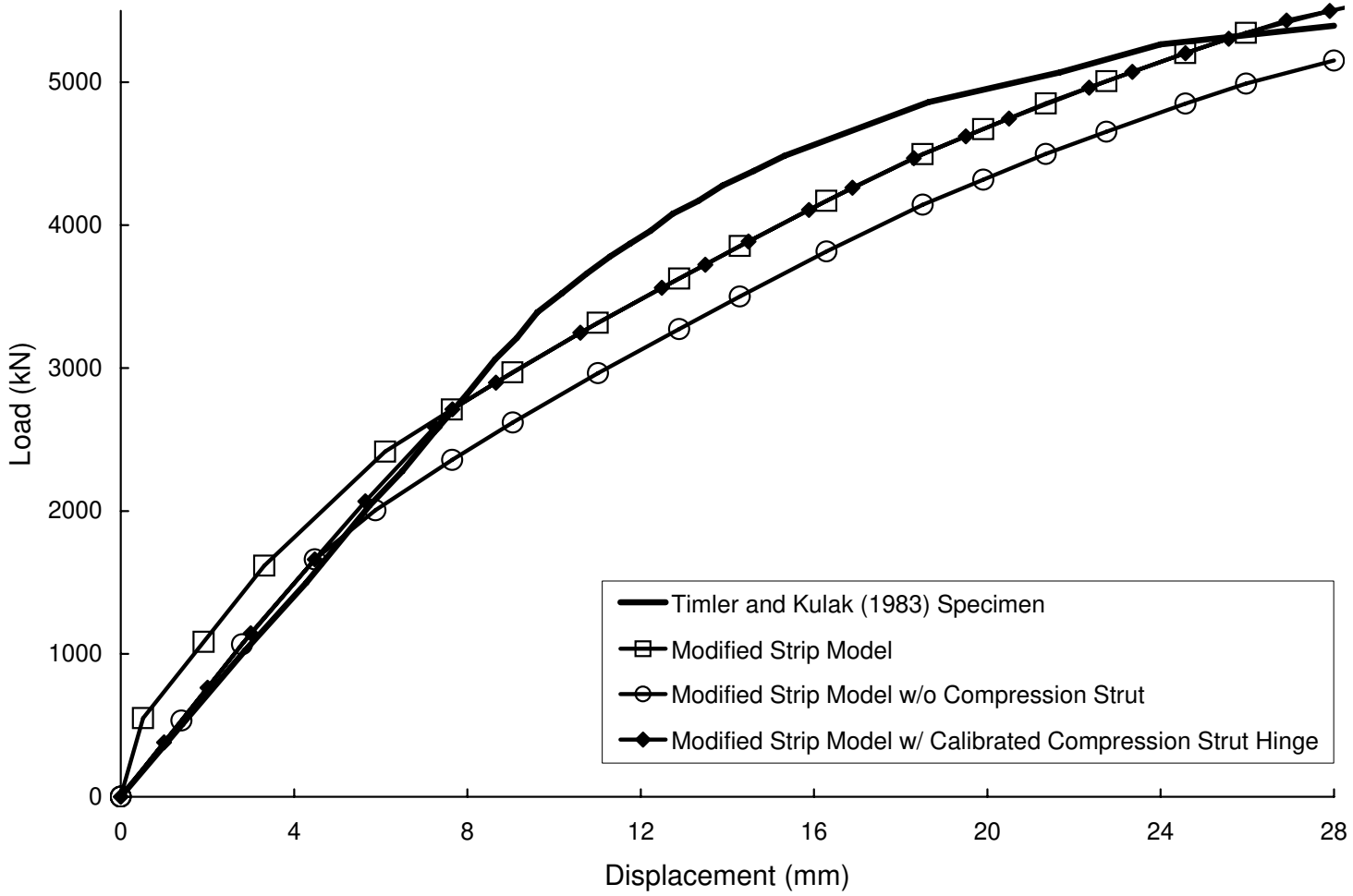

Figure 5.2 - Response Curves for Timler and Kulak (1983) Specimen and Various Modified Strip Models

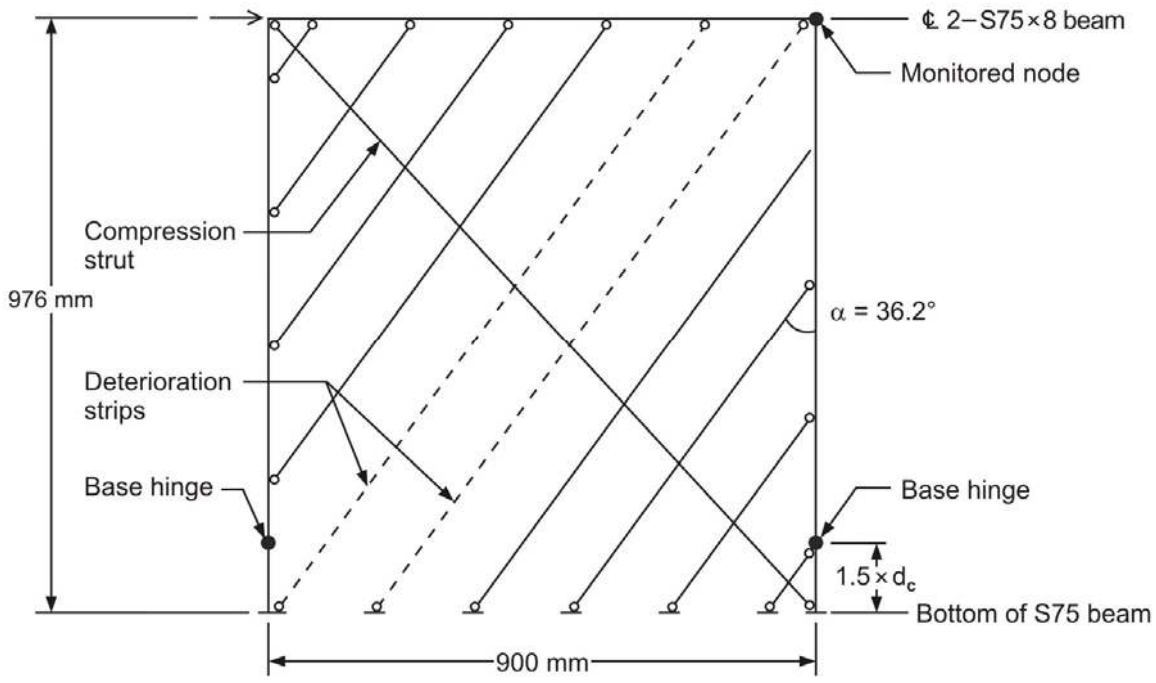

Figure 5.3 - Geometric Arrangement of SPSW2 (Lubell 1997) Specimen Using the Modified Strip Model

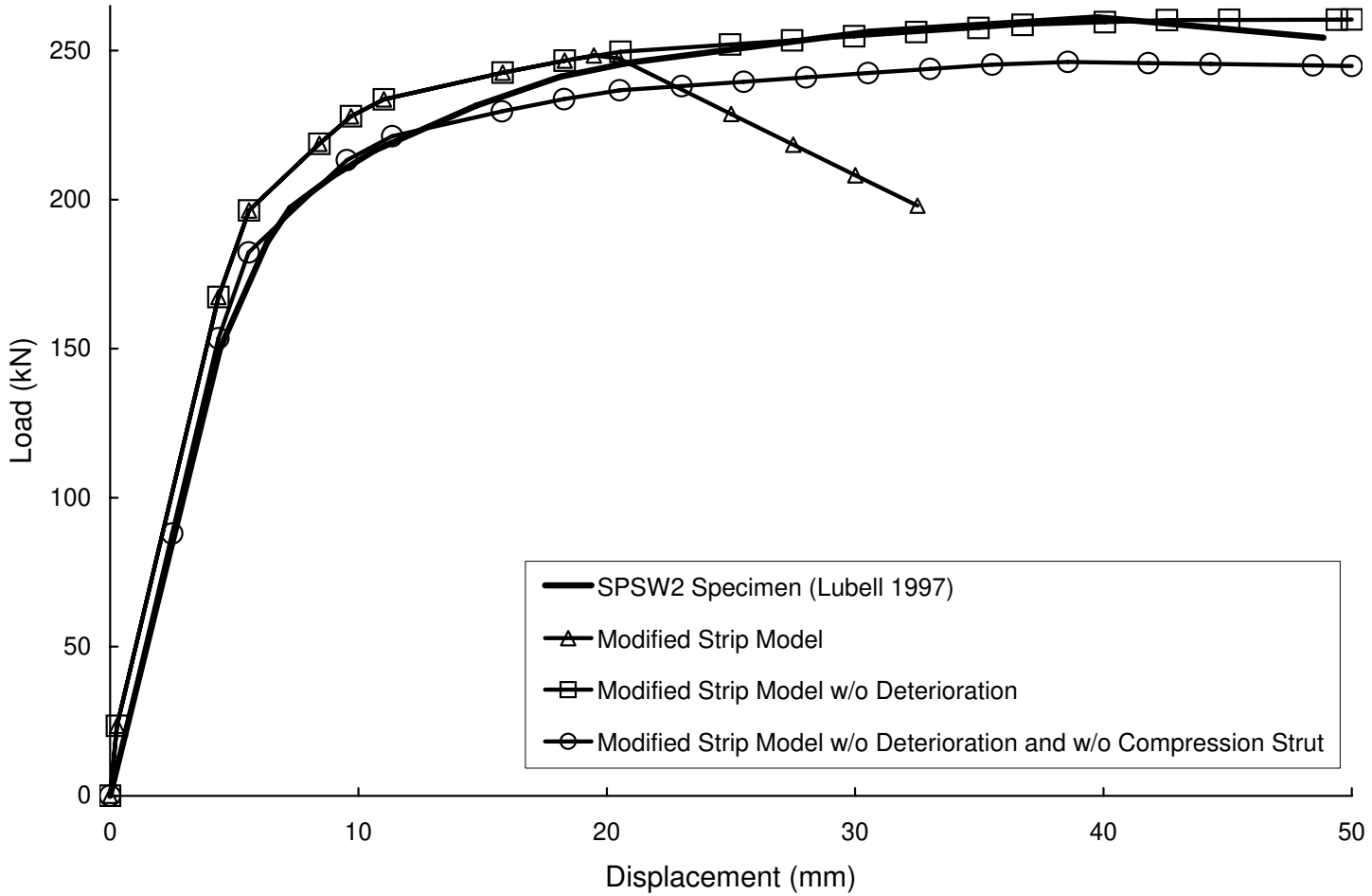

Figure 5.4 - Response Curves for SPSW2 (Lubell 1997) Specimen and Various Modified Strip Models

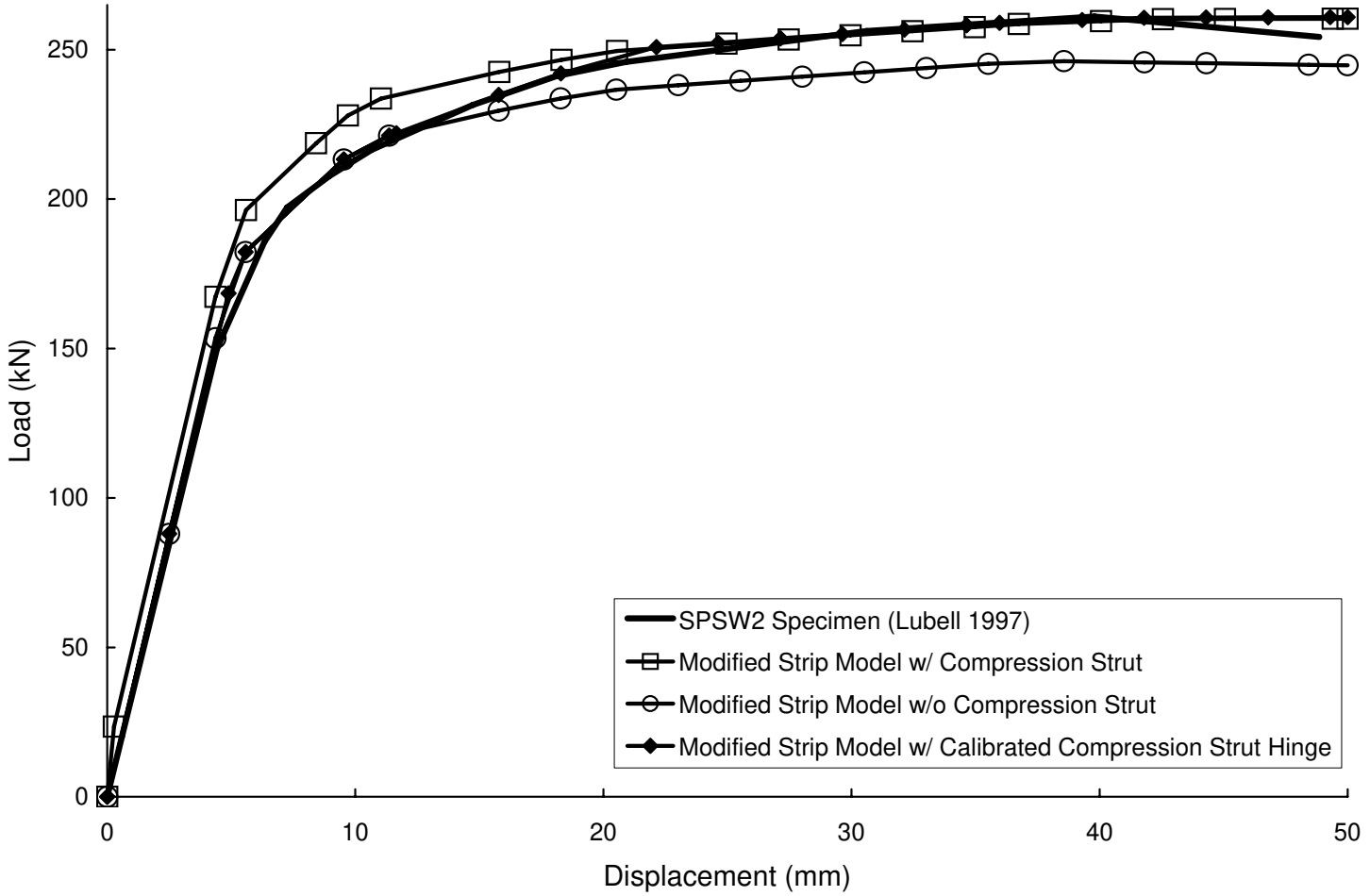

Figure 5.5 - Response Curves for SPSW2 (Lubell 1997) Specimen and Various Modified Strip Models

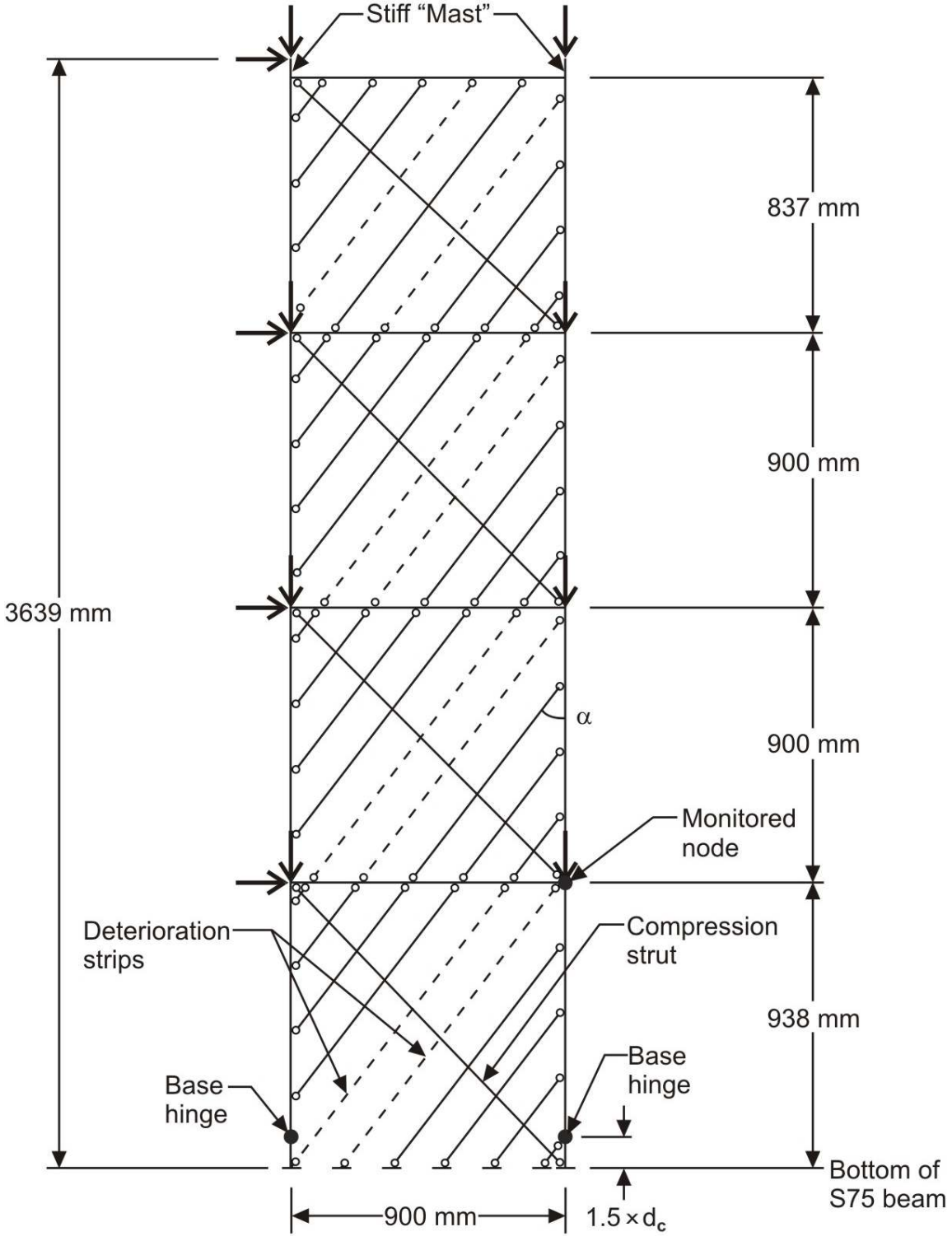

Figure 5.6 - Geometric Arrangement of SPSW4 (Lubell 1997) Specimen Using the Modified Strip Model

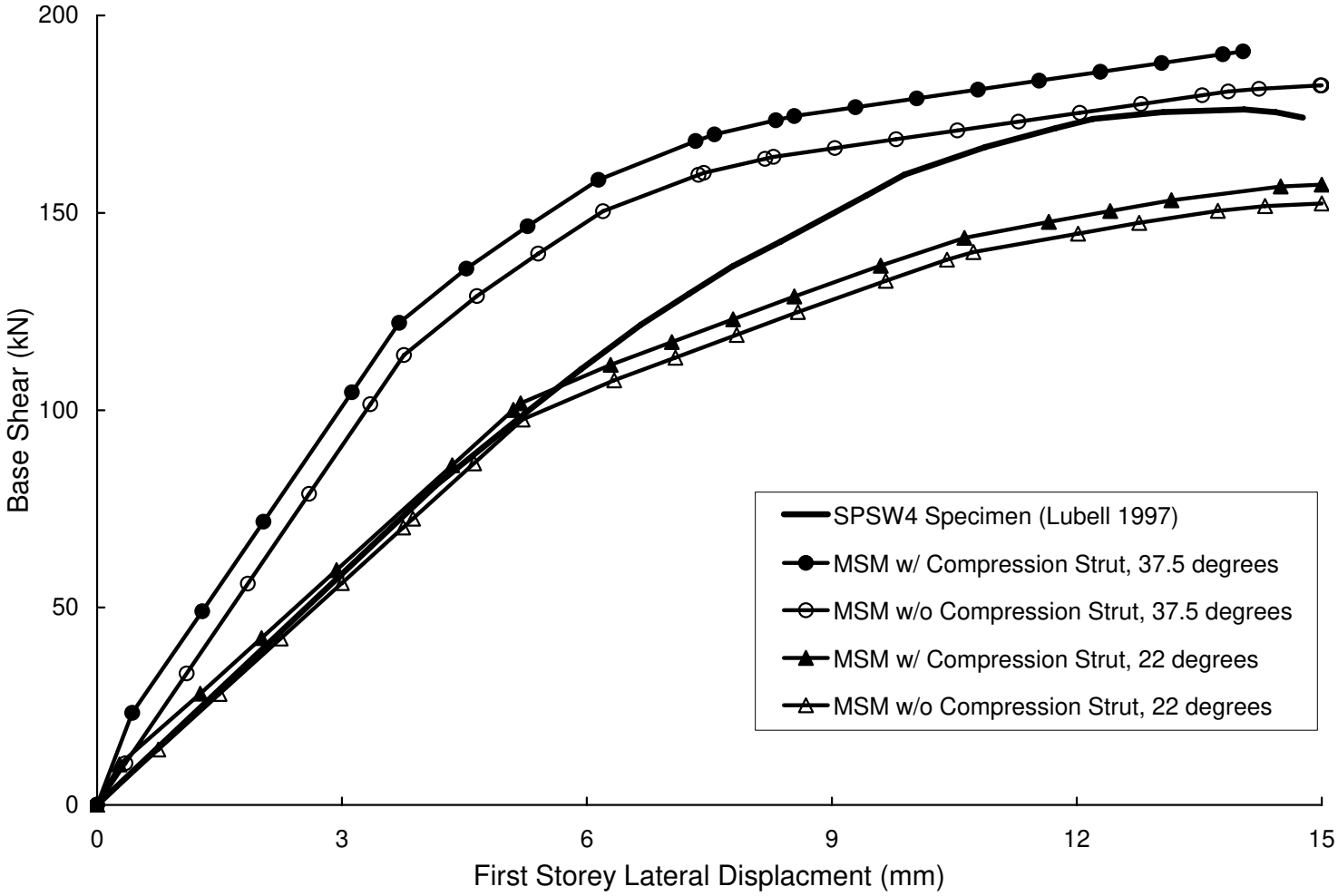

Figure 5.7 - First–Storey Response Curves for SPSW4 (Lubell 1997) Specimen and Various Modified Strip Models

6. PARAMETRIC STUDY

6.1 Introduction

The value for the angle of inclination of the tension field that develops in the infill plate, α, as described in Equation 2.3 or in Clause 20.3.1 of the Canadian steel design standard (CAN/CSA S16-01), is dependent on the thickness of the infill plate, the cross-sectional properties of the boundary members, and the height and width of each panel. Although the bay size and storey height of a building are normally fixed early in the design development, alterations to the boundary members or the infill plate can be a regular occurrence during the design of a steel plate shear wall. As a result, the value of α changes, thus requiring the strip model to be regenerated. Factors such as the lack of availability of a particular wide flange section or plate thickness and architectural changes can require alterations to the strip model. Thus, the design of steel plate shear walls can be a highly iterative and time-consuming process. It would be more convenient for the design engineer to be able to assume a single value of α throughout the design process, even though the columns, beams or infill plates could change.

This chapter investigates the influence that varying the value of α has on the inelastic behaviour of steel plate shear walls as predicted by the modified strip model. The parametric study described in this chapter stems from the findings of Driver *et al.* (1998b) that varying the value of α significantly had little effect on the predicted pushover curve of the four-storey one–bay specimen as represented by the original strip model. The modified strip model was applied to one-, four-, and fifteen-storey one–bay steel plate shear walls with either rigid or pinned beam-to-column connections. Certain non-dimensional parameters, as described in Section 6.3, were selected for study and incorporated into the models.

6.2 Design Criteria

The seismic loads for the design and analysis of the modelled steel plate shear walls were determined using the equivalent static force procedure, as described in the 2005 National Building Code of Canada (NBCC 2005) seismic load criteria. Each steel plate shear wall was designed as a "ductile frame plate shearwall," resulting in the assignment of a

ductility modification factor, R_d, of 5.0 and an overstrength modification factor, R_o, of 1.6. Also, each model was assumed to be one of two steel plate shear walls in a symmetric and regularly–shaped office building of normal importance located in Vancouver, British Columbia, Canada. It was assumed that each steel plate shear wall resists one-half of the design seismic loads, and torsional effects were assumed to be carried by transverse elements. Each building was assumed to contain a floor and roof area of 2000 m^2 and a foundation that was built upon rock (Site Class B).

The gravity loads, applied to the columns at each storey as a point load, consisted of dead, live, and snow loads. Dead loads were determined based on the assumed loads listed in Table 6.1. Snow loads were calculated based on criteria from NBCC 2005. For simplicity, it was assumed that the building had a flat roof with no parapets, the wind exposure was such that the snow load was not reduced, and no accumulations occurred. The live load on all floors was taken to be 2.4 kPa (NBCC 2005). The load combination, as defined by NBCC 2005, is as follows:

$$1.0D + 0.5LL + 0.25S + 1.0EQ \tag{6.1}$$

where D is the dead load, LL is the live load, S is the snow load, and EQ is the seismic (earthquake) load (the notation in the equation is slightly different from that used in the NBCC to avoid duplication of symbols used elsewhere in this report.). The tributary area for each column was assumed to be six metres times the centre-to-centre distance of the columns of the modelled steel plate shear wall. Live load reduction factors were not used in determining the design load at each level.

The design of the steel plate shear wall members for each parametric study model was based on the requirements of CAN/CSA S16-01. Because the infill plate is the primary energy-dissipating member, the boundary members were designed for a probable infill plate yield stress ($R_y \times F_{yPL}$) of 385 MPa, as required by the standard, where R_y is a factor applied to F_{yPL} to estimate the probable yield stress. An infill plate thickness of 3.0 mm was assumed to be the minimum practical thickness based on handling and welding considerations. The nominal yield stress of the beams and columns was assumed to be 350 MPa and all steel members were assumed to have a modulus of elasticity of

200 000 MPa. All boundary members were selected to be Class 1 sections. Capacity design was used on all models and thus, to ensure ductile behaviour, the seismic design loads in the columns were increased by an amplification factor, B, defined as the ratio of the probable shear resistance at the base of the steel plate shear wall, V_{re}, to the factored lateral seismic base force as determined by the equivalent static force method. CAN/CSA S16-01 states that B shall have a maximum value of R_d (5.0 for steel plate shear walls). V_{re} is defined as follows:

$$V_{re} = 0.5 R_y F_{yPL} t L \sin 2\alpha \tag{6.2}$$

A preliminary design was performed on all parametric study models using the equivalent brace method (Thorburn *et al.* 1983) to determine the forces in the plate—which is represented by a brace—and column sections. The effective length factors were assumed to be 1.0 for the preliminary design of the columns. Final design forces, obtained through a second–order elastic analysis using the modified strip model, are input into the beam-column interaction equations of CAN/CSA S16-01 to determine the final column cross-section. For this final column design check, the effective length factors of the columns were conservatively assumed to be 0.7 since the base of the columns were fixed. The compression strut axial force is checked to ensure it is below the limiting force value in the second–order elastic analysis. If it is not, this strut is removed and a "propping" force in the direction of the strut of $0.08 F_{yPL} A_{CS}$, where F_{yPL} is the infill plate yield stress and A_{CS} is the cross-sectional area of the strut, is applied at the panel corners where the strut was removed.

The top beam was designed assuming the formation of a full tension field along with the gravity roof loads acting on the section. Because of the minimum plate thickness selected, which was always greater than the thickness needed to carry the storey shear, the top beams for the wider steel plate shear walls were very heavy. In all cases, a standard rolled W-shape section was selected, although deeper welded sections may have been lighter. Intermediate beams were selected using factored dead and live floor loads since the tension field forces on either side of the section tend to offset one another. The beams were then checked under the forces obtained from the second-order elastic

analysis and found to be adequate. Pinned end conditions for the top and intermediate beams were conservatively assumed. In order to keep the intermediate beam cross-section constant during the parametric study, a W410×100 section was selected for each multi-storey model.

6.3 Parameters

Behbahanifard *et al.* (2003) selected eight scale–independent and non-dimensional parameters that have the potential to influence the predicted non-dimensional inelastic pushover curve of steel plate shear walls. It was found that only three of the parameters—aspect ratio, column flexibility, and normalised gravity load—had a significant influence on behaviour and also were relevant to the parametric study of the modified strip model. During the design process, it was found that the normalised gravity load parameter did not vary much (between 0.01 and 0.03.) Thus, to maintain a reasonably straightforward design process, the normalised gravity load parameter was not considered in the study. Therefore, the nonlinear behavioural effects of varying the value of α on structures with different aspect ratios and column flexibilities are investigated in this parametric study. The aspect ratio was varied by changing the length (distance between steel plate shear wall column centrelines), L, and keeping the storey height, h, constant. The column flexibility parameter was varied by using different column cross-sections while keeping the infill plate thickness and aspect ratio constant. CAN/CSA S16-01 defines the column flexibility parameter, ω_h, as follows:

$$\omega_h = 0.7\sqrt[4]{\frac{h^4 t}{2LI_c}} \tag{6.3}$$

where t is the infill plate thickness, I_c is the column moment of inertia, and the other parameters are as defined in Figure 6.1.

The effect of different beam-to-column connection types—rigid or pinned—on the nonlinear response as predicted by the modified strip model was also investigated. For the pinned beam-to-column models, no flexural plastic hinges or panel nodes were located on the beam elements and the strong–axis moment was released at the ends of

each beam. The flexural hinges and panel nodes remained on the columns at intermediate levels, but were removed at the top. The axial hinge for each compression strut was as developed for the Timler and Kulak specimen (with pinned beam-to-column connections) in Chapter 5.

Figure 6.1 shows the typical geometric arrangement of the first storey for each parametric study model, where L is the distance between the centrelines of each column and h is the interstorey height or the distance between the centrelines of each successive beam. For the first level, h is the height from the base of the model to the centreline of the first–storey beam. In order to apply the equivalent static force procedure, the building must be a regular structure that is less than 60 m in height with a fundamental period of less than 2 seconds (NBCC 2005). Selecting a constant value of $h = 3800$ mm, the structure can have a maximum number of fifteen storeys. Therefore, fifteen-storey structures were analysed in the parametric study, along with one- and four-storey steel plate shear walls. All parametric study models have fixed column bases.

A pushover analysis is conducted for each parametric study model. Gravity loads are first applied to their full value according to Equation 6.1, followed by the application of the seismic loads using displacement control. For all models in the parametric study, the node on the "lee" column at the first–storey beam is monitored for lateral deflections. The first storey is where interstorey deflections and shears are the largest under these loading conditions.

6.4 One-Storey Models

6.4.1 Model Arrangement and Design

Table 6.2 lists the parameters and designed members for the one-storey models. To facilitate the comparison of models with similar parameters, the models are arranged in four groups. Group 1-A keeps the values of ω_h constant at 2.5—the maximum allowed by CAN/CSA S16-01—while the aspect ratio varies among four values: 0.75, 1.0, 1.5, and 2.0. For Group 1-B, the aspect ratio has a constant value of 1.5 while the column sections are varied to reflect a column flexibility at the CAN/CSA S16-01 limit ($\omega_h = 2.5$) as well as column flexibilities below and above

the limit, herein referred to as "rigid" and "flexible" columns, respectively, for convenience. Both preceding groups employed rigid beam-to-column connections. Groups 1-C and 1-D are similar to Groups 1-A and 1-B, respectively, except pinned beam-to-column connections are utilised. Certain parameters that are a part of Groups 1-A and 1-B are not included in Groups 1-C and 1-D since similar patterns to that in Groups 1-A and 1-B could be discerned using fewer models.

For each set of parameters, two models with values of α at the limits prescribed by CAN/CSA S16-01 (38° and 50°) are analysed. For comparison purposes, the predicted value of α for each model is determined using the equation from CAN/CSA S16-01 (Equation 2.3) and is also shown in Table 6.2. Although Equation 2.4 appears to be more appropriate for one-storey models, it was found that for some models Equation 2.4 predicts an almost horizontal tension field. Therefore, to provide a better prediction for the value of α for each model, a slightly modified form of the finite element model using shell elements presented by Behbahanifard *et al.* (2003) is applied to each model to give the dominant value of α. Since the calculated values of α are all within the range of 38° and 50°, no additional models were included in the one-storey parametric study.

Using the equivalent static force procedure (NBCC 2005), the design base shear for each of the one-storey models is 119 kN. It should be noted that the minimum infill plate thickness required to resist the design forces is considerably lower than the assumed minimum practical plate thickness of 3.0 mm. Because of this, the value of B for all one-storey models is $R_d = 5.0$, the maximum value required by CAN/CSA S16-01. Even though the values of the design forces suggest lighter column sections could be used for the models than those listed in Table 6.2, the column flexibility requirement of CAN/CSA S16-01 ($\omega_h \leq 2.5$) demands the use of stockier sections. The design moments and axial forces in the columns are obtained from a second–order elastic analysis using the modified strip model with seismic loads determined from the equivalent static method (NBCC 2005) and amplified by the capacity design factor, B. From this analysis, it was found that the columns for all

the one-storey models, as listed in Table 6.4, easily met the CAN/CSA S16-01 beam-column interaction requirements.

6.4.2 Analysis and Results

Pushover curves were obtained from the one-storey models and arranged in their respective groups. Figure 6.2 shows the response curves for the one–storey models with rigid beam-to-column connections, column flexibilities at the CAN/CSA S16-01 limit, and various aspect ratios (Group 1-A). For each set of aspect ratios, the ultimate strengths for each model ($\alpha = 38°$ and 50°) are nearly identical. For the panel aspect ratio of 1.0, the initial stiffnesses were also nearly equal (2% difference) for $\alpha = 38°$ and 50°. For all parametric study models, the initial stiffness was calculated from the point closest to initial yield and with the origin as the reference point. As the aspect ratio increases, the predicted initial stiffnesses of models with $\alpha = 38°$ become somewhat lower than those with $\alpha = 50°$. Figure 6.3 shows the pushover curves for the models with rigid beam-to-column connections, an aspect ratio of 1.5, and various column flexibilities (Group 1-B). In all cases, the models with $\alpha = 38°$ provided a more conservative estimate of the initial stiffness than those with $\alpha = 50°$ (between 10 and 15% difference) and the predicted ultimate strengths are in good agreement with one another. Table 6.3 shows the comparison of the predicted ultimate strength values for the one-storey parametric study models. With the exception of the 1-B model that violated the column flexibility design criterion, the 38° models with rigid beam-to-column connections always predicted slightly lower strengths than the 50° models.

Figure 6.4 shows the response curves for the models with pinned beam-to-column connections, $\omega_h = 2.5$, and various aspect ratios (Group 1-C), while Figure 6.5 shows the response curves for the models with pinned beam-to-column connections, an aspect ratio of 1.5, and two different column flexibilities (Group 1-D). The pushover results from Groups 1-C and 1-D are similar to those of Groups 1-A and 1-B, respectively. As shown in Table 6.3, for the one-storey steel plate shear walls with pinned beam-to-column connections, in some cases the 38° model provided the lower

strength and in others it was the 50° model, although the results are similar in all cases.

Table 6.3 and Figures 6.2 through 6.5 demonstrate that the value of α does not greatly influence the predicted inelastic response of the modified strip model for one-storey steel plate shear walls of various geometric arrangements, column flexibilities, and beam-to-column connection types. In particular, the prediction of the ultimate strength for these models is relatively insensitive to the angle of inclination of the tension strips. It would seem reasonable that a single value of $\alpha = 40°$ could be specified for any one-storey steel plate shear wall, which would result in generally conservative pushover curves—in terms of both initial stiffness and ultimate strength—as long as the wall proportions are within or near the range considered. It should be noted that the capacities of all the steel plate shear walls exceed the design base shear, as determined by the equivalent static force procedure (NBCC 2005), by a considerable amount. This reflects the fact that the minimum practical plate thickness selected is significantly in excess of that theoretically required, which in turn increases the column sizes required to meet the column flexibility limit (CAN/CSA S16-01) and the demand increased by the capacity design factor, *B*.

6.5 Four-Storey Models

6.5.1 Model Arrangement and Design

Table 6.4 lists the parameters and the designed members for the four-storey models, which are grouped in a similar fashion to the one-storey models. For each set of parameters, one model is analysed with the tension–only strips oriented at 38°, while another is analysed with the strips oriented at 50°. For comparison purposes, the average values of α, calculated using the CAN/CSA S16-01 equation (Equation 2.3) for each level, are shown in Table 6.4. Since the calculated values of α are all within the range of 38° and 50°, no additional models are created using these values.

Using the equivalent static force procedure (NBCC 2005), the design base shear for each of the four-storey models is 1142 kN. The column cross-section and infill plate

thickness selected for each model is the same for each storey. As in the case of the one-storey models, the assumed minimum practical plate thickness of 3.0 mm is sufficient for all four-storey models. However, the difference between 3.0 mm and the minimum infill plate thickness required, as determined by the design forces, is less than that for the one–storey models. Thus, the values of *B*, as listed in Table 6.4, are less than the maximum value specified by CAN/CSA S16-01.

For the case of the models with aspect ratios of 1.5 and 2.0, the values of ω_h used for the one–storey models could not be used without unrealistically thick infill plates. (The reason for this is that a column section selected to obtain a value of ω_h equal to the limit specified in CAN/CSA S16-01, along with the minimum practical infill plate thickness, would not satisfy the design capacity requirements. Increasing the plate thickness also increases the design forces in the columns until the maximum value of the parameter *B* is reached and only then could the column flexibility limit and the capacity requirements be satisfied simultaneously.) Therefore, keeping the infill plate at the assumed minimum practical thickness of 3.0 mm, the column sections for the models with aspect ratios of 1.5 and 2.0 were designed so that ω_h would be as close to 2.5 as the design column forces would allow. Due to this restriction, a reasonable design for the flexible column could not be obtained and thus was omitted from the four-storey parametric study. The moments and axial forces of the columns are obtained from a second–order elastic analysis using the modified strip model with seismic loads determined from the equivalent static method (NBCC 2005) and amplified by the capacity design factor, *B*. From this analysis, it was found that the columns for all the four-storey models, as listed in Table 6.4, met the CAN/CSA S16-01 beam-column interaction requirements.

6.5.2 Analysis and Results

Pushover curves were obtained from the four-storey models and arranged in their respective groups. It should be noted that for the models with pinned beam-to-column connections (Groups 4-C and 4-D), a slight slope (0.0001:1) had to be input on the zero compression portion of the tension–only strip and deterioration axial hinges to achieve convergence. Even though the effect of this was determined to be negligible,

it was found that convergence could not be attained for the model with an aspect ratio of 0.75 and pinned beam-to-column connections. Thus, the pushover results of this model could not be presented.

Figure 6.6 shows the pushover curves for the four-storey models with rigid beam-to-column connections, column flexibilities at or as near as possible to the CAN/CSA S16-01 limit while maintaining the minimum practical infill plate thickness, and various aspect ratios (Group 4-A). For each aspect ratio, it can be seen that there is little difference between the curves for the two models ($\alpha = 38°$ and 50°) up to the ultimate strength (between 2 and 10% difference in initial stiffness). Figure 6.7 shows the pushover curves for the four-storey models with rigid beam-to-column connections, an aspect ratio of 1.5, and two different column flexibilities (Group 4-B). For each column flexibility, the initial stiffnesses of the two models ($\alpha = 38°$ and 50°) are nearly identical, varying between 0 and 3%. Also, the ultimate strength predicted by the 38° model either agreed well with or was slightly lower than that of the 50° model.

Figure 6.8 shows the response curves for the four-storey models with pinned beam-to-column connections, column flexibilities as near as possible to ω_h=2.5, and various aspect ratios (Group 4-C), while Figure 6.9 shows the pushover curves for the four-storey models with pinned beam-to-column connections, an aspect ratio of 1.5, and two different column flexibilities (Group 4-D). The pushover results from Groups 4-C and 4-D are similar to those of Groups 4-A and 4-B, respectively, with the exception that the curves for the models with an aspect ratio of 2.0 in Group 4-C tend to diverge somewhat near the peak of the curve. In this latter case, however, the prediction of the ultimate strength for $\alpha = 38°$ is again lower than that for $\alpha = 50°$. Table 6.5 shows the comparisons of the predicted ultimate strength values for the four-storey parametric study models. The predicted shear wall capacities using the two extremes of the angle of inclination of the tension field are close in all cases, and with only one exception the angle $\alpha = 38°$ leads to a lower value.

Table 6.5 and Figures 6.6 through 6.9 suggest that the value of α does not greatly influence the predicted inelastic response of the modified strip model for four-storey steel plate shear walls of various geometric arrangements, column flexibilities, and beam-to-column connection types. As in the case of the one-storey models, it would seem reasonable that a value of $\alpha = 40°$ could be specified for any four-storey steel plate shear wall, which would result in generally conservative pushover curves. It should be noted that the capacities of all the four-storey steel plate shear wall models significantly exceed the design base shear as determined by the equivalent static force procedure (2005 NBCC), although not to the same degree as the one-storey models due to the lower value of the capacity design factor, *B*.

The moments and axial forces for the first–storey columns of each four-storey model were extracted from the pushover analysis at the peak level of the respective response curve. The interaction equations of CAN/CSA S16-01 predict that the columns experiencing combined compression and bending moment forces for each model would be inadequate by approximately 30%. For columns experiencing combined tension and bending moment forces, it was found that most column sections were adequate, although there were some cases where the interaction equations predicted an understrength. These results seem to imply that the pushover curves may not be accurate in terms of overall system strength and ductility due to the column capacity limit. For comparison, the first–storey column forces were also extracted from the modified strip model of the Driver *et al.* (1998a) specimen at the peak overall capacity. Using the nominal yield strength and modulus of elasticity of the columns for the specimen, the first–storey column of the specimen was also found to be inadequate in compression–moment interaction by approximately 45% and tension–moment interaction by approximately 35% (the understrength is approximately 40% and 30%, respectively, when measured material properties are utilised). However, failure of the specimen did not occur until well after the maximum strength of the specimen was achieved. This suggests that the beam-column interaction equations of CAN/CSA S16-01 provide conservative results when frame forces from the modified strip model are used.

6.6 Fifteen-Storey Models

6.6.1 Model Arrangement and Design

Table 6.6 lists the parameters and designed members for the fifteen-storey models. For each set of parameters, one model is analysed with the tension–only strips oriented at 38° and the another is analysed with the strips oriented at 50°. For comparison, the average values of α, calculated using the CAN/CSA S16-01 equation (Equation 2.3) for each level, are also presented in Table 6.6. For the fifteen-storey case, only steel plate shear walls with rigid beam-to-column connections are analysed.

Using the equivalent static force procedure (NBCC 2005), the design base shear for each of the fifteen-storey models is 1800 kN. For the design of these models, a reduction in the overturning moments is implemented as permitted by NBCC 2005 to account for higher modes of vibration. However, this reduction is not present in the pushover analysis of the models. Three-storey column lifts of a single section are assumed for the design of each steel plate shear wall. It was found that the minimum practical infill plate thickness of 3.0 mm was again adequate to resist the base shear in all storeys. For the case of the model with an aspect ratio of 0.75, the capacity design factor for the column, B, is determined to be 0.9. Since B only considers the contribution of the infill plate and not the steel frame, a value of less than one is possible. Due to the high column loads, the lowest column cross-sections could not be designed at $\omega_h = 2.5$ with the selected infill plate thickness. Therefore, the column sections at the bottom of each model are sized based on the design column forces only. Because of this restriction and the low values of ω_h for the lower column sections, a separate model group that varies the column flexibilities is not included for the fifteen-storey parametric study. Also, near the top of the modelled steel plate shear walls, the size of the column cross-section is governed by the $\omega_h \leq 2.5$ requirement rather than the column design forces. The moments and axial forces in the columns are obtained from a second–order elastic analysis using the modified strip model with seismic loads determined from the equivalent static method (NBCC 2005) and amplified by the capacity design factor, B. From this analysis, it

was found that the columns for all the fifteen-storey models, as listed in Table 6.6, met the CAN/CSA S16-01 beam-column interaction requirements.

6.6.2 Analysis and Results

Pushover curves were obtained from the fifteen-storey models. A slight slope (0.0001:1) had to be input on the zero compression portion of the tension–only strip and deterioration axial hinges for all models to assist in achieving convergence. Also, at the start of the analysis, the models had to be pushed slightly using the seismic load pattern in order to avoid numerical instabilities while the gravity loads were applied. Despite these efforts, full pushover curves could not be obtained for some models, as can be seen in Figure 6.10. However, these "partial" pushover curves define the initial stiffness, initial yield, and post-yield portions of the predicted steel plate shear wall inelastic response up to very near to the ultimate capacity, but they do not predict the deterioration of strength. Even though only partial pushover curves could be obtained for some models, a comparison between the 38° and 50° models is still possible.

Figure 6.10 shows the pushover curves for the fifteen-storey models. It can be seen that for each aspect ratio, the curves of the two models ($\alpha = 38°$ and 50°) are nearly identical, with the initial stiffnesses differing by between 0 and 5%. Table 6.7 shows a comparison of the predicted ultimate strength (base shear) values for the fifteen-storey parametric study models. Where partial pushover curves are concerned, the final point is taken as the ultimate strength. Table 6.7 and Figure 6.10 suggest that the value of α does not significantly influence the predicted inelastic response of the modified strip model for fifteen–storey steel plate shear walls of various geometric arrangements with rigid beam-to-column connections. As for the cases of the one- and four-storey models, it would seem reasonable that a value of $\alpha = 40°$ could be specified for any fifteen-storey steel plate shear wall. Figure 6.10 also shows that the capacities of all the steel plate shear walls exceed the design base shear as determined from the 2005 NBCC. The pushover curves for the models with an aspect ratio of 0.75 reach the design base shear just before significant yielding of the model begins.

For the models with aspect ratios of 1.5 and 2.0, the design base shear is well within the elastic range of each steel plate shear wall model.

6.7 Summary

A parametric study was conducted to determine the effect of varying the value of α on the inelastic response of steel plate shear walls modelled using the modified strip model. Each model represents one of two identical steel plate shear walls that equally share the seismic load imposed on a regular office building located in Vancouver, British Columbia. Each member of each steel plate shear wall was designed according to the seismic requirements of NBCC 2005 and CAN/CSA S16-01. Two values of α (38° and 50°) were applied to one-, four-, and fifteen-storey steel plate shear walls of different aspect ratios, column flexibilities, and beam-to-column connection types.

It was found that the predicted inelastic response of the modified strip model was fairly insensitive to the value of α selected. Most importantly, the values of the ultimate base shear varied little when the angle of inclination of the tension strips changed from 38° to 50°, the extreme values permitted by CAN/CSA S16-01. This phenomenon arises because as the orientation of the tension strip force changes, so does the area of each individual strip. These effects tend to offset one another, resulting in similar base shear capacities. Since the pushover results for the 38° models were generally slightly conservative when compared to those for the 50° models, it is proposed that a value of $\alpha = 40°$ could be used throughout the entire design procedure of a steel plate shear wall and give conservative but accurate results. In any case, the values of α determined using the current CAN/CSA S16-01 procedure are generally close to 40° for the entire range of parameters studied (see Tables 6.2, 6.4, and 6.6). Although estimates of the initial stiffness could be significantly conservative for certain cases of one-storey shear walls, thus leading to an overestimate of lateral deflections, for such low structures deflections are unlikely to be a concern for design.

It is evident from the parametric study that the minimum practical plate thickness has a large effect on the economics of low- and mid-rise steel plate shear walls, even in high

seismic zones. The column cross-sections required for each steel plate shear wall model are extremely stocky in order to meet the capacity design requirements and the column flexibility limit. To improve the economic viability of steel plate shear walls, the use of low-yield steel grades for the infill plates may be required. It was also found that for certain cases (*i.e.*, one-storey buildings or near the top of multi-storey buildings), the limiting value of $\omega_h \leq 2.5$ (CAN/CSA S16-01), rather than the design forces, can govern the column design of a steel plate shear wall. For the one- and four-storey parametric study models, the predicted capacity of the steel plate shear walls exceeded the design base shear, as determined by the equivalent static force method (NBCC 2005), by a significant amount due to the overstrength of the infill plates and the resulting heavy boundary members.

Table 6.1 - Summary of Dead Loads

Roof Loads		Floor Loads	
Steel deck	0.10 kPa	Steel deck	0.10 kPa
Insulation	0.10 kPa	Normal density concrete deck slab	2.55 kPa
Asphalt and gravel	0.32 kPa	Carpeting	0.10 kPa
Suspended ceiling with light fixtures	0.20 kPa	Suspended ceiling with light fixtures	0.20 kPa
HVAC ducts/wiring allowance	0.25 kPa	HVAC ducts/wiring allowance	0.25 kPa
Steel allowance	0.15 kPa	Partitions	0.50 kPa
		Steel allowance	0.56 kPa
Total	1.12 kPa	Total	4.26 kPa

Table 6.2 - Summary of One-Storey Models

Group	α (degrees)			Aspect Ratio, L/h	ω_h	B	Beam-to-Col. Conn. Type	Column Section	Top Beam Section	t (mm)
	Model	S16-01	FEA							
1-A	38	39.7	41.0	0.75	2.5	5.0	Rigid	W310×253	W310×143	3.0
	50									
	38	40.4	42.5	1.0	2.5	5.0	Rigid	W310×202	W530×196	3.0
	50									
	38	42.4	42.0	1.5	2.5	5.0	Rigid	W310×143	W610×372	3.0
	50									
	38	43.3	47.0	2.0	2.5	5.0	Rigid	W250×149	W760×582	3.0
	50									
1-B	38	44.7	45.0	1.5	1.7	5.0	Rigid	W610×174	W610×372	3.0
	50									
	38	42.4	42.0	1.5	2.5	5.0	Rigid	W310×143	W610×372	3.0
	50									
	38	40.3	42.0	1.5	3.1	5.0	Rigid	W250×89	W610×372	3.0
	50									
1-C	38	39.7	—	0.75	2.5	5.0	Pinned	W310×253	W310×143	3.0
	50									
	38	42.4	—	1.5	2.5	5.0	Pinned	W310×143	W610×372	3.0
	50									
	38	43.3	—	2.0	2.5	5.0	Pinned	W250×149	W760×582	3.0
	50									
1-D	38	44.7	—	1.5	1.7	5.0	Pinned	W610×174	W610×372	3.0
	50									
	38	42.4	—	1.5	2.5	5.0	Pinned	W310×143	W610×372	3.0
	50									

Table 6.3 - Predicted Ultimate Strengths of One-Storey Models

Group	Aspect Ratio, L/h	ω_h	α (degrees)	Predicted Ultimate Strength (kN)	% diff*.
1-A	0.75	2.5	38	3066	+1.6%
			50	3115	
	1.0	2.5	38	3447	+0.8%
			50	3473	
	1.5	2.5	38	4041	+2.0%
			50	4120	
	2.0	2.5	38	5065	+1.4%
			50	5138	
1-B	1.5	1.7	38	5228	+3.0%
			50	5384	
	1.5	2.5	38	4041	+2.0%
			50	4120	
	1.5	3.1	38	3499	-3.7%
			50	3369	
1-C	0.75	2.5	38	2492	+0.1%
			50	2493	
	1.5	2.5	38	3684	-2.5%
			50	3590	
	2.0	2.5	38	4747	-2.5%
			50	4630	
1-D	1.5	1.7	38	4223	+2.6%
			50	4332	
	1.5	2.5	38	3684	-2.5%
			50	3590	

* 50 degree model as compared to 38 degree model

Table 6.4 - Summary of Four-Storey Models

Group	α (degrees)		Aspect Ratio, L/h	ω_h	B	Beam-to-Col. Conn. Type	Column Section	Top Beam Section	t (mm)
	Model	S16-01							
4-A	38	38.9	0.75	2.5	1.4	Rigid	W310×253	W310×143	3.0
	50								
	38	39.5	1.0	2.5	1.9	Rigid	W310×202	W530×196	3.0
	50								
	38	41.2	1.5	2.2	2.8	Rigid	W310×226	W610×372	3.0
	50								
	38	42.2	2.0	2.0	3.7	Rigid	W310×253	W760×582	3.0
	50								
4-B	38	42.5	1.5	1.6	2.8	Rigid	W610×217	W610×372	3.0
	50								
	38	41.2	1.5	2.2	2.8	Rigid	W310×226	W610×372	3.0
	50								
4-C	38	41.2	1.5	2.2	2.8	Pinned	W310×226	W610×372	3.0
	50								
	38	42.2	2.0	2.0	3.7	Pinned	W310×253	W760×582	3.0
	50								
4-D	38	42.5	1.5	1.6	2.8	Pinned	W610×217	W610×372	3.0
	50								
	38	41.2	1.5	2.2	2.8	Pinned	W310×226	W610×372	3.0
	50								

Table 6.5 - Predicted Ultimate Strengths of Four-Storey Models

Group	Aspect Ratio, L/h	ω_h	α (degrees)	Predicted Ultimate Strength (kN)	% diff*.
4-A	0.75	2.5	38	2347	+0.4%
			50	2357	
	1.0	2.5	38	2680	-0.6%
			50	2665	
	1.5	2.2	38	3913	0.0%
			50	3913	
	2.0	2.0	38	5244	+0.8%
			50	5285	
4-B	1.5	1.6	38	4362	+4.2%
			50	4546	
	1.5	2.2	38	3913	0.0%
			50	3913	
4-C	1.5	2.2	38	3861	+0.8%
			50	3892	
	2.0	2.0	38	5159	+6.3%
			50	5484	
4-D	1.5	1.6	38	4187	+2.0%
			50	4272	
	1.5	2.2	38	3861	+0.8%
			50	3892	

* 50 degree model as compared to 38 degree model

Table 6.6 - Summary of Fifteen-Storey Models

α (degrees)		L/h	ω_h (First storey)	B	Storeys 1-3		Storeys 4-6		Storeys 7-9		Storeys 10-12		Storeys 13-15	
Model	S16 -01				Column Sections	*t* (mm)	Column Sections	*t* (mm)	Column Sections	*t* (mm)	Column Sections	*t* (mm)	Column Sections	*t* (mm)
38	39.4	0.75	1.7	0.9	W360×818	3.0	W360×592	3.0	W360×382	3.0	W360×216	3.0	W360×216	3.0
50														
38	41.0	1.5	1.4	1.8	W360×744	3.0	W360×551	3.0	W360×347	3.0	W360×196	3.0	W360×110	3.0
50														
38	41.6	2.0	1.3	2.4	W360×744	3.0	W360×551	3.0	W360×382	3.0	W360×216	3.0	W360×91	3.0
50														

Table 6.7 - Predicted Ultimate Strengths of Fifteen-Storey Models

Aspect Ratio, L/h	ω_h	α (degrees)	Predicted Ultimate Strength (kN)	% diff*.
0.75	1.7	38	2491	+0.5%
		50	2503	
1.5	1.4	38	4012	-0.2%
		50	4003	
2.0	1.3	38	5172	+1.3%
		50	5239	

* 50 degree model as compared to 38 degree model

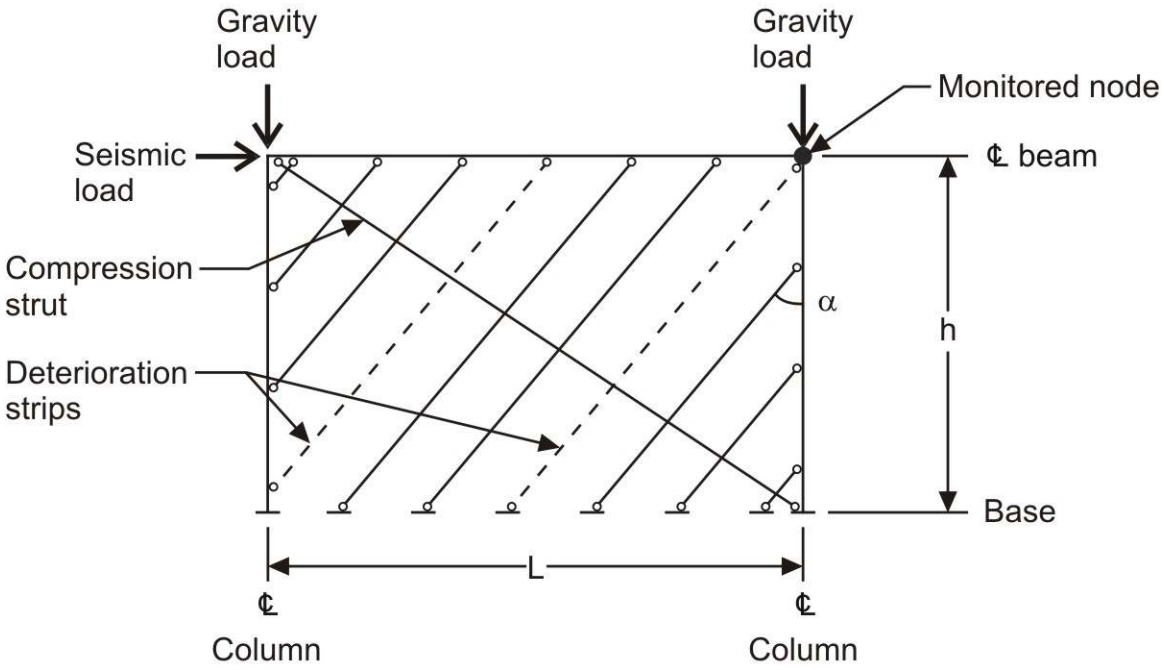

Figure 6.1 - Typical Geometric Arrangement for Parametric Study Models

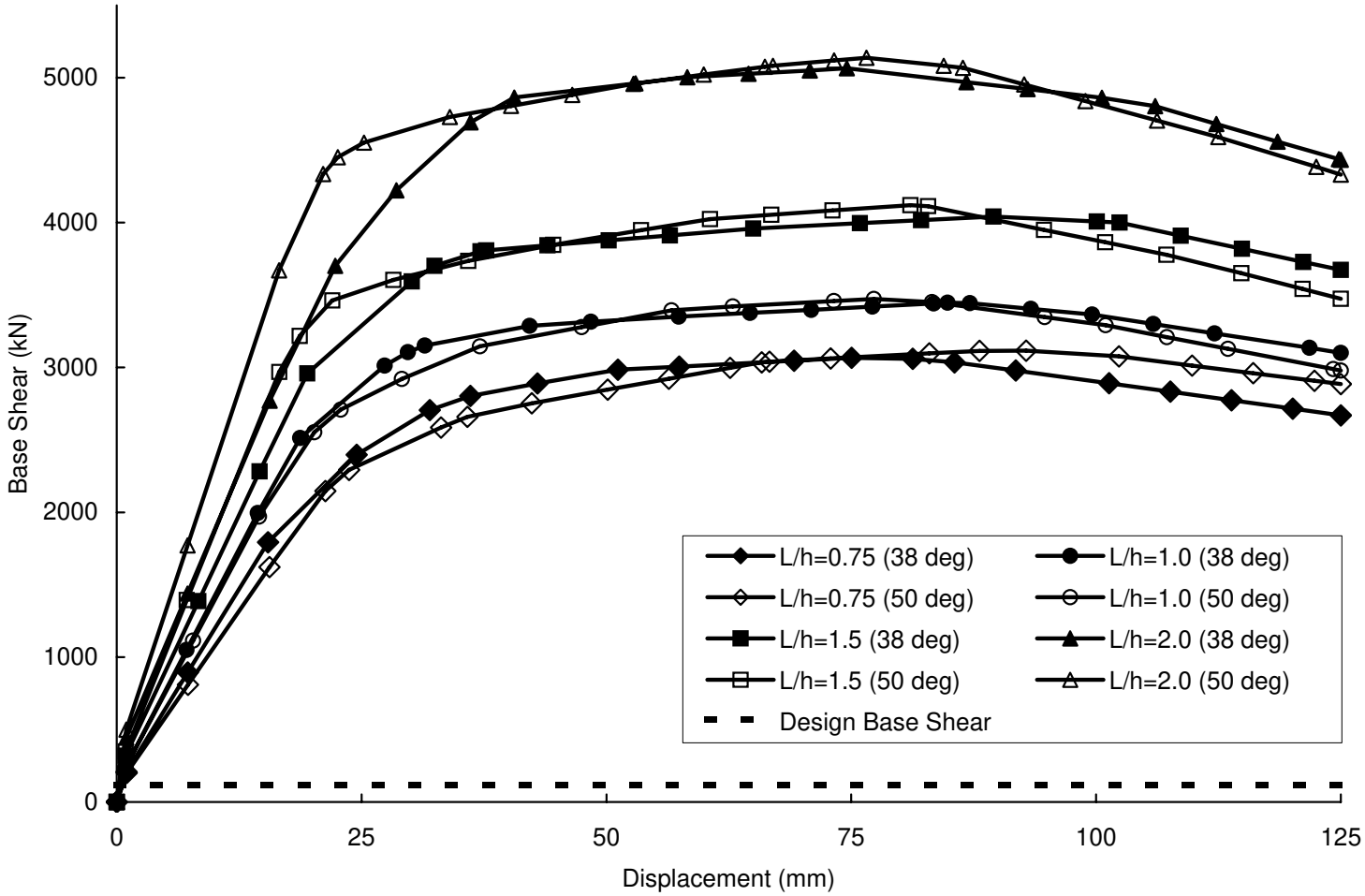

Figure 6.2 - Response Curves for Group 1-A Models

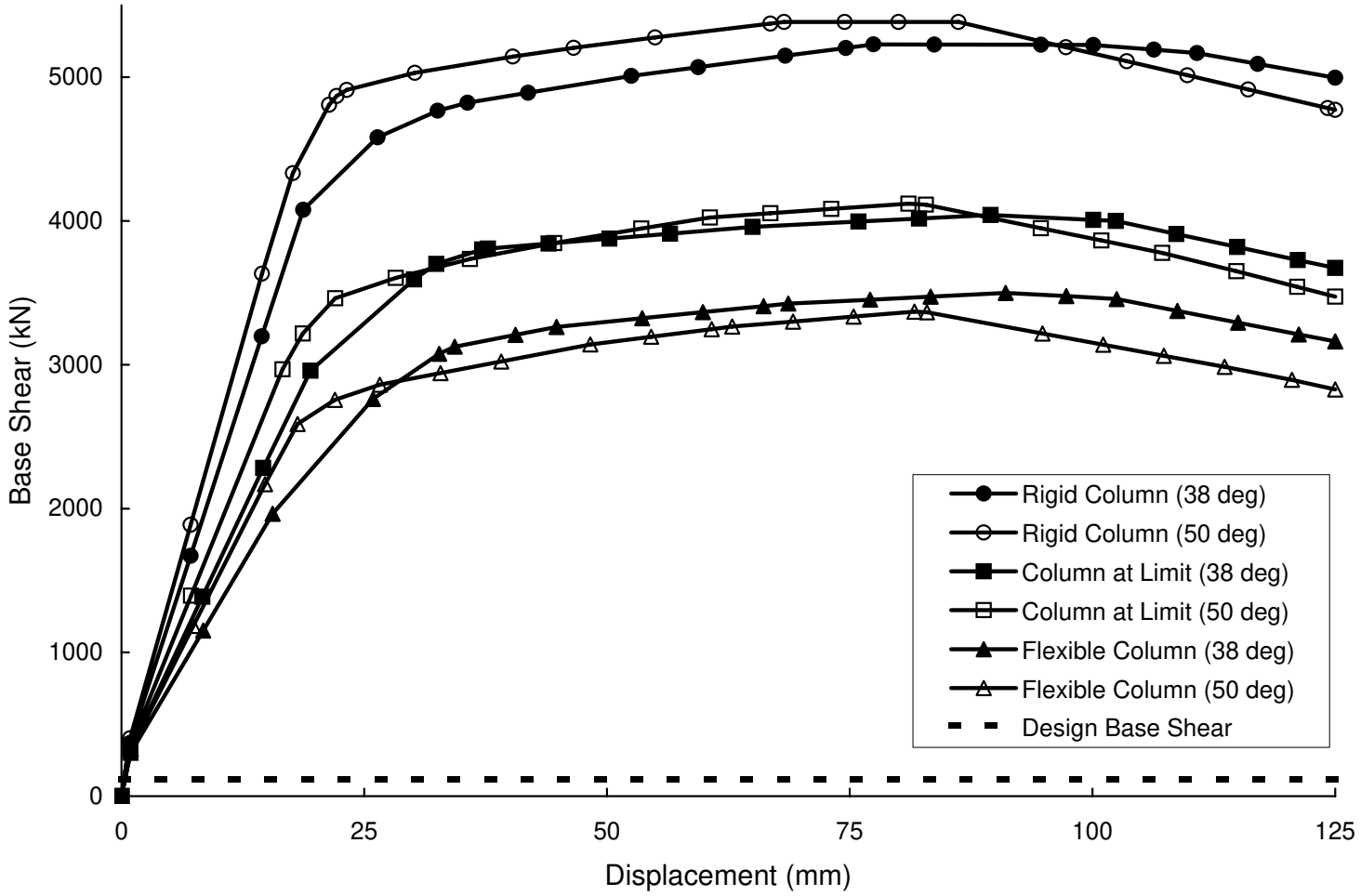

Figure 6.3 - Response Curves for Group 1-B Models

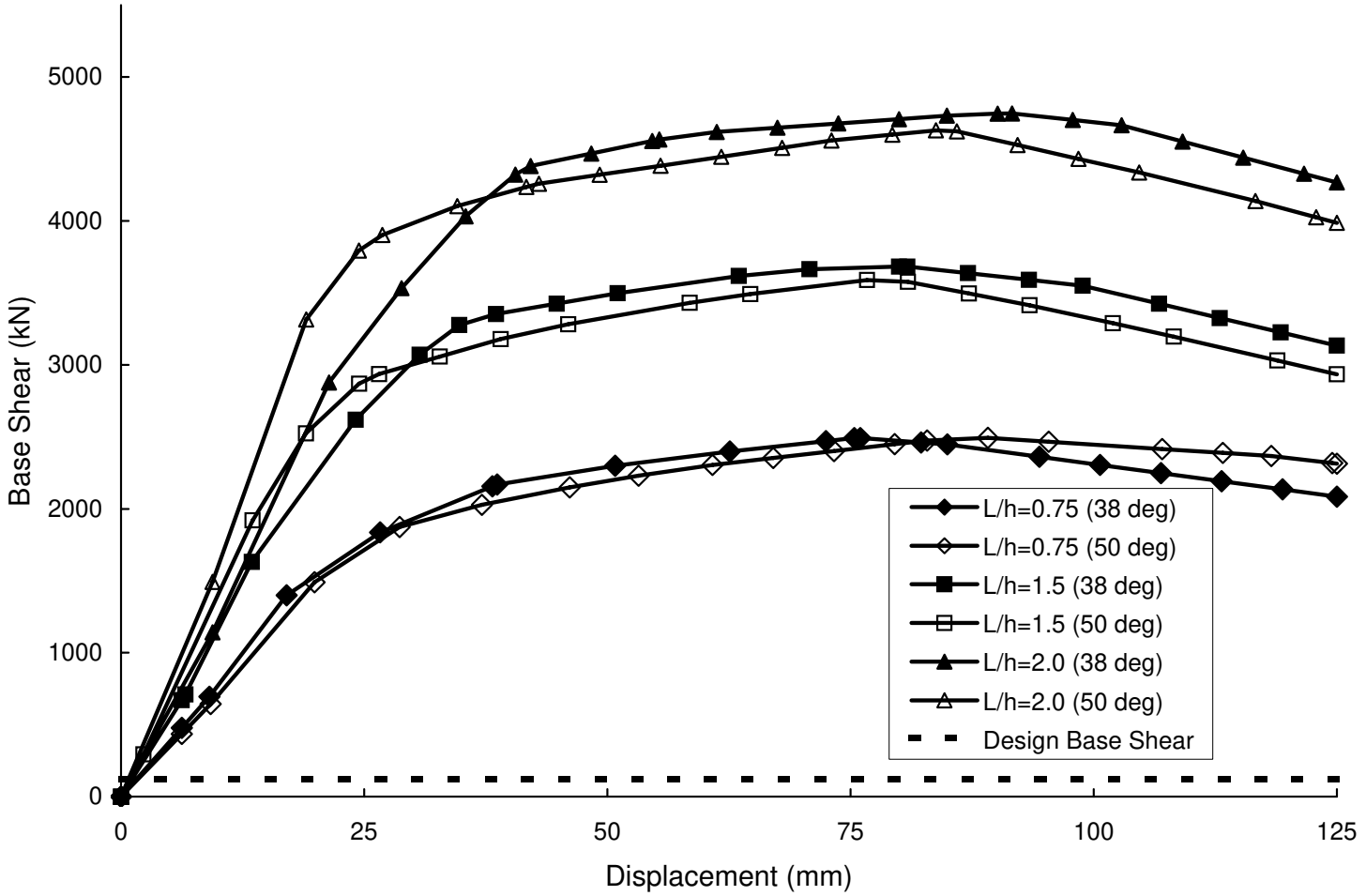

Figure 6.4 - Response Curves for Group 1-C Models

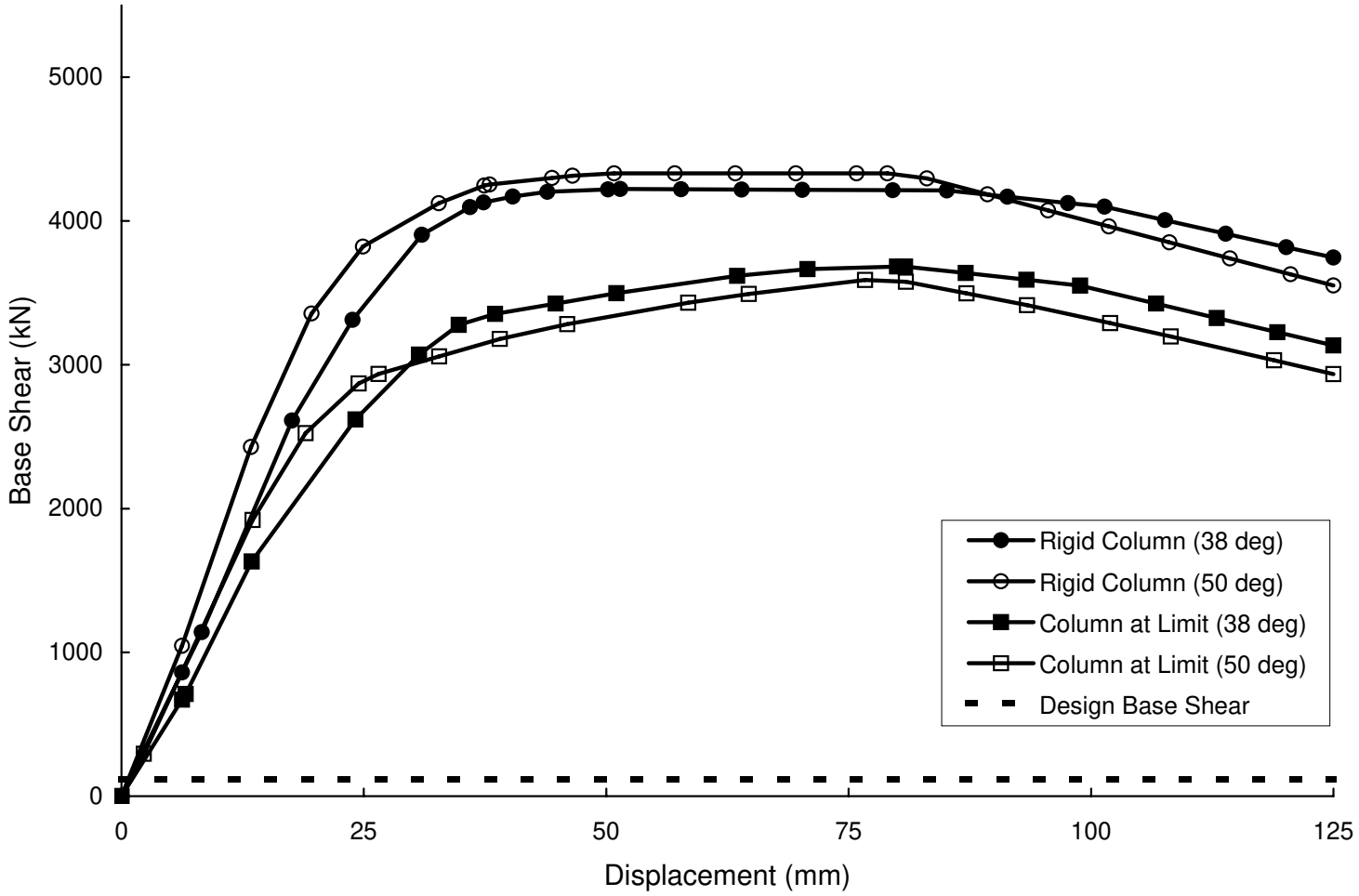

Figure 6.5 - Response Curves for Group 1-D Models

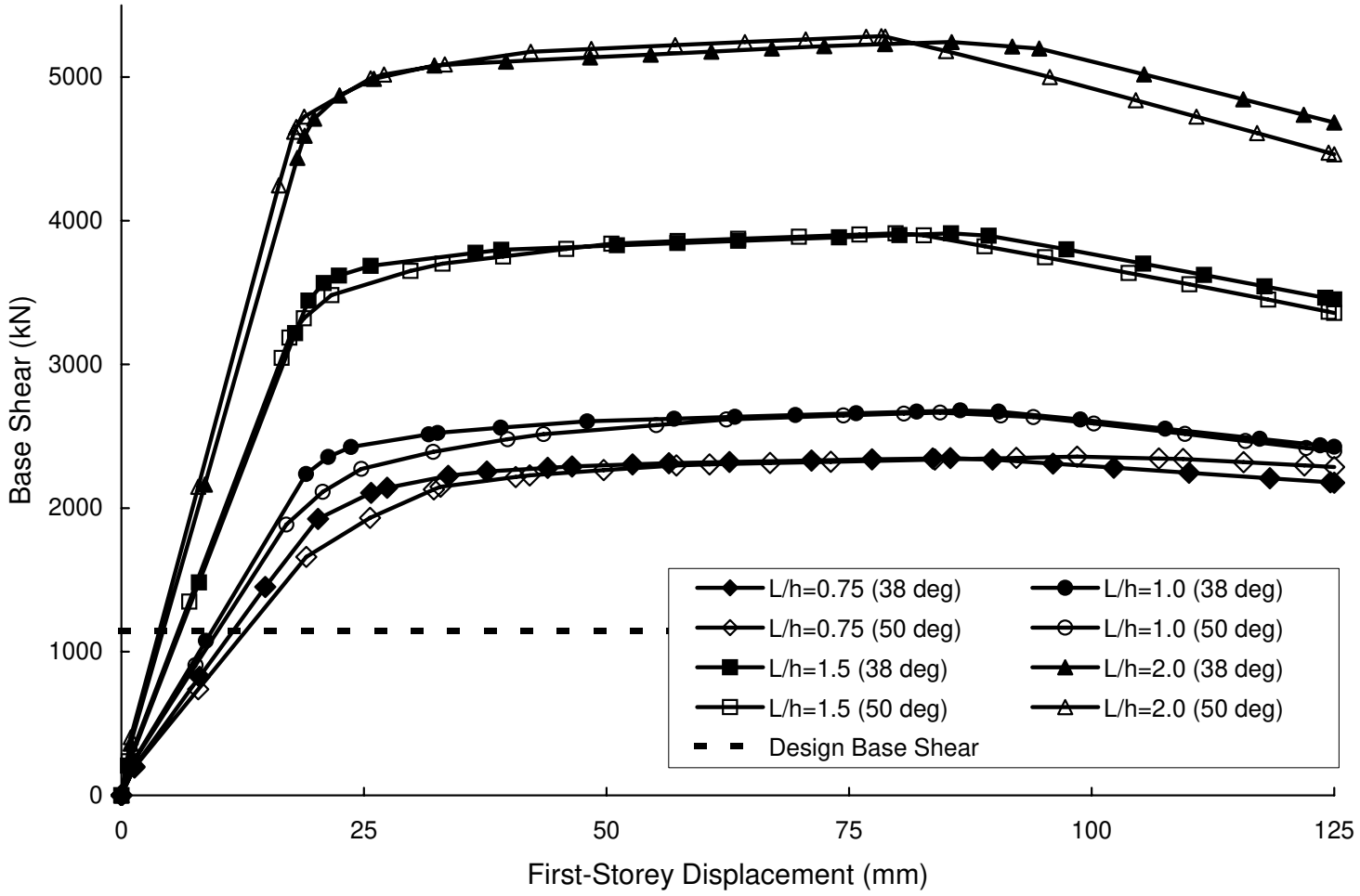

Figure 6.6 - Response Curves for Group 4-A Models

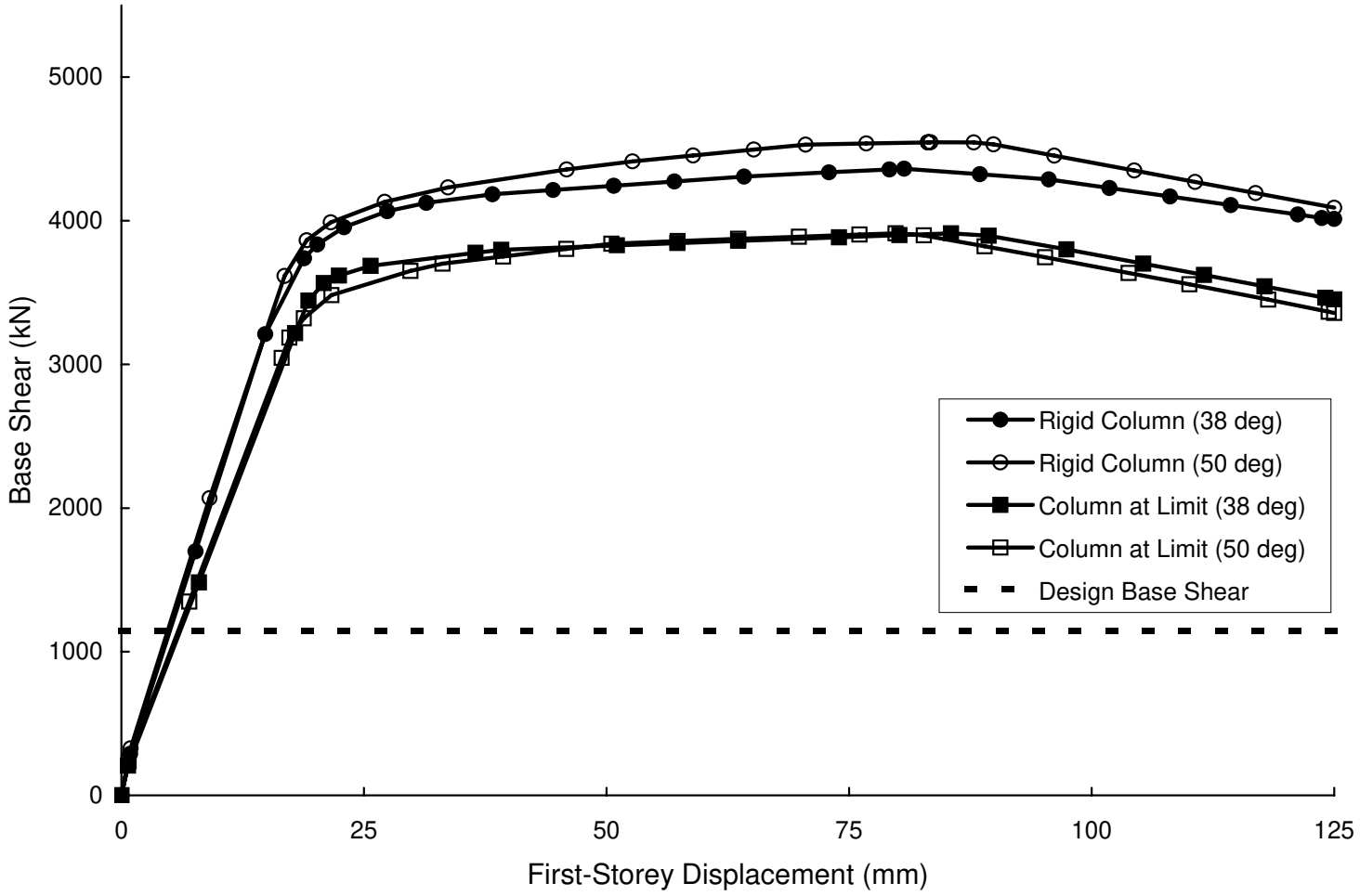

Figure 6.7 - Response Curves for Group 4-B Models

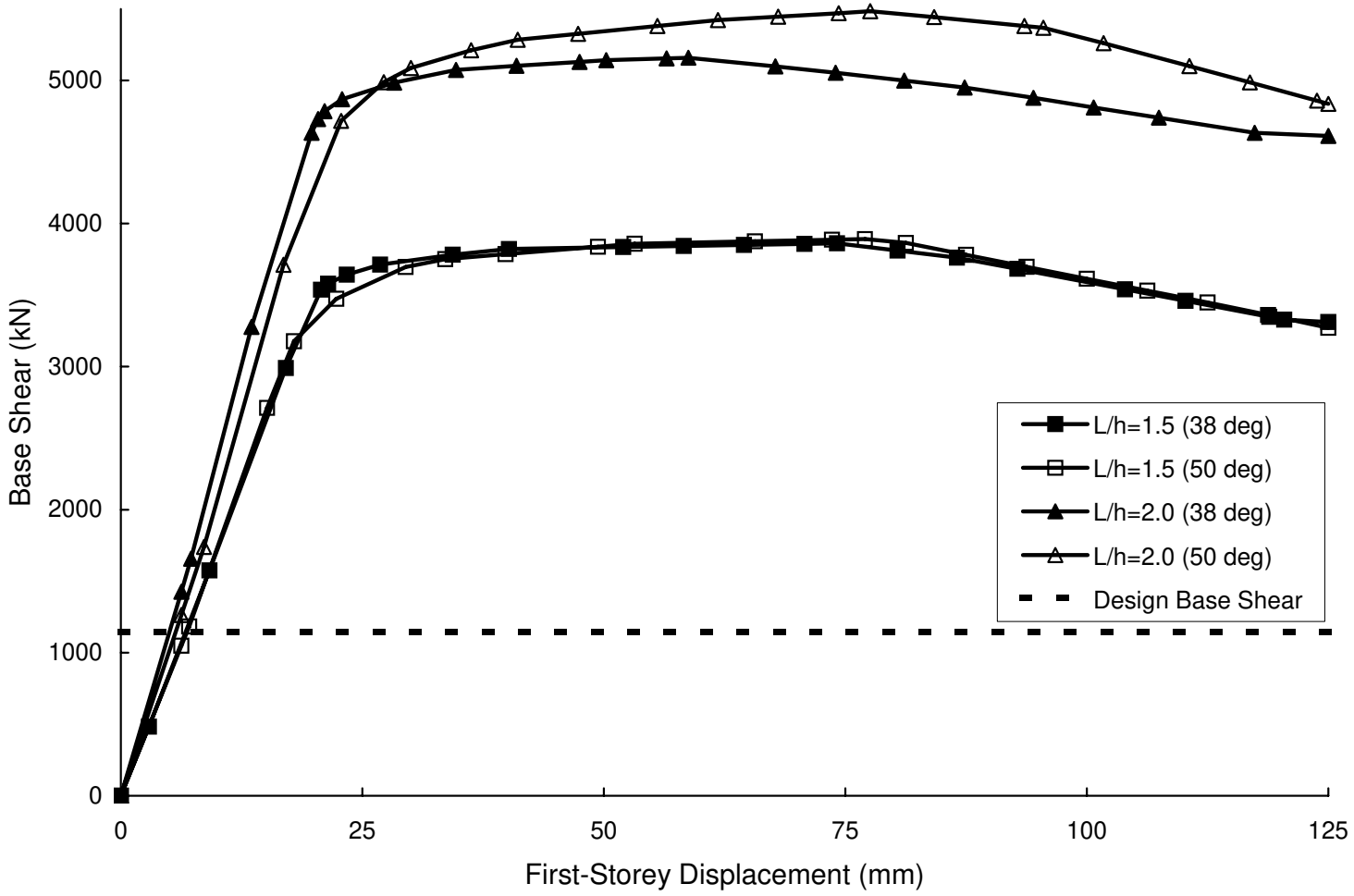

Figure 6.8 - Response Curves for Group 4-C Models

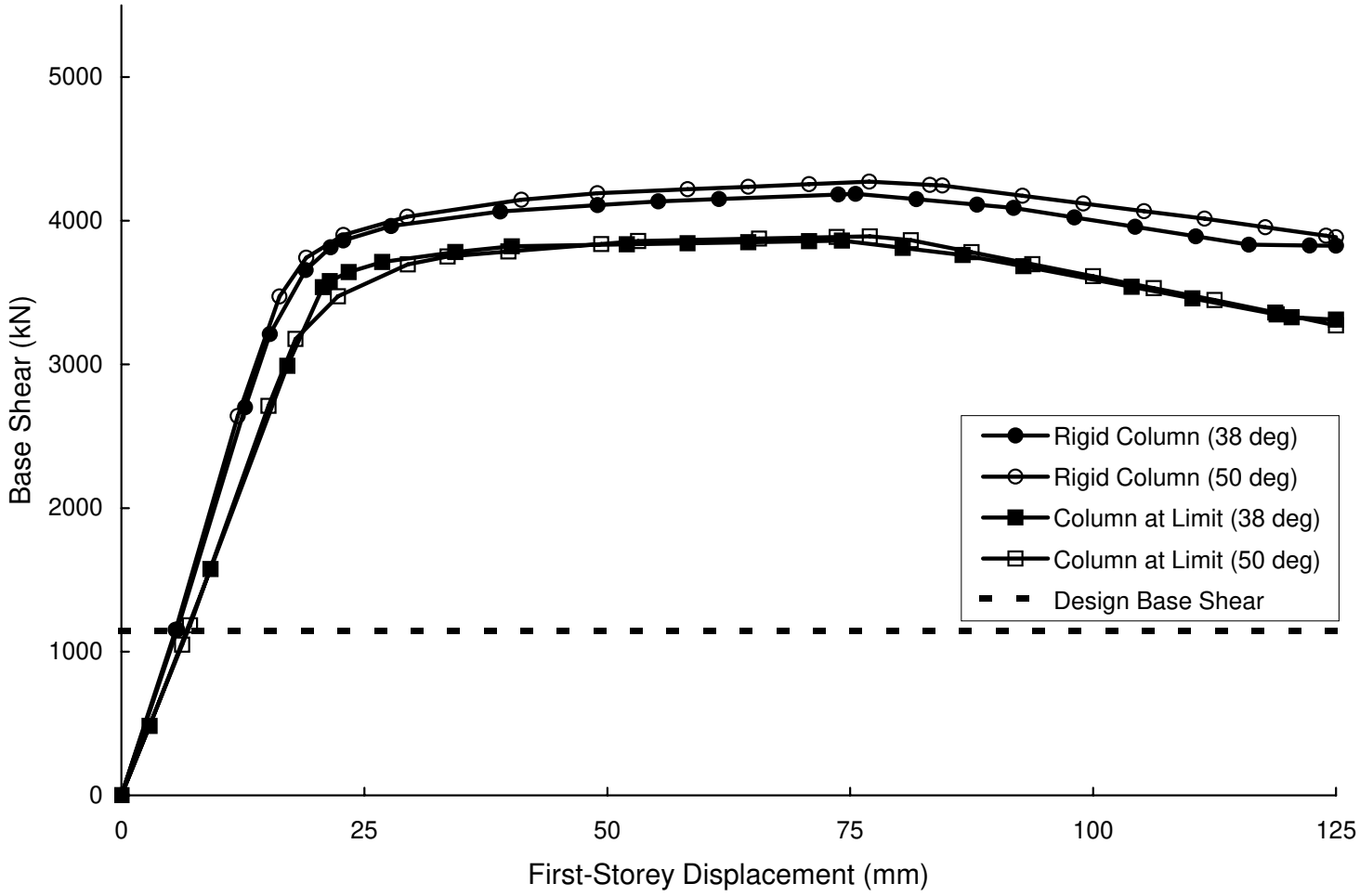

Figure 6.9 - Response Curves for Group 4-D Models

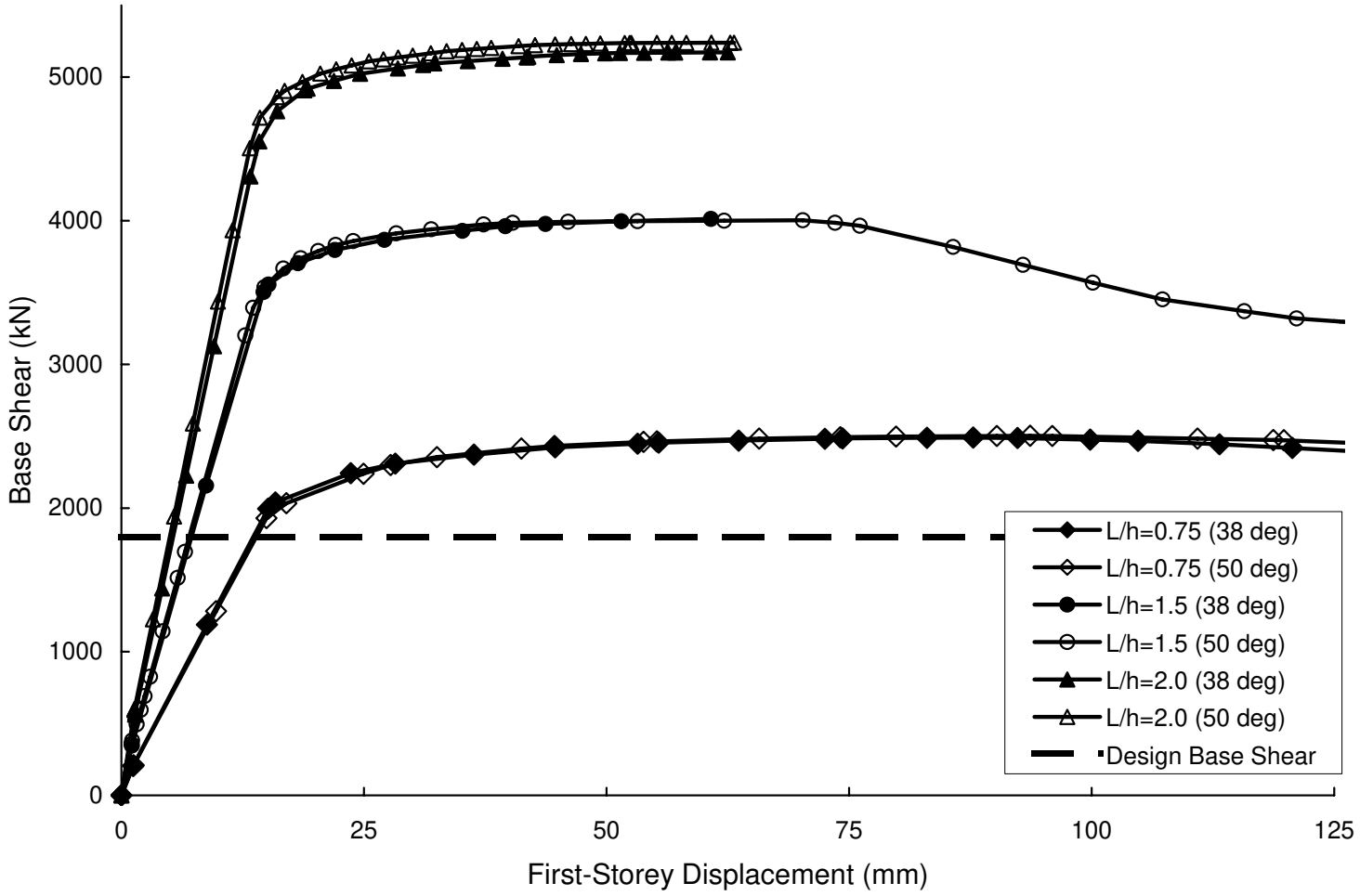

Figure 6.10 - Response Curves for Fifteen–Storey Models

7. SUMMARY AND CONCLUSIONS

7.1 Summary

The strip model, originally developed by Thorburn *et al.* (1983), was refined based on observed phenomena during loading of test specimens in order to better represent steel plate shear wall pushover behaviour. To reflect the fact that deformations observed in the panel zones during the loading of a steel plate shear wall specimen were negligible, the panel zones of the model were stiffened by increasing the modulus of elasticity of the members in this region. Multilinear rigid-inelastic flexural and axial hinges, based on the stress vs. strain material curve of each member and neglecting local buckling, were used to model the inelastic response of steel plate shear walls. The flexural hinges were located a distance of one-half the boundary frame member depth from the edge of the panel zone and the axial hinges were located at a discrete point along the length of the tension–only strip. The compression field in each panel, as described in Chapter 3, was modelled by a compression–only diagonal strut. The limiting stress of the strut ($F_{yCS} = 0.08 \times F_{yPL}$) was modelled using a bilinear axial hinge that was located at a discrete point along the length of the strut. Deterioration axial hinges, located on the strips that came closest to the corners of each panel, modelled the tearing of the infill plate corners.

The detailed strip model was applied to the four–storey one–bay steel plate shear wall specimen tested by Driver *et al.* (1998a). Using a conventional structural analysis software package, the detailed model underwent a pushover analysis to obtain a pushover curve that was compared to the envelope of the hysteresis curve of the specimen. It was found that the detailed model was in excellent agreement with the initial stiffness of the specimen, while providing a slightly conservative estimate of the ultimate strength. For comparison, the same specimen was modelled using the strip model described in CAN/CSA S16-01 with rigid–inelastic hinges located at the connection nodes, which was called the basic strip model, and a pushover curve was obtained from this model. The detailed model was found to be more accurate than the basic strip model in predicting both the initial stiffness and ultimate strength of the test specimen.

Each parameter of the detailed model was examined more closely to determine if it could be made simpler to generate while still retaining a high degree of accuracy in overall inelastic behaviour. The frame–joint arrangement was simplified such that the panel zone contained a nominal or measured modulus of elasticity and the flexural hinges were located at the edges of the panel zones, eliminating the need for creating additional nodes half the member depth from the panel zone boundaries. The tension–only strips were spaced so that strips on either side of a beam element shared a common node. Also, all plastic hinges were made to be bilinear. It was found that these simplifications had a negligible effect on the predicted inelastic behaviour, while reducing modelling effort considerably.

A pushover analysis of the Driver *et al.* (1998a) specimen was performed using the simplified model and the resulting curve was compared to the response curves of the detailed model, basic strip model, and the test specimen. It was found that the simplified model provided an excellent prediction of the initial stiffness of the specimen and a good, but conservative, estimate of the ultimate strength. In the region of initial yielding, the simplified model actually provided more accurate results than the detailed model. The simplified model was also more accurate in predicting the inelastic behaviour than the basic strip model. Since little accuracy was lost in simplifying the detailed model, while the model became considerably more efficient to generate, the simplified model was selected for validation and was re-named the modified strip model. The value of the compression strut limiting stress ($0.08 \times F_{yPL}$) was validated by a sensitivity analysis performed on the modified strip model. Frame forces were extracted from the modified strip model and compared to those of the Driver *et al.* (1997) specimen. For most cases, the model provided conservative results, with the exception of the columns in tension where the axial force was underestimated. When compared to the frame forces predicted by the basic strip model, the modified strip model proved to be more accurate, although the frame forces were still overly conservative in several cases. It was also found that using twenty tension–only strips per panel instead of ten did not improve the accuracy of the frame force predictions.

The modified strip model was validated using results of the specimen tested by Timler and Kulak (1983), which had pinned beam-to-column connections, and the Lubell (1997) one–storey specimen, which had a very thin infill plate and flexible columns. The initial stiffnesses of both specimen response curves were estimated well by the modified strip model when the compression strut was omitted from the model. This was attributed to the fact that the pinned connections and the very thin plates delayed the development of the compression fields in the panel corners. However, it was found that the compression strut was still required to obtain a good estimate of the post-yield portion of the envelope curves. Thus, the compression strut axial hinge for both specimens was calibrated by delaying the point at which it engages and reducing its stiffness but not its strength to capture the full nonlinear behaviour of each specimen. Even though the compression strut required some degree of refinement, the validation process supported the use of the strut for predicting the ultimate strength of a steel plate shear wall specimen. The modified strip model was also applied to the Lubell (1997) four–storey specimen, which also had very thin infill plates and highly flexible columns. It was found that one model could not accurately capture the inelastic behaviour of the specimen because, as noted by Lubell (1997), the angle of inclination of the infill plate tension field increased steadily as the applied load was increased. Because of the use of flexible columns that would not be permitted by CAN/CSA S16-01, angles outside the usual range were observed and this result is not considered to impact the validity of the modified strip model. It was also found that the deterioration behaviour of the modified strip model did not accurately describe the deterioration of the validation test specimens, although it is considered to be conservative for most cases.

A parametric study was performed on the modified strip model to determine the sensitivity of the predicted inelastic behaviour to varying the angle of inclination of the infill plate tension strips, α. One-, four-, and fifteen-storey steel plate shear walls were modelled and analysed with various aspect ratios, column flexibilities, and beam-to-column connection types. Each steel plate shear wall was designed using the seismic requirements of the current Canadian codes and standards (*i.e.*, NBCC 2005, CAN/CSA S16-01). During the design process, it was found that for all models, the

required infill plate thickness was below that of the minimum practical thickness (taken as t = 3.0 mm). It was also found that for one–storey buildings and the top of multi-storey buildings, the maximum column flexibility limit of CAN/CSA S16-01 ($\omega_h \leq 2.5$) was the governing factor in the design of the column cross-section rather than the column design forces. The pushover curves were obtained for each model and it was determined that the predicted inelastic behaviour of the modified strip model was generally insensitive to variations of α. It was also found that for the one- and four-storey models, the capacity far exceeded the design base shear, as determined by the equivalent static force procedure (NBCC 2005). The required column and beam cross-sections of each steel plate shear wall model were very stocky due to the minimum practical plate thickness used.

7.2 Conclusions

It was demonstrated that the modified strip model is an accurate tool for predicting the inelastic behaviour of steel plate shear walls, while providing generally conservative results for the frame forces. The modified strip model is based on the original strip model by Thorburn *et al.* (1983), but incorporates bilinear flexural hinges at the edges of the panel zones, a simplified method of spacing tension–only strips, a compression strut with a bilinear axial hinge to represent the buckling of the compression field, and bilinear axial hinges plus a conservative deterioration behaviour for the tension strips that come closest to the panel corners.

Use of the compression strut, which represents the small compressive capacity of the infill plate along with other phenomena that could not be modelled using a tension–only strip model, contributes significantly to improving the prediction of the initial stiffness and capacity of steel plate shear walls with moment-resisting beam-to-column connections and infill plate thicknesses suitable for ease of handling and welding. The calibrated value of the limiting stress for the compression strut (8% of the infill plate yield stress) was confirmed. For cases with pinned beam-to-column connections or with very thin infill plates, the compression strut axial hinge requires calibration so one model can accurately capture all elements of the inelastic response curve. Such hinges are proposed herein based on available test results. Alternatively for these special cases, the

compression strut can be omitted from the modified strip model to obtain the initial stiffness and retained to obtain the ultimate capacity.

It was shown that the deterioration axial hinge, as described in Chapter 3, did not accurately describe the behaviour of the validation specimens. For the Timler and Kulak (1983) specimen, the pushover curve of the model kept on gaining strength even after the maximum deflection of the specimen was reached. However, it should be noted that Timler and Kulak (1983) expected a higher capacity and larger deflections if the connection plate at one of the pinned connection had not buckled. For the Lubell (1997) one–storey specimen, the model predicted deterioration to occur at an earlier deflection than what occurred for the specimen. This is attributed principally to the fact that the thin sheet material used for the infill plate would be less susceptible to severe kinking than the plate used for deriving the deterioration behaviour in the model. Moreover, no gravity loads were applied to this test specimen, negating any potential P-Δ effect.

The modified strip model was found to be relatively insensitive to variations in the angle of inclination for the infill plate tension field, α. This finding, which supports that of Driver *et al.* (1998b), applies to multi-storey structures of different geometries, column stiffnesses, and beam-to-column connection types. It is recommended that a single value of $\alpha = 40°$ could be used throughout the design process of a steel plate shear wall to achieve accurate, but generally slightly conservative, results.

The analysis results from the one- and four-storey parametric study models showed that the predicted capacities exceed the design base shear (NBCC 2005) by a considerably large margin due to the fact that the minimum practical plate thickness selected was significantly in excess of that theoretically required. Thus, to meet the column flexibility limit (CAN/CSA S16-01) and to resist the demand increased by the capacity design factor, B, the column sizes were increased. Also, it was found that the column flexibility limit of CAN/CSA S16-01 ($\omega_h \leq 2.5$) governed for the design of columns in one-storey steel plate shear walls and near the top of multi-storey steel plate shear walls.

The design of the parametric study models demonstrates that the thickness of the infill plate has a considerable effect on the economics of small and medium sized steel plate

shear wall buildings. The frame sections were selected to resist the design frame forces (amplified according to capacity design principles) and to meet the column flexibility requirement of CAN/CSA S16-01, resulting in extremely stocky sections. This suggests that the use of infill plates with a low-yield strength could result in a dramatic improvement in the economic viability of the system.

Moments and axial forces in the columns of the four–storey models and the Driver *et al.* (1998a) specimen were extracted at the peak level of the pushover curves. When they were applied to the CAN/CSA S16-01 beam-column interaction equations, the columns were found to be inadequate in cross-sectional strength. However, the columns of the test specimen did not fail until after the ultimate strength was achieved, which suggests that the interaction equations represent a conservative estimate of the ultimate member strength when used with frame forces derived from the modified strip model.

7.3 Recommendations for Future Research

While the modified strip model generally produced conservative estimates of the boundary member frame forces, the degree of accuracy was not at the same level as that of the predicted overall inelastic behaviour, even when twenty tension–only strips per panel were used instead of ten. It would be desirable for the design engineer to have one model that is able to predict accurately the overall inelastic behaviour of steel plate shear walls and the resulting boundary member frame forces, simultaneously. Therefore, further research should be conducted to achieve this goal.

The validation of the modified strip model resulted in compression strut axial hinges that were calibrated separately for steel plate shear walls with pinned beam-to-column connections and very thin infill plates. Additional tests are required to validate these hinge models further.

A more detailed investigation into the deterioration behaviour of various specimens should be performed to support or refine the deterioration axial hinge proposed.

During the design of the parametric study models, it was found that the frame of the steel plate shear walls utilised very stocky cross-sections. The use of low-yield infill plates

should be investigated as a means to reduce the size of the boundary members of steel plate shear walls designed according to capacity design principles.

REFERENCES

Applied Technology Council, 1992, "Guidelines for Cyclic Seismic Testing of Component of Steel Structures." ATC–24, Redwood City, CA

Astaneh-Asl, A., 2001, "Seismic Behaviour and Design of Steel Shear Walls." Steel TIPS Report, Structural Steel Educational Council, July, Moraga, CA.

Basler, K., 1961, "Strength of Plate Girders in Shear." ASCE Journal of the Structural Division, Vol. 87, No. ST7, pp. 151–180.

Behbahanifard, M.R, Grondin, G.Y., and Elwi, A.E., 2003, "Experimental and Numerical Investigation of Steel Plate Shear Walls." Structural Engineering Report No. 254, Department of Civil and Environmental Engineering, University of Alberta, Edmonton, Canada.

Berman, J., and Bruneau, M., 2003, "Plastic Analysis and Design of Steel Plate Shear Walls." ASCE Journal of Structural Engineering, November, pp. 1448–1456.

Berman, J., and Bruneau, M., 2004, "Steel Plate Shear Walls Are Not Plate Girders." AISC Engineering Journal, Third Quarter, pp. 95–106.

Caccese, V., Elgaaly, M., and Chen, R., 1993, "Experimental Study of Thin Steel-Plate Shear Walls Under Cyclic Load." ASCE Journal of Structural Engineering, Vol. 119, No. 2, pp. 573–587.

Caccese, V., Elgaaly, M., and Chen, R., 1994, Closure to "Experimental Study of Thin Steel-Plate Shear Walls Under Cyclic Load." ASCE Journal of Structural Engineering, Vol. 120, No. 10, pg. 3074.

Canadian Standard Association, CAN/CSA S16.1-94, 1994, "Limit States Design of Steel Structures." Toronto, Ontario.

Canadian Standard Association, CAN/CSA S16-01, 2001, "Limit States Design of Steel Structures." Toronto, Ontario.

Computers and Structures, Inc., 1984-2000, SAP2000 Nonlinear, Computers and Structures, Inc., Berkeley, CA.

Driver, R.G., Kulak, G.L., Kennedy, D.J.L., and Elwi, A.E., 1997, "Seismic Behaviour of Steel Plate Shear Walls." Structural Engineering Report No. 215, Department of Civil and Environmental Engineering, University of Alberta, Edmonton, Canada.

Driver, R.G., Kulak, G.L., Kennedy, D.J.L, Elwi, A.E., 1998a, "Cyclic Test of a Four–Storey Steel Plate Shear Wall." ASCE Journal of Structural Engineering, Vol. 124, No. 2, pp. 112–120.

Driver, R.G., Kulak, G.L., Elwi, A.E., Kennedy, D.J.L, 1998b, "FE and Simplified Models of Steel Plate Shear Wall." ASCE Journal of Structural Engineering, Vol. 124, No. 2, pp. 121–130.

Elgaaly, M., Caccese, V., and Du, C., 1993a, "Postbuckling Behaviour of Steel-Plate Shear Walls Under Cyclic Loads." ASCE Journal of Structural Engineering, Vol. 119, No. 2, pp. 588–605.

Elgaaly, M., Caccese, V., and Martin, D.K., 1993b, "Experimental Investigation of the Behavior of Bolted Thin Steel Plate Shear Walls." Civil Engineering Department, University of Maine, Orono, Maine.

Elgaaly, M., Caccese, V., and Du, C., 1994, Closure to "Postbuckling Behaviour of Steel-Plate Shear Walls Under Cyclic Loads." ASCE Journal of Structural Engineering, Vol. 120, No. 7, pp. 2251–2255.

Elgaaly, M., and Liu, Y., 1997, "Analysis of Thin-Steel-Plate Shear Walls." ASCE Journal of Structural Engineering, Vol. 123, No. 11, pp. 1487–1496.

FEMA, 2000, "Prestandard and Commentary for the Seismic Rehabilitation of Buildings (FEMA 356)." Washington, D.C.

Kennedy, D.J.L., Kulak, G.L., and Driver, R.G., 1994, Discussion of "Postbuckling Behaviour of Steel-Plate Shear Walls Under Cyclic Loads." ASCE Journal of Structural Engineering, Vol. 120, No. 7, pp. 2250–2251.

Kharrazi, M.H.K., Ventura, C.E., Prion, G.L., and Sabouri-Ghomi, S., 2004, "Bending and Shear Analysis and Design of Ductile Steel Plate Walls." Proceedings of the the 13th World Conference on Earthquake Engineering, August, Vancouver, B.C., Canada.

Krawinkler, H. and Popov, E.P., 1982, "Seismic Behavior of Moment Connections and Joints." ASCE Journal of the Structural Division, Vol. 108, No. ST2, pp. 373–391.

Kuhn, P., Peterson, J.P., and Levin, L.R., 1952, "A Summary of Diagonal Tension, Part I – Methods of Analysis." Technical Note 2661, National Advisory Committee for Aeronautics, Washington, D.C.

Kulak, G.L., Kennedy, D.J.L., and Driver, R.G, 1994, Discussion of "Experimental Study of Thin Steel-Plate Shear Walls Under Cyclic Load." ASCE Journal of Structural Engineering, Vol. 120, No. 10, pp. 3072–3073.

Kulak, G.L., Kennedy, D.J.L, Driver, R.G., and Medhekar, M., 2001, "Steel Plate Shear Walls—An Overview" American Institute of Steel Construction Engineering Journal, First Quarter, pp. 50–62.

Lubell, A.S, 1997, "Performance of Unstiffened Steel Plate Shear Walls Under Cyclic Quasi-Static Loading." M.A.Sc. Thesis, Department of Civil Engineering, University of British Columbia, Vancouver, BC, Canada.

Lubell, A.S., Prion, H.G.L, Ventura, C.E., and Rezai, M., 2000, "Unstiffened Steel Plate Shear Wall Performance Under Cyclic Loading." Journal of Structural Engineering, Vol. 126, No. 4, pp. 453–460.

Mimura, H. and Akiyama, H., 1977, "Load-Deflection Relationship of Earthquake-Resistant Steel Shear Walls With a Developed Diagonal Tension Field." Transactions, Architectural Institute of Japan, 260, October, pp. 109–114 (in Japanese).

NBCC, 2005, “National Building Code of Canada.” National Research Council of Canada, Ottawa, ON.

Popov, E.P., Amin, N.R., Louie, J.J.C., and Stephen, R.M., 1986, “Cyclic Behavior of Large Beam–Column Assemblies.” AISC Engineering Journal, Vol. 23, No. 1, pp. 9–23.

Rezai, M., 1999, “Seismic Behaviour of Steel Plate Shear Walls by Shake Table Testing.” PhD Dissertation, Department of Civil Engineering, University of British Columbia, Vancouver, BC, Canada.

Rezai, M., Ventura, C.E., and Prion, H.G.L., 2000, “Numerical Investigation of Thin Unstiffened Steel Plate Shear Walls.” Proceedings, World Conference of Earthquake Engineering, pp. 0801-1–0801-8.

Takahashi, Y., Takemoto, Y., Takeda, T., and Takagi, M. 1973. “Experimental Study on Thin Steel Shear Walls and Particular Bracings Under Alternative Horizontal Load.” Preliminary Report, IABSE Symposium on Resistance and Ultimate Deformability of Structures Acted on by Well-defined Repeated Loads, Lisbon, Portugal, pp. 185–191.

Thorburn, L.J., Kulak, G.L., and Montgomery, C.J., 1983, “Analysis of Steel Plate Shear Walls” Structural Engineering Report No. 107, Department of Civil Engineering, University of Alberta, Edmonton, Canada.

Timler, P.A., Kulak, G.L., 1983, “Experimental Study of Steel Plate Shear Walls.” Structural Engineering Report No. 114, Department of Civil Engineering, University of Alberta, Edmonton, Canada.

Timler, P.A., 1998, “Design Procedures Development, Analytical Verification, and Cost Evaluation of Steel Plate Shear Wall Structures.” Earthquake Engineering Research Facility Technical Report No. 98-01.

Timler, P.A., Ventura, C.E., Prion, H., and Anjam, R., 1998, “Experimental and Analytical Studies of Steel Plate Shear Walls as Applied to the Design of Tall Buildings.” Structural Design of Tall Buildings, Vol. 7, pp. 233–249.

Tromposch, E.W., Kulak, G.L., 1987, “Cyclic and Static Behaviour of Thin Panel Steel Plate Shear Walls.” Structural Engineering Report No. 145, Department of Civil Engineering, University of Alberta, Edmonton, Canada.

Wagner, H., 1931, “Flat Sheet Metal Girders with Very Thin Webs, Part I – General Theories and Assumptions.” Technical Memo No. 604, National Advisory Committee for Aeronautics, Washington, D.C.

Xue, M., and Lu, L.-W., 1994, “Interaction of Infilled Steel Shear Wall Panels With Surrounding Frame Members.” Proceedings, Structural Stability Research Council Annual Technical Session, Bethlehem, PA, pp. 339–354.

APPENDIX A

COMPARISON OF MODELS WITH TEN AND TWENTY STRIPS PER PANEL

Chapter 4 describes how the Driver *et al.* (1997) specimen was analysed using the modified strip model. One of the features of the model is the representation of the tension field of the infill plate by ten tension–only strips oriented at the average angle of inclination of the tension field, α, of all the panels in the structure. After the model underwent a pushover analysis, the nonlinear response curve of the critical panel and the frame forces in the lower two storeys were extracted and compared to the respective specimen data. The modified strip model accurately predicted the elastic and initial inelastic regions of the first–storey response of the specimen, and due to modelling simplifications over the detailed model it provided a conservative, but reasonable, estimate of the ultimate strength. It was found, however, to be generally conservative—and sometimes by a significant margin—in predicting the frame forces of the boundary members, although it was somewhat non-conservative in a few cases (see Chapter 4 for details).

To determine if greater accuracy could be attained in predicting the frame forces, the Driver *et al.* (1997) specimen was analysed similarly to the modified strip model, but with twenty strips per panel representing the diagonal tension field instead of ten. (The analysis described above is referred to as the twenty–strip model while the modified strip model from Chapter 4 is the ten–strip model.) Figure A.1 shows the pushover curves for the ten– and twenty–strip models compared to the envelope curve of the specimen. Both models agree very well with the initial stiffness of the specimen. The twenty–strip model underestimates the ultimate strength of the specimen by 6.9% as compared to 5.3% for the ten strip model (2868 kN for the twenty–strip model, 2916 kN for the ten–strip model, and 3080 kN for the specimen.) Therefore, the accuracy of the two models in predicting the inelastic behaviour is essentially the same.

Frame forces were extracted at certain increments of the pushover analysis of the twenty–strip model. At one such increment, a total base shear of 2035 kN was recorded, which is 0.7% above the base shear for the first–storey frame forces of the specimen (2021 kN). At a subsequent increment, a total base shear of 2574 kN was recorded, which is 0.2% above the base shear for the second–storey frame forces of the specimen (2570 kN). Therefore, it can be assumed that the frame forces extracted from the twenty–strip model

can be directly compared to those from the ten–strip model and the Driver *et al.* (1997) specimen.

Figures A.2 through A.13 show that there is little or no difference between the frame forces of the ten– and twenty–strip models. Therefore, it was determined that using ten tension–only truss members per panel to represent the infill plate tension field is sufficient. It should be noted that previous research supports these findings (*e.g.*, Thorburn *et al.* 1983, Driver *et al.* 1997).

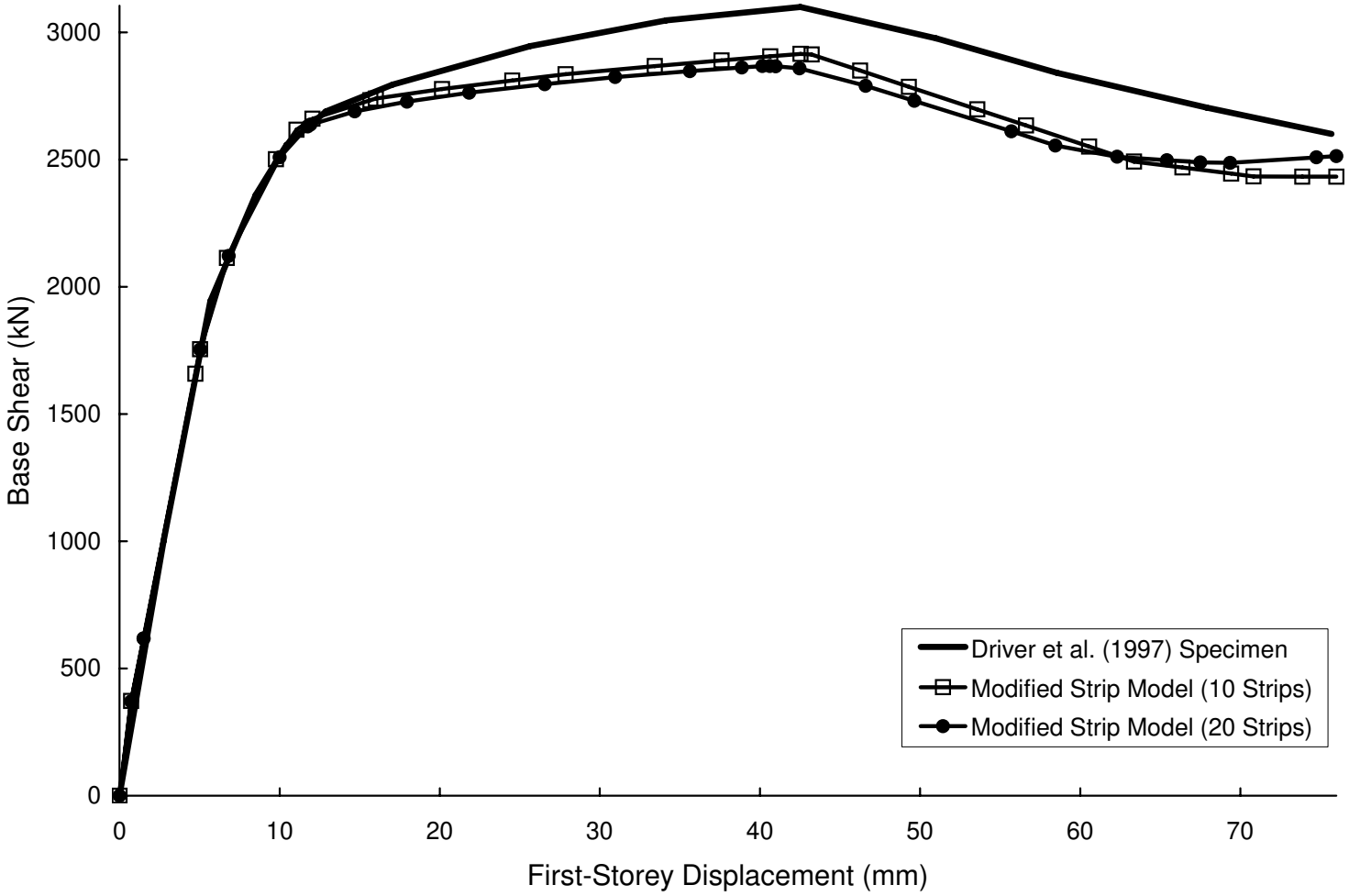

Figure A.1 - First–Storey Response Curves for Ten and Twenty Strip Modified Strip Model and Driver et al. (1997) Specimen

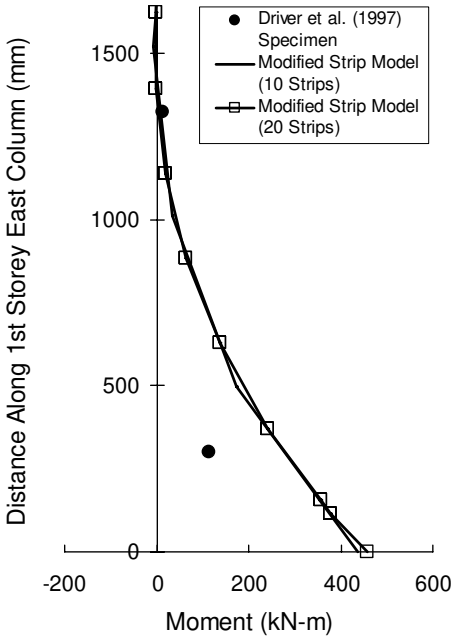

Figure A.2 - First–Storey East Column Moments

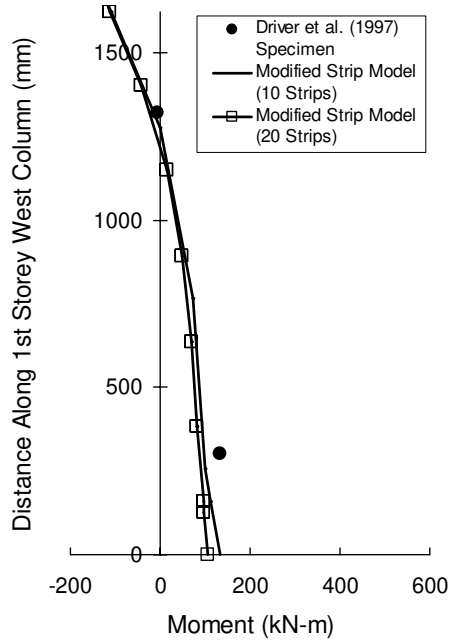

Figure A.3 - First–Storey West Column Moments

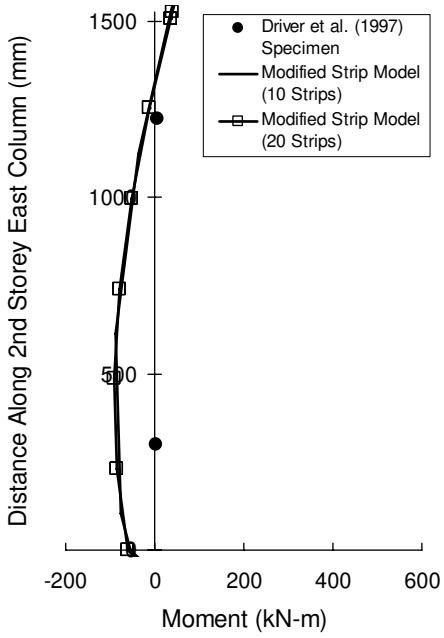

Figure A.4 - Second–Storey East Column Moments

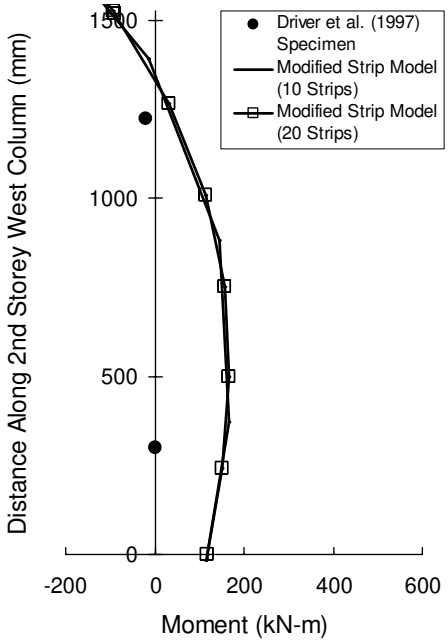

Figure A.5 - Second–Storey West Column Moments

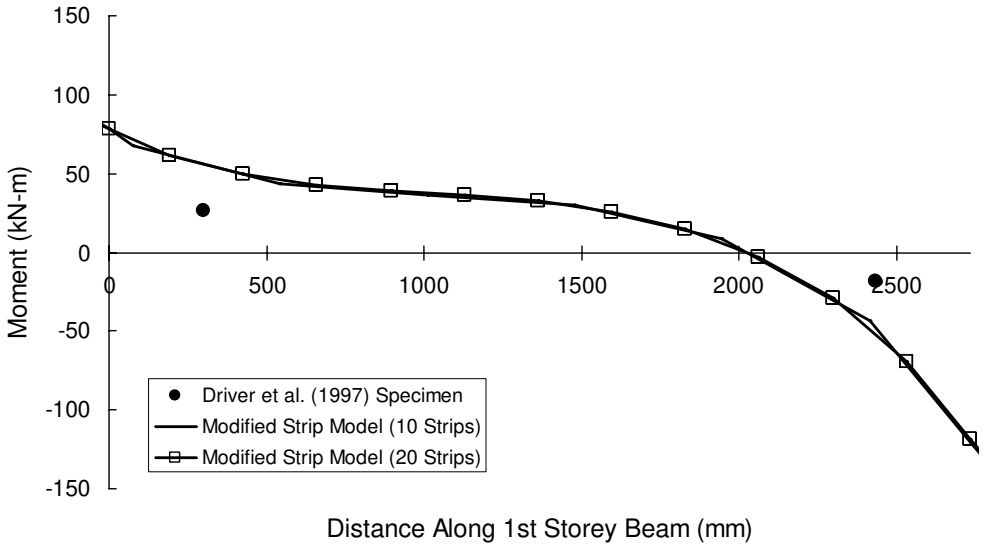

Figure A.6 - First–Storey Beam Moments

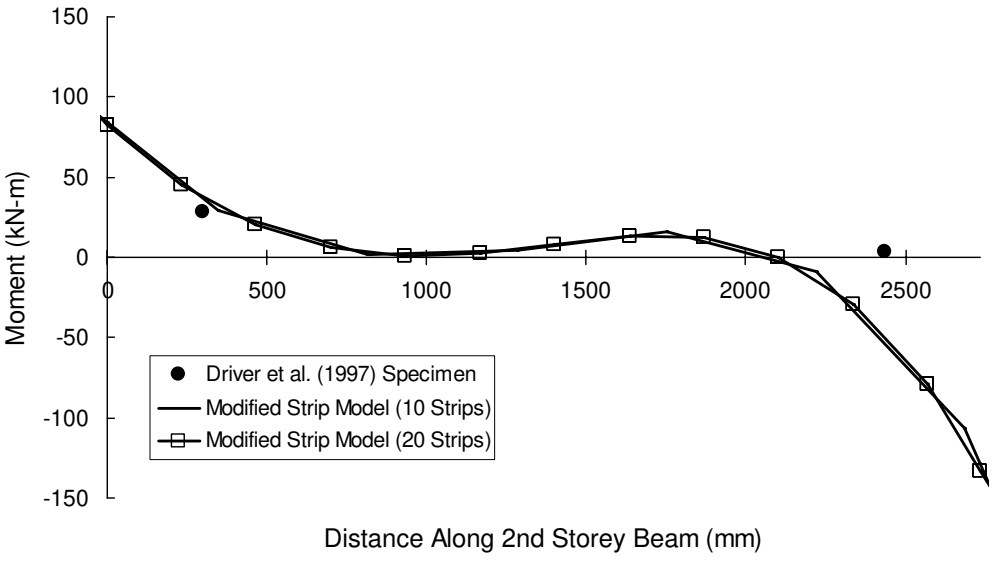

Figure A.7 - Second–Storey Beam Moments

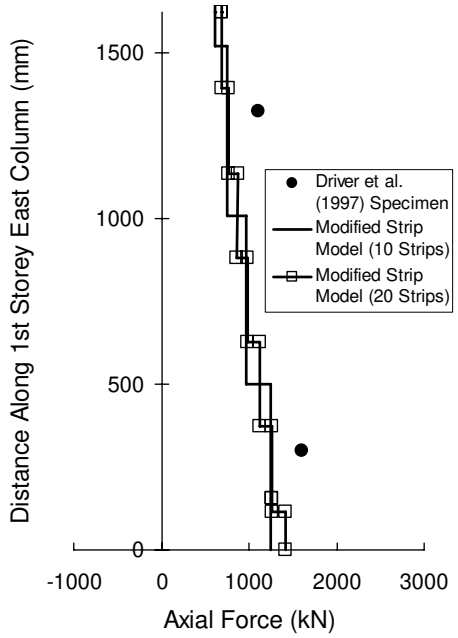

Figure A.8 - First–Storey East Column Axial Forces

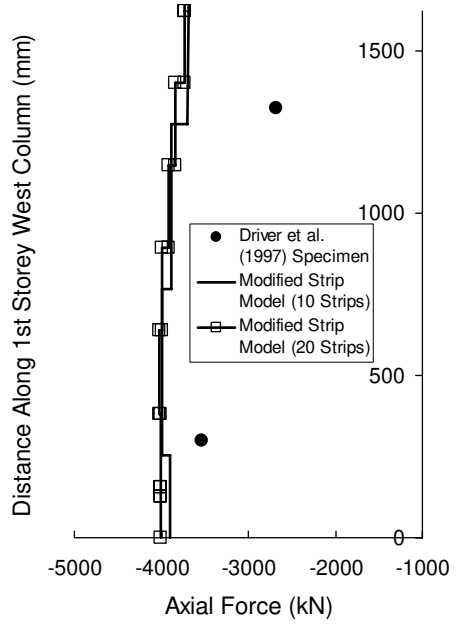

Figure A.9 - First–Storey West Column Axial Forces

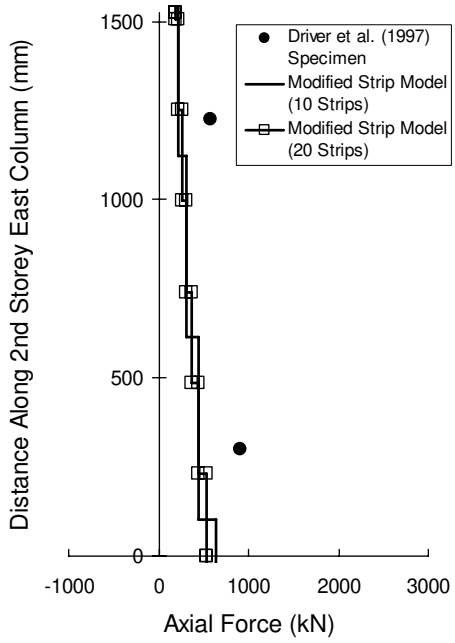

Figure A.10 - Second–Storey East Column Axial Forces

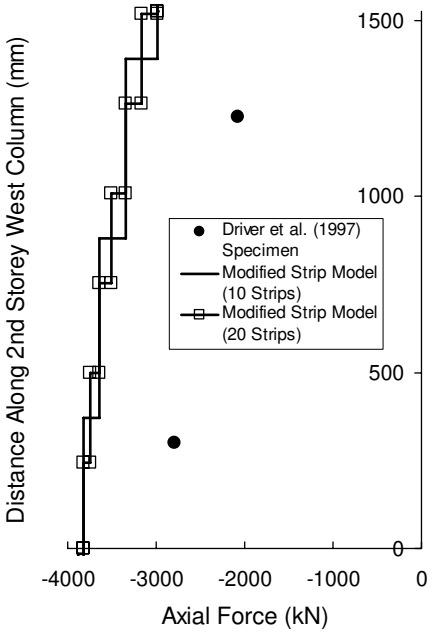

Figure A.11 - Second–Storey West Column Axial Forces

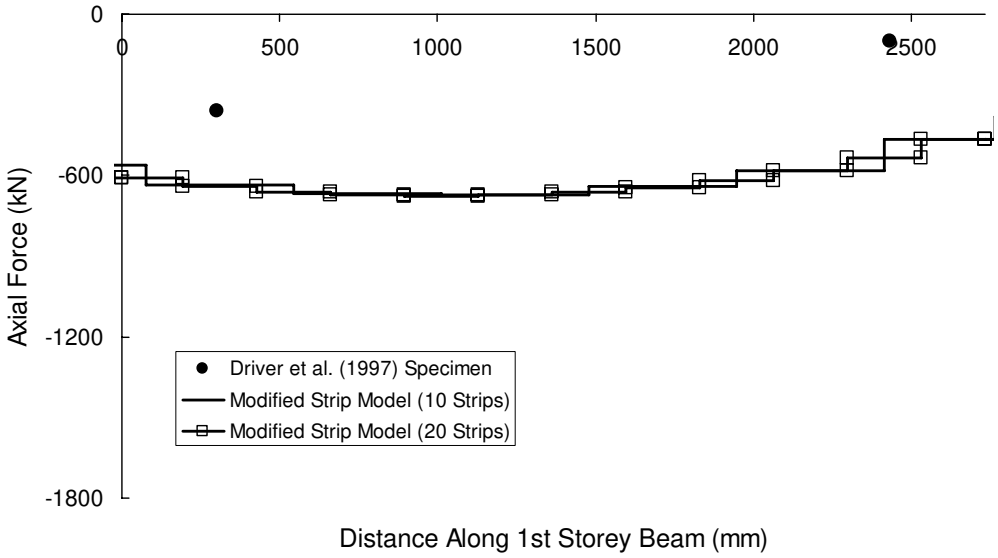

Figure A.12 - First–Storey Beam Axial Forces

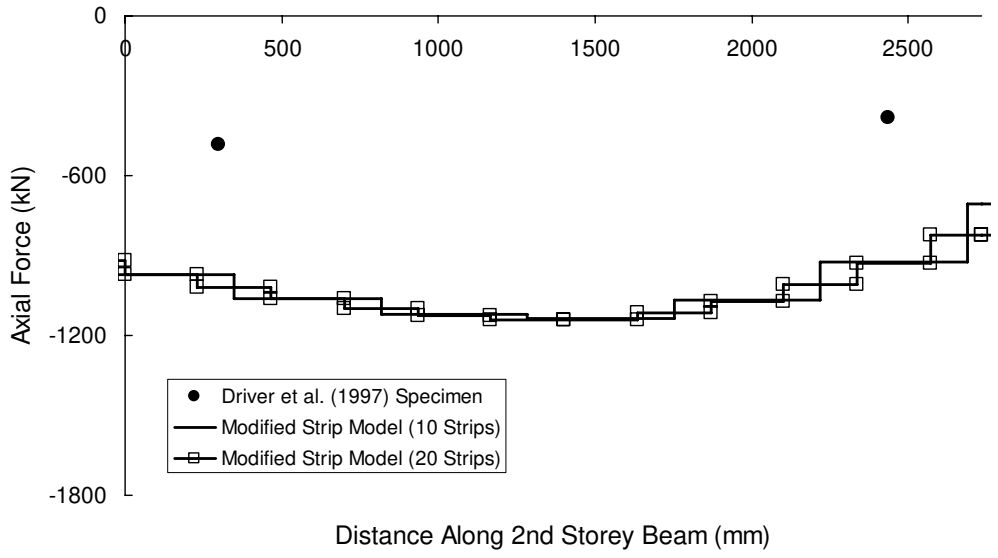

Figure A.13 - Second–Storey Beam Axial Forces